A STUDY INTO THE EARTHQUAKE RESISTANCE OF CIRCULAR ADOBE BUILDINGS

by

Watcharin Jinwuth

A thesis submitted in fulfilment of the requirements

For the degree of

Doctor of Philosophy

Faculty of Design Architecture and Building

University Technology of Sydney

CERTIFICATE OF AUTHORSHIP/ ORIGINALITY

I certify that the work in this thesis has not previously been submitted for a degree nor has it been submitted as part of requirements for a degree except as fully acknowledged within the text.

I also certify that the thesis has been written by me. Any help that I have received in my research work and the preparation of the thesis itself has been acknowledged. In addition, I certify that all information sources and literature used are indicated in the thesis.

Production Note:
Signature removed prior to publication.

Watcharin Jinwuth

November 2012

ACKNOWLEDGMENTS

The thesis has not been completed without the support and encouragement of a number of people. In particular, I would like to thank;

- My supervisor, Prof. Bijan Samali, who provided the invaluable support, motivation and time throughout the process of the dynamic testing and writing this thesis.
- My ex-supervisor, Dr. Kevan Heathcote, for his tireless contributions to many aspects of this project and his understanding during difficult times, which have been greatly appreciated.
- My co-supervisor, Dr. Cynthia Wang, for her constant advice, proof-reading, critical comments and encouragement throughout the period of my research.
- My mudbrick helper: Peter Hickson, for his guidance, friendship and support.
- The Lapaloma hotel technician: Khemachat Phaensanit and his staff, for their support in relation to tilt table construction and testing.
- The Thai government for financial support for this research project.
- The University of Technology, Sydney (UTS) and the Faculty of Design Architecture and Building staff, especially Ann Hobson for her friendship and support.
- The UTS Engineering structures laboratory staff: Rami Haddad, David Hooper, Dave Dicker, Peter Brown, Ulrike Dackermann and Scott Graham, for their extensive and willing assistance in all aspects of the experimental testing.
- Hamidreza Valipour, for his willing assistance in FEM analysis and experimental testing.
- My family who provided continual support and love during the past four years.
- Ian, a primary proof-reader and his family for their hospitality and assistance during my time in Australia.
- Nuch, Wise and Ward for their enduring love, support and patience.

PUBLICATIONS

The following publications have been generated as part of this research project.

Conference papers

Jinwuth, W., Samali, B., Heathcote, K. & Wang, C. 2010, '*A Study into the earthquake resistance of circular adobe buildings using static tilt tests'*, paper presented to the 2010 AEES Conference, Perth, 26-28 November.

Samali, B., Jinwuth, W., Heathcote, K. & Wang, C. 2011, *'Seismic capacity comparison between square and circular plan adobe construction'*, paper presented to the Twelfth East Asia-Pacific Conference on Structural Engineering and Construction (EASEC-12), Hong Kong, 26-28 January.

TABLE OF CONTENTS

CERTIFICATE OF AUTHORSHIP/ ORIGINALITY……………………….………....ii

ACKNOWLEDGMENTS……………………………………………………………iii

PUBLICATIONS…………………………………….…………………………iv

TABLE OF CONTENTS……………………………………………………………..v

LIST OF FIGURES……………………………………………………………..xi

LIST OF TABLES……………………………………………………………...xx

ABSTRACT…………………………………………………………………xxiii

Chapter 1 Introduction………………………………………………………………1

1.1 Background to adobe construction………………………………….………..1

1.2 Seismic vulnerability of adobe buildings……………………………….………5

1.2.1 Distribution of adobe buildings in seismic areas………………………..7

1.2.2 Historical earthquake damage to conventional adobe buildings……..….8

1.2.3 Factors affecting building damage……………………………….…..11

1.3 Effect of shape on earthquake resistance……………………………….…12

1.4 Aim of thesis……………………………………………………………………15

1.5 Scope of the study……………………………………………………………15

1.6 Limitations…………………………………………………………………...16

1.7 Research methodology………………………………………………….……16

1.8 Thesis layout…………………………………………………………………17

Chapter 2 Previous Researches into the Seismic Resistance of Earth Buildings……..19

2.1 Introduction…………………………………………………………………….19

2.2 Adobe researches of the Catholic University of Peru………………………….21

2.3 Static tilt tests of a tall cylindrical liquid storage tank…………………………26

2.4 Tilt-table-testing of the FUNDASAL, El Salvador……………………….………30

2.5 Seismic strengthening of adobe-mud brick houses……………………….………33

2.6 Getty Seismic Adobe Project, U.S.A. …………………………………………40

2.7 Shake table testing of scaled geogrid-reinforced adobe models…….……….47

2.8 Adobe models testing of the University of Kassel, Germany……….………50

2.9 Adobe guidelines and manuals…………………………………………………52

2.9.1 International Association for Earthquake Engineering (IAEE)…..……53

2.9.2 The Australia Earth Building Handbook…………………………..…56

2.9.3 Earthquake Tips……………………………………………………...59

2.9.4 Earthquake-Resistant Construction of Adobe Buildings: A Tutorial…..61

2.10 Summary………………………………………………………………………64

Chapter 3 Seismic Performance of Adobe Buildings…………………………..…..66

3.1 Introduction…………………………………………………………………….66

3.2 Earthquake Definition………………………………………………………….66

3.3 Typical damage patterns and failure mechanisms………………...………….68

3.4 Static and Dynamic Analysis ………………………………………………….74

3.4.1 Static method…………………………………………………………...74

3.4.2 Dynamic method………………………………………….……………75

3.5 Seismic Design Code for Earth Building Regions……………………..……77

3.5.1 Concept of seismic code……………………………………….…….77

3.5.2 The earthquake codes of case studies' regions…………………...…….81

3.6 Summary……………………………………………………………….....…..87

Chapter 4 Performance of Existing Circular Earthen Houses located in Seismic Regions……………………………………………………………………88

4.1 Introduction…………………………………………………………….…….88

4.2 Hakka earth buildings in China……………………………….…………..91

4.2.1 Background…………………………………………………………..91

4.2.2 Architectural and structural features……………………………………92

4.2.3 Building performance in earthquake…………………………….…...99

4.3 Bhunga houses in India…………………………………………………..100

4.3.1 Background……………………………………………………………100

4.3.2 Architectural and structure features……………………….…….….104

4.3.3 Building performance in earthquake…………………………….….104

4.4 Yomata houses in Malawi…………………………………………….….106

4.4.1 Background……………………………………………………………106

4.4.2 Architectural and structural features………………..………………108

4.4.3 Building performance in earthquakes ……………………………....110

4.5 Summary……………………………………………………………….…112

Chapter 5 Simple Static Earthquake Design Method……………….……………114

5.1 Introduction……………………………………………………………....114

5.2 Description of static design method…………………………….………..…114

5.3 Relationship between design loads and tilt table performance………………..117

5.3.1 Maximum normal stress for design condition…………..……….......117

5.3.2 Maximum normal stress for models………………….……….......119

5.3.3 Hypothesis of the failure criteria as link between design and model behaviours…………………………………………………………...120

5.4 Theory of reduced model testing…………………….…………….......121

5.5 Calculations of static design loads of the existing circular adobe houses……..123

5.6 Summary……………………………………………………………….…127

Chapter 6 Brick Fabrication and Material Property Tests…………………...……128

6.1 Introduction……………………………………………………………....128

6.2 Brick fabrication……………………………………………...……..128

6.3 Material property testing…………………………………….......….132

6.3.1 Specifications……………………………………………………………132

6.3.2 Testing method…………………………………………………….…..135

6.3.3 Results…………………………………………………………….…...137

6.4 Summary………………………………………………………………………139

Chapter 7 Seismic Capacity Comparison between Square and Circular Plan Adobe Construction using Tilt-table Testing…………………………………...140

7.1 Introduction……………………………………………………………...….140

7.2 The relationship between the static design load and tilt table testing………....141

7.3 Static tilt table ……………………………………………………………..…..141

7.4 Specimen fabrication and specifications……………………………….....…144

7.5 Results of the specimens tested......... ……………………………………….....146

7.6 Social aspect of circular building…………………………………………...…149

7.7 Summary……………………………………………………………………....153

Chapter 8 Capacity Estimation of Circular Adobe Buildings by Tilt-table Testing...154

8.1 Introduction……………………………………………………………...….154

8.2 The hypothesis of the typical failure mechanism………………………....…..156

8.3 Specimen design and construction…………………………………….....….157

8.4 Detail of experimental procedures of static test……………………………....160

8.4.1 Procedures of static tilt-table tests…………………………..……...160

8.4.2 Specimen 1A…………………………………………………………..…162

8.4.3 Specimen 2A…………………………………………………….……164

8.4.4 Specimen 3A…………………………………………………….……166

8.4.5 Specimen 2B…………………………………………………….……168

8.4.6 Specimen 3B…………………………………………………….……170

8.4.7 Specimen 2C…………………………………………………….……172

8.4.8 Specimen 3C…………………………………………………….……174

8.4.9 Specimen 2D……………………………………………………….…176
8.4.10 Specimen 3D……………………………………………………….…178
8.5 Comparative analysis of results from the static tests ………………………...180
8.5.1 Effect of roof load……………………………………….………..…181
8.5.2 Effect of wall height-to-thickness ratios……………………..…..…182
8.5.3 Effect of wall height-to-diameter ratio…………………….……..…184
8.6 Analysis of crack patterns and failure mechanisms ……………...……...186
8.7 Predicted performance of the tilt tests…………………………………..…187
8.7.1 Prediction based on maximum normal stress ………………………...187
8.7.2 Prediction based on overturning about toe……….……………..…189
8.7.3 Discussion of the proposed method………………………………...192
8.8 Summary……………………………………………………………………194
Chapter 9 Comparison between Predicted Performances of Tilt Table Test Specimens with Performance on Shake Table…………………………………….……195
9.1 Introduction……………………………………………………………..…195
9.2 Brick fabrication and material properties tests…………………………..…197
9.2.1 Brick fabrication……………………………………………………....197
9.2.2 Material properties tests……………………………………………198
9.3 Adobe specimens construction………….……………………………….208
9.4 Static pushover test………………………………………………………210
9.4.1 Specimen description and test setup…………………………..…210
9.4.2 Testing procedure………………………………………………….....212
9.4.3 Experimental result and discussion…………………..……………..212
9.5 Shake table testing………………………………………..………………217
9.5.1 UTS shake table……………………………….……………………218
9.5.2 Simulated earthquake motions………………..…………………..…219

9.5.3 Scaling of the input time histories……………………………………220

9.5.4 Predicted results for the dynamic shake tests………….……………..228

9.5.5 Test setup and instrumentation……………..………………………230

9.5.6 Testing procedure……………………………………………………..232

9.5.7 Testing and results of specimen 1A……………………………..…234

9.5.8 Testing and results of specimen 3D with openings………………..…237

9.6 Summary……………………………………………………………………...241

Chapter 10 Application of Design Methodology………………………...………242

10.1 Introduction……………………………………………………...…….…..242

10.2 Evaluation of an existing building……………………………..………..…243

10.3 Summary……………………………………………………………...…..247

Chapter 11 Conclusions and Recommendations for Further Research……..…...…248

11.1 Conclusions………………………………………………………………248

11.2 Recommendation for further research………………………………...…..250

References……………………………………………………………………………252

Appendices……………………………………………………………………………260

LIST OF FIGURES

Figure 1.1: Taos Pueblo's Mud Villages (built ca. 1000 A.D.)(McHenry 1985)………..2

Figure 1.2: Traditional adobe brick fabrication (Keefe 2005)…………………………...3

Figure 1.3: Construction of a circular adobe house for a homeless project in Thailand……………………………………………………………………….4

Figure 1.4: A typical circular adobe house for homeless people in Thailand.………..…4

Figure 1.5: Breakdown of earthquake-related fatalities in the 20th century (Coburn 1993)…………………………………………………………….....5

Figure 1.6: World maps of earthen architecture (a) and seismic hazard risk areas(b) from www.terracruda.com (De Sensi 2003)…………………………………….…..…7

Figure 1.7: Earthquake damage to adobe houses Peru-Aug 16, 2007 (Jean Luis Arce /Reuters)………………………………………………………………………9

Figure 1.8: Collapsed Adobe structures by Bam Earthquake Jan 14, 2004 (World Housing Encyclopedia)………………………………………………….….9

Figure 1.9: Losses in the 2001 earthquake in Bhuj, India © Randolph Langenbach, 2007…………………………………………………………………….….11

Figure 1.10: The quake-safe circular Adobe houses in India (swissinfo.ch) ……….....14

Figure 2.1: Seismic Performance of an Unreinforced and a Strengthened Adobe Building in PUCP………………………………………………………….…...22

Figure 2.2: Lateral load deformation of static test of unreinforced and reinforced adobe wall's panels in PUCP (Blondet, Garcia & Loaiza 2003)…………………...…22

Figure 2.3: Adobe research at PUCP in 1979………………………………………..…24

Figure 2.4: Dynamic test of adobe model with cane reinforcement in PUCP………..…25

Figure 2.5: View of the tilt test facilities (Clough & Niwa 1979)……………………...26

Figure 2.6: Resultant Forces on Inclined Cylinder (Clough & Niwa 1979)……………27

Figure 2.7: The plan of the tilt table (Clough & Niwa 1979)…………………………..28

Figure 2.8: The elevations of the tilt table (Clough & Niwa 1979)…………………….28

Figure 2.9: Deflected shapes of the model tanks with different base conditions (Clough & Niwa 1979)……………………………………………………………..29

Figure 2.10: Basic concept of the static tilt testing (Pena & Lopez 2007)……………..30

Figure 2.11: Tilt table with 40 degrees for maximum angle (Pena & Lopez 2007)........31

Figure 2.12: The collapsed of the front wall of traditional adobe house when tilting reach 14 degree (Pena & Lopez 2007)……………….………………………31

Figure 2.13: Commencement of cracking of reinforcement house in the side wall at 30 degrees and cracking in the front and rear walls at 34 degrees (Pena & Lopez 2007)…………………………………………………………...…...….31

Figure 2.14: Specimen configuration and dimensions of u-shaped wall unit (Dowling 2006).………………………………………………………………….....33

Figure 2.15: Vertical corner cracking of unreinforced u-shaped adobe wall testing at UTS, Sydney (Dowling 2006)…………………………………...……...…34

Figure 2.16: Preparation of reinforced u-shaped adobe wall unit at UTS (Dowling 2006)……………………………………………………………………....34

Figure 2.17: Detail reinforcement of model adobe house at UTS (Dowling 2006)……………..…………………………………………………………...37

Figure 2.18: Damaged model adobe house retrofitted with string, bamboo, wire and timber ring beam at UTS (Dowling 2006)………………………. ……….…37

Figure 2.19: Model house 4 (a) and model house 7 (b) prior to testing (E. Leroy Tolles 2000)……………………………………………………………………....41

Figure 2.20: Model house 10 (a) and model house 11 (b) configuration (E. Leroy Tolles 2000)……………………………………………………………………....42

Figure 2.21: East wall of Model house 4 (a) after test level X and east wall of model house 7 (b) after test level X(2) (E. Leroy Tolles 2000)………………………43

Figure 2.22: West wall of Model house 6 (a) after test level VIII and west wall of model house 8 (b) after test level X (E. Leroy Tolles 2000)…………………………..43

Figure 2.23: Out-of-plane failure of Model house 10 (a) after test level VIII and north wall of model house 11 (b) after test level VIII (E. Leroy Tolles 2000)……….43

Figure 2.24: U-shaped adobe wall configuration (Tipler et al. 2010)………………....48

Figure 2.25: Tilt testing of the U-shaped adobe wall (Tipler et al. 2010)…….……..48

Figure 2.26: Tilt testing of the U-shaped adobe wall (Tipler et al. 2010)…………..…..49

Figure 2.27: Simulation of seismic shocks (Minke 2000)………………..…..…...…50

Figure 2.28: Earthquake resistant of earthen buildings in circular shape (left) and square shape (right)(Minke 2001)……………………………………………...51

Figure 2.29: Field strength test of soil (a) and adobe block (b) (IAEE 1986)……….....55

Figure 2.30: Ribbon test (Walker & Standards Australia 2002)…………………..…56

Figure 2.31: Sedimentation test (Walker & Standards Australia 2002)………………..56

Figure 2.32: Roll Test (CTAR/COPASA,2002 cited in Blondet, M. & Brzev 2003).…62

Figure 2.33: Configuration of opening guideline (RESESCO, 1997 from WHE)……..63

Figure 3.1: Types of Fault (NICEE 2002a)……………………………………….…67

Figure 3.2: Earthquake-induced inertia force of masonry houses (Source: IITK-Earthquake Tips)………………………………………………………..68

Figure 3.3: Definition of In-plane and Out-of-plane walls.(Source: City University, London)…………………………………………………………..…...69

Figure 3.4: In-plane crack pattern……………………………………………………70

Figure 3.5: Inclined cracking in the wall in Pinarkaya (Source: GFZ-German Research Centre for Geosciences)…………………………………………………...70

Figure 3.6: Out-of-plane flexural crack pattern……………………………………...71

Figure 3.7: Cracking and separation of walls in 1997 Jabalpur Earthquake (Source: World housing Encyclopedia, reports # 23)……………………………………71

Figure 3.8: In-plane failure pattern……………………………………………..….72

Figure 3.9: In-plane shear failure – San Giuliano (Marrow) (Source: Conservationtech.com)……………………………………………………72

Figure 3.10: Various types of failure in adobe structures under seismic excitations (GINELL & Tolles (n.d.))……………………………………………...73

Figure 3.11: Seismic zoning map of peak ground acceleration (PGA) of China (RP = 475 years; PE = 10%/50 years) (GB 18306 – 2001 – A1)…………………………..…82

Figure 3.12: Seismic effective coefficient curve of GB50011-2001 (IISEE 2002)……83

Figure 3.13: Seismic zoning map of India (IS 1893:2002) (Source: The Institute of Seismological Research (ISR))…………………………………………………84

Figure 3.14: Seismic hazard map of Africa (Source: GSHAP-Global Seismic Hazard Assessment Project)……………………………………………………….…86

Figure 4.1: Seismic Hazard map of Asia (Source: Global Seismic Hazard Assessment Program, Switzerland)………………………………………………......…..88

Figure 4.2: Seismic Hazard map of the Western Hemisphere (left) and Europe, Africa and the Middle East (right) (Source: Global Seismic Hazard Assessment Program, Switzerland)………………………………………………….……89

Figure 4.3: Seismic intensity zoning map in China……………………………………91

Figure 4.4: The map shows the location of Hongkeng village…………………………93

Figure 4.5: The view of Hongkeng village where the most earth buildings are located…………………………………………..……………………...95

Figure 4.6: The Zhencheng Buidling was built in 1912 is the biggest circular earthen form at Hongkeng village (Source: www.painaima.com)…..............................95

Figure 4.7: Ground floor plan of the circular earthen form……………………………96

Figure 4.8: The 2nd- 4th floor plans of the circular earthen form……………………...96

Figure 4.9: The roof plans of the circular earthen form………………………………..97

Figure 4.10: The cross section of the circular earthen form…………………………....97

Figure 4.11: The wooden frame supported the inner earthen wall (Prof. Sunny Cai, 2008)…………………………………………………………………….....98

Figure 4.12: Earthen wall with small openings (Prof. Sunny Cai, 2008)……………....98

Figure 4.13: Seismic zoning map of Gujarat (Source: The Institute of Seismological Research (ISR))…………………………………………………………..…100

Figure 4.14: Map of district of Kutch of Gujarat State (India)……………………..…101

Figure 4.15: Typical circular earthen hut of Kutch district (Amir January 2005)…….101

Figure 4.16: Plan of the circular typical building……………………………………..102

Figure 4.17: Section of the circular house……………………………………………103

Figure 4.18: Light roof structure of Bhunga house…………………………………...103

Figure 4.19: Bhunga houses in India…………………………………………………104

Figure 4.20: Seismic hazard map of Africa…………………………………………...107

Figure 4.21: A traditional Yomata with thatched roof………………………………...108

Figure 4.22: Typical Yomata buildings………………………………………………109

Figure 4.23: The typical plan of Yomata house………………………………….……109

Figure 4.24: The typical roof structure of Yamata house………….……………........110

Figure 4.25: The typical section of Yamata house…………………………………..…110

Figure 5.1: Horizontal design earthquake loads for single story building…………….118

Figure 5.2: Shear forces of circular adobe building…………………………………...118

Figure 5.3: Shear forces on circular adobe model at failure angle……………………119

Figure 5.5: Comparison between the seismic zoning maps produced by China Earthquake Administration (CEA) (right) and that produced by the Global Seismic Hazard Assessment Program (GSHAP) (left)………………………..124

Figure 5.6: Comparison of the peak ground acceleration for each case study's region rely on the global seismic hazard map……………………….……………..124

Figure 6.1: Mixing of mud for adobe bricks……………………………………..….…130

Figure 6.2: Making adobe bricks by mould………………………………….....……130

Figure 6.3: (a)Drying of adobe bricks; (b) Stacked adobe bricks……………………..130

Figure 6.4: Sedimentation test……………………………………………………….…131

Figure 6.5: The sequence of construction for adobe compression prisms…………….134

Figure 6.6: Compression machine at NU……………………………………………...135

Figure 6.7: Compression test with specimen C1…………………………………….…136

Figure 6.8: Types of failure pattern of compression prisms (specimen C3 & C5)…....137

Figure 7.1: Conceptual scheme of the static testing…………………………….……..141

Figure 7.2: Tilt table configuration and dimensions……………………………..…142

Figure 7.3: Construction of the tilt table……………………………………………143

Figure 7.4: Tilt testing of a square adobe model…………………………………...143

Figure 7.5: Square and circular specimens' configurations and dimensions………..145

Figure 7.6: Tilting the square specimen and first crack appearing at 20 degrees……..146

Figure 7.7: The failure modes of the square specimen when tilted further……........146

Figure 7.8: Tilting the circular specimen and first crack appearing at 29 degrees……147

Figure 7.9: The failure modes of the circular specimens when tilted further……….....147

Figure 7.10: The performance of functional areas in circular adobe houses…………151

Figure 7.11: Circular-adobe-wall construction……………………………………..152

Figure 8.1: Conceptual failure pattern of a circular adobe model in static testing ...…156

Figure 8.2: Typical specimen configuration…………………………………..…157

Figure 8.3: Construction of a circular adobe specimen……………………………….159

Figure 8.4: The wooden roof cover with bracing…………………………….….160

Figure 8.5: Roof and sand bags installation………………………………….…..161

Figure 8.6: Tilting the specimen until cracking and subsequent failure………………161

Figure 8.7: Reading the result of failure angle……………………………………..161

Figure 8.8: Specimen 1A prior to testing……………………………………..…162

Figure 8.9: Testing sequence of specimen 1A……………………………………...163

Figure 8.10: Specimen 2A prior to testing…………………………………….…164

Figure 8.11: Testing sequence of specimen 2A………………………………………165

Figure 8.12: Specimen 3A prior to testing……………………………………………166

Figure 8.13: Testing sequence of specimen 3A………………………………………167

Figure 8.14: Specimen 2B prior to testing……………………………………………168

Figure 8.15: Testing sequence of specimen 2B……………………………………..169

Figure 8.16: Specimen 3B prior to testing……………………………………………….170

Figure 8.17: Testing sequence of specimen 3B……………………………………….171

Figure 8.18: Specimen 2C prior to testing……………………………………………….172

Figure 8.19: Testing sequence of specimen 2C…………………………………..…173

Figure 8.20: Specimen 3C prior to testing……………………………………………….174

Figure 8.21: Testing sequence of specimen 3C……………………………………….175

Figure 8.22: Specimen 2D prior to testing……………………………………………....176

Figure 8.23: Testing sequence of specimen 2D……………………………………….177

Figure 8.24: Specimen 3D prior to testing……………………………………………....178

Figure 8.25: Testing sequence of specimen 3D…………………………………..…179

Figure 8.26: Relationship between roof load and the percentage of horizontal force compare to model own weight……………………………………...……181

Figure 8.27: Relationship between wall height-to-thickness ratio and the percentage of horizontal force compare to model own weight………………………………183

Figure 8.28: Relationship between wall height-to-diameter ratio and the percentage of horizontal force compare to model own weight……………………………....184

Figure 8.29: Typical failure mechanisms of circular adobe structures……………….…186

Figure 8.30: Failure analysis of the circular adobe specimen………………………...189

Figure 8.31: Variation of the first crack angle with the predicted angle…………….…..192

Figure 9.1: Adobe brick fabrication for the dynamic testing……………………….……198

Figure 9.2: Sedimentation test of soil composition for dynamic tests……….……..…199

Figure 9.3: Compressive strength test set up……………………………………….201

Figure 9.4: Typical failure patterns of the compression tests' prisms at UTS………..202

Figure 9.5: The typical load and time curve from the compression tests (specimen D1)…………………………………………………………………………..202

Figure 9.6: Test setup for the compressive strength test of adobe prisms…………….205

Figure 9.7: Chord modulus of elasticity (MSJC 2005; Rai 2005)…………………….205

Figure 9.8: The typical stress-strain curve of the adobe prisms (specimen D1)……...206

Figure 9.9: Specimen 1A and 3D (with openings): configuration and dimensions…...208

Figure 9.10: Three circular adobe models under construction at UTS………………..209

Figure 9.11: Completed three specimens and drying………………………….……209

Figure 9.12: The pushover test setup of the specimen 1A…………………………….210

Figure 9.13: The curve push-plate…………………………………………………….211

Figure9.14: Instrument locations for the pushover test……………….……………….211

Figure 9.15: Specimen 1A prior to the pushover testing………………………………212

Figure 9.16: Failure crack patterns at the southwest side wall………………………..213

Figure 9.17: Failure crack patterns at the southeast side wall…………………………213

Figure 9.18: Displacement graph of the pushover-testing result………………………214

Figure 9.19: Damages sequence of the specimen from the static pushover testing…...215

Figure 9.20: UTS shake table………………………………………………….………218

Figure 9.21: The acceleration time history of 1940 El-Centro earthquake with Peak Ground Acceleration of 0.35g registering 7.1 magnitude……………………..220

Figure 9.22: Simulation of the specimen 1A using FEM…………………….…………224

Figure 9.23: Test set up for the impact hammer testing……………………….……….226

Figure 9.24: Impact hammer hit……………………………………….………………….227

Figure 9.25: Modal Analysis of the circular model…………………….………………228

Figure 9.26: Instrumentation locations and direction of motion………………………230

Figure 9.27: LVDT displacement transducer and accelerometer at the north wall (specimen 1A and 3D)…………………………………………………...231

Figure 9.28: Instrumentation locations of the specimen 3D with openings…………..231

Figure 9.29: Specimen 1A and 3D: instrumented and ready for testing………………233

Figure 9.30: Specimen 1A after simulation S13…………………….…………………235

Figure 9.31: Specimen 1A after simulation S14 and its damage at the SE wall…...…235

Figure 9.32: Specimen 3D after simulation S13……………………………………….238

Figure 9.33: Specimen 3D: damage from simulation S14…………………………….238

Figure 9.34: Failure analysis of the specimen 3D with openings……….…………….239

Figure 10.1: Failure analysis of the existing circular adobe house…………….…....243

Figure A-1: The acceleration time history of 1940 El-Centro earthquake with Peak Ground Acceleration of 0.35g…………………………………………..….262

Figure A-2: The acceleration time history of 1994 Northridge earthquake with Peak Ground Acceleration of 0.88g…………………………………………...262

Figure A-3: The acceleration time history of 1995 Kobe earthquake with Peak Ground Acceleration of 0.84g……………………………………………………263

Figure A-4: The acceleration time history of 2001 El Salvador earthquake with Peak Ground Acceleration of 0.74g…………………………………………...263

Figure A-5: Failure analysis of specimen 3D with openings…………………………264

Figure A-6: Failure mode of the Bhunga house………………………………………266

LIST OF TABLES

Table 1.1: Major earthquakes in regions where adobe buildings are located………..…10

Table 2.1: U-shaped adobe wall units testing at UTS: specifications and results (Dowling 2006)…………………………………………………………...35

Table 2.1: (continued) U-shaped adobe wall units testing at UTS: specifications and results (Dowling 2006)……………………………………………………....36

Table 2.2: Simulated seismic motions for GSAP testing………………………………42

Table 2.3: Specifications and results of adobe model testing at GSAP (E. Leroy Tolles 2000)……………………………………………………………………44

Table 2.3 (continued): Specifications and results of adobe model testing at GSAP (E. Leroy Tolles 2000)…………………………………………………………..45

Table 2.4: Earthquake scale factors of the research at University of Auckland………..48

Table 2.5: Recommendation from IAEE guidelines (1986)…………………………....54

Table 2.6: Recommendations from the Australia Earth Building Handbook (Walker & Standards Australia 2002)……………………………………….………...58

Table 3.1: Selection of method of seismic analysis (Dowrick 1977)…………………..76

Table 3.2: Design characteristic period of ground motion……………….…………...83

Table 4.1: History of post-earthquakes in Malawi………….……………..……….106

Table 4.2: Comparison of the existing adobe houses' configuration…………….…112

Table 5.1: Values for specific shape factors……………………………………..116

Table 5.2: Similitude requirements (Moncarz & Krawinkler 1981)……………….…122

Table 5.3: Comparison parameters of the existing circular adobe buildings……...….126

Table 5.4: Comparison of the horizontal forces of three case studies' buildings……..126

Table 6.1: Specifications of compression prisms…………….…………………...132

Table 6.2: Results from compression tests of adobe prisms………………….…….137

Table 7.1: Comparison of specifications between square and circular models……….145

Table 7.2: Results of the square specimen subjected to static tilt testing……………..148

Table 7.3: Results of the circular specimen subjected to static tilt testing…………......148

Table 8.1: Small Scale Adobe Models: specifications……………………….………..155

Table 8.2: Results of the tilt-table testing of the nine circular adobe models……….....180

Table 8.3: The comparative results of varying roof loads…………………………..….181

Table 8.4: The comparative results of wall height-to-thicknesses ratio…….…….……182

Table 8.5: The comparative results of wall height-to-diameter ratio……………...…...184

Table 8.6: Results of the static tilt testing based on maximum normal stress……….…..187

Table 8.7: Predicted angles using the mean value of the maximum normal stress…...188

Table 8.8: Results of the prediction based on overturning about toe…………………191

Table 9.1: Adobe prisms specifications for compressive strength testing…………….…200

Table 9.2: The results of compressive strength of tested prisms…………………….…..201

Table 9.3: Comparisons of the compressive strength of adobe bricks………………..203

Table 9.4: UTS shake table specifications……………………………………………..…218

Table 9.5: Earthquake records for the shake testing…………………………………..219

Table 9.6: Comparison of the prototype and small-scale parameters…………………222

Table 9.7: Comparisons of the building period's formulas from a various earthquake codes…………………………………………………………………………..223

Table 9.8: Values of the fundamental natural of frequencies and scale-differences between prototypes and scale models……………………………………...…..225

Table 9.9: Specimens 1A and 3D: natural frequencies and damping ratios…………..228

Table 9.10: Testing sequence of the shake table testing for each simulation…………232

Table 9.11: Classification of damage to buildings (IAEE 1986)…………………….…..233

Table 9.12 Specimen 1A: testing sequence and summary of observations………….…..234

Table 9.13 Specimen 3D: testing sequence and summary of observations…………...237

Table 10.1: Summarization of the specification of Bhunga house ……………………243

Table 10.2: Ranges of PGA for Modified Mercalli Intensities (Wald et al. 1999)…...245

Table A-1: Results of the compression tests at UTS lab…………………………...…261

ABSTRACT

Unreinforced adobe or mud-brick structures have in the past suffered severe damage from seismic forces and have caused a vast number of deaths. However, a number of adobe buildings located in seismic regions have performed well under several seismic events. Most of these traditional buildings are symmetrical in shapes which have significant bearing on the performance of the buildings during strong earthquakes. Most existing circular adobe houses have performed well in withstanding earthquakes even though some did not have any additional ductile reinforcements.

This thesis presents a series of tilt table tests conducted to study the performance of unreinforced circular adobe buildings subjected to earthquake forces. Nine small-scale models (1:3 scale) of adobe structures were built with a variety of configurations and roof loads. The adobe house models were subjected to a constant acceleration when tilted on a tilt-up table. The lateral component of the models weight was used as a parameter to quantify the maximum seismic force for each model. The results then developed a methodology for designing circular adobe buildings to resist earthquakes in specific seismic zones and for specific site conditions.

A static pushover test and two shake table tests were also conducted in order to evaluate the reliability of the predictive model from the tilt table tests. The research outcomes give simple and effective solutions for construction of new adobe buildings located in seismic hazard areas. It can also be applied to evaluate existing circular adobe buildings for their seismic resistance which can assist in predicting the likely outcome in the event of an earthquake.

Keywords: Adobe construction, mud-brick, earthquake resistance, circular building, tilt table test, static pushover test, shake table test.

Chapter 1 Introduction

1.1 Background to adobe construction

Accommodation is the foundation of human need for shelter. People should have a place to live as a family and to protect themselves from the elements and natural disasters, especially earthquakes. In many developing countries, people do not have the resources to buy houses built by professionals but to build them by relying on their own labour, using local materials.

Earth is one of the most ancient construction materials used to construct houses. Earthen buildings are the most common type of human dwelling found throughout Africa, the Middle East and Latin America. In China, this type of structure has a long history since 214 A.D. (Heathcote 2002) and has remained to be the vernacular dwelling to this day (Doat et al. 1991). Earthen structures can be found in Sweden, Denmark, Germany, Middle East, North Africa and the eastern European countries, as well as in Australia and New Zealand. Adobe has also been used by indigenous people of the Americas, Mesoamerica, and the Andean region of South America for several thousand years (Wikimedia Foundation 2007).

Approximately one-third of the world's population lives in unbaked earthen buildings with about half of the population in developing countries, which accounts for the majority of the rural population and at least one-fourth of the urban and suburban population (Houben & Guillaud 1994; Wojciechowska 1967). For example, approximately 60 percent of houses in Peru are built with earth and approximately 73 percent of all buildings in India are made out of earth (67 million houses inhabited by 375 million people) (Blondet, M. & Brzev 2003). Earthen houses are still being used by millions of people in developing countries, especially in rural areas, because they are cheap, can be built with local materials and little technical expertise, and are comfortable as they have excellent thermal properties if designed properly (Heathcote 2005).

There are many reasons why earth is a desirable building material. Its use does not require high level of skills and more importantly, it provides good thermal and acoustic insulation with low energy consumption and can have aesthetics qualities (Christie 1990). It also has a number of disadvantages such as being weak under seismic forces and the actions of water (NICEE 2002c).

Adobe or Mud brick construction is one earthen technique that has been known for more than nine thousand years (Minke 2000). Adobe is defined as an air dried brick made from a puddle earth mix cast in a mould, which contains a mixture of clay, sand and silt or straw or a stabiliser (Earth Building Association of Australia(EBAA) 2005). It is also known as *earth brick* or *mud brick or sun-dried earth block*. The term "*Adobe*" derives from the Egyptian "*Thobe*" which means brick. It is made by using moulds without compaction and letting the bricks dry in the sun (Doat et al. 1991). Adobe are constructed with a wide variety of building shapes such as conical, cylindrical, trapezoidal, dome, vault or free-form and can include a combination of these shapes as well as being integrated with other earth building technologies, e.g., rammed earth. Each adobe house is a unique result of the materials at hand with the inspiration of the builder or owner (Christie 1989). The technology of earth construction was developed by trial and error for adaptation to the particular environment and context in which the building is located (McHenry & May 1984). This technology does not require special skills, therefore skilled technicians (engineers and architects) are generally not involved in this type of construction, hence the term "*non-engineered construction*".

Figure 1.1: Taos Pueblo's Mud Villages (built ca. 1000 A.D.)(McHenry 1985).

Adobe structures are easy to make using hand tools because the construction practice is simple. Furthermore, one person can build his own single house. The size and weight of brick is determined as suitable for handling by the mason (Keefe 2005). The size of adobe blocks varies from region to region depending on the local custom, which in part might be due to thermal and stability factors. The most common size, adopted as a UN standard, is about 150 mm wide by 300 mm long by 100 mm high (Keefe 2005). It can be made in square or rectangular shape in either wood or metal mould. Adobe buildings can be simple, single-story houses or large and elaborate monuments, like churches and cultural sites (Dowling 2006).

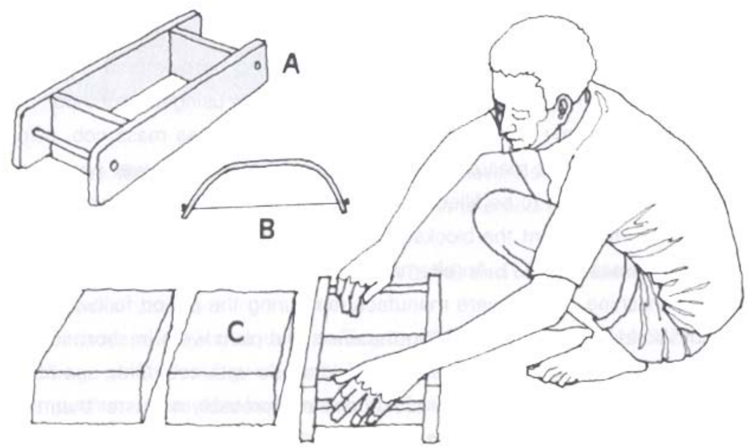

(A) mould box   (B) wire for trimming   (C) completed adobe brick

Figure 1.2: Traditional adobe brick fabrication (Keefe 2005).

Worldwide use of adobe is mainly in rural areas, where houses are typically single storey; about 3m in height, with wall thicknesses ranging from 0.25 m to 0.80 m. Architectural characteristics are similar in most countries (Figure 1.3 and Figure 1.4). Foundations are made of large stones joined with mud or mortar. Walls are made with unburned-bricks joined with mud mortar using same mixture of the bricks. Sometimes straw, wheat, or rice husk is added to the soil to make the blocks and mortar. Roofs are made from various structural types and materials (Blondet & M. (n.d.)). A roof can be made using similar materials as the brick and therefore called "*adobe roof*" or as a contemporary lightweight roof using thatch, sheet metal or a heavyweight tiled roof such as baked clay or concrete tiles, etc.

Figure 1.3: The researcher and local people helped to build the adobe house (below) in Thailand.

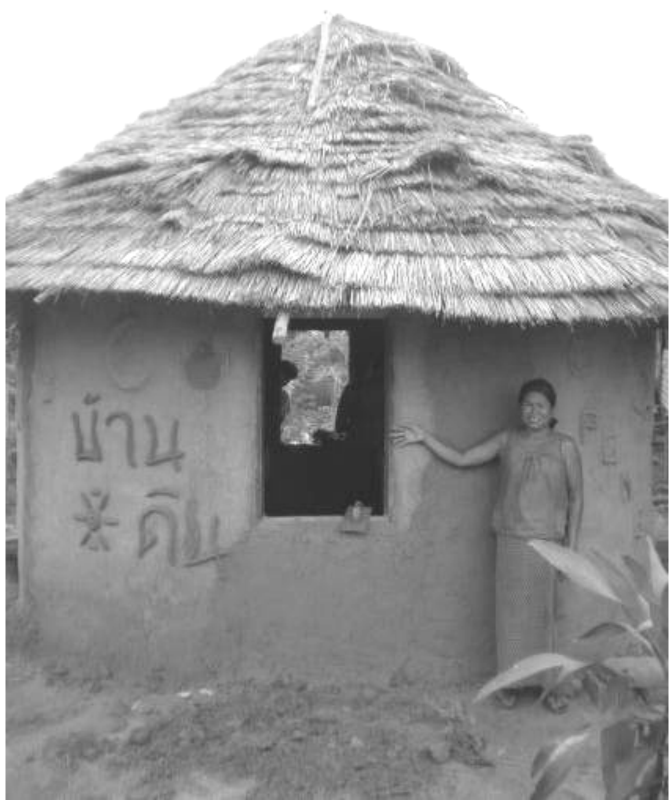

Figure 1.4: A typical circular adobe house for homeless people in Thailand.

1.2 Seismic vulnerability of adobe buildings

Earthquakes is caused by underground movement along a fault plane or by volcanic activity. There are many effects of earthquakes including landslides and avalanches, fires, soil liquefaction, tsunami, floods, ground shaking, and ground rupture (Wikimedia Foundation 2009a). These events cause damages to buildings, economic and social infrastructures, and even the loss of human life. Besides the loss of life, the worst effect from earthquakes is the deconstruction of building structures.

Unreinforced masonry buildings are the cause of the vast majority of deaths caused by the destructive force of earthquakes. On average, about 10,000 people die from earthquakes each year (Naeim 1989). Coburn and Spence (1992) state that the total number of people killed by 87 of the most significant earthquakes during the twentieth century is likely to be greater than 1.7 million people in 80 earthquake prone countries. These statistics highlight the extent of fatal events caused by the destructive force of earthquakes. Coburn (1993) reported that the principal cause of death by earthquakes is the collapse of buildings especially in weak masonry buildings. Figure 1.5 illustrates the comparison of earthquake fatalities since 1900-1999. It shows that the collapse of masonry buildings has the greatest proportion of death. These types of buildings are unreinforced earthen unfired or fired brick or concrete block masonry which are vulnerable to serve damage even at low seismicity. Adobe or unreinforced unfired brick is a weak low-strength masonry when compared to the others. It is one of the most commonly used building materials available to the poor as it is readily available and very cheap.

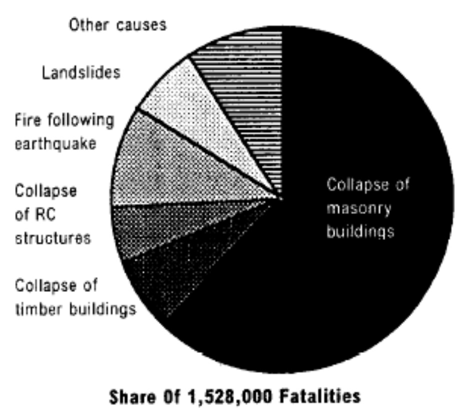

Figure 1.5: Breakdown of earthquake-related fatalities in the 20th century (Coburn 1993).

Adobe as unreinforced masonry does not perform well in major seismic activities and it is reported that it regularly contributed to the scale of disasters (Smith 1941). Adobe structure is naturally an inflexible material when subjected to shear or tension forces (Webster 1995). The low tensile strength of this material is the primary cause of building damage which results in both shear and flexural cracking. The continued cracking of a wall can result in a bearing wall failure. This type of wall typically falls outward allowing the heavy roof structures to collapse, killing occupants inside the building (Tolles & Krawinkler 1990a). The details on typical damage patterns of adobe structures are presented in Section 3.3 of Chapter 3.

1.2.1 Distribution of adobe buildings in seismic areas

Abode buildings are very brittle and weak when subjected to lateral forces, even in areas of moderate seismic activity (Christie 1989). Typically damage to adobe buildings occurs in areas such as Asia, the Middle East, Africa and Latin America where the poor local inhabitants have inadequate knowledge of seismic design and construction. Figure 1.6 shows world maps indicating the distribution of earthen architecture, and the regions of moderate and high seismic risk.

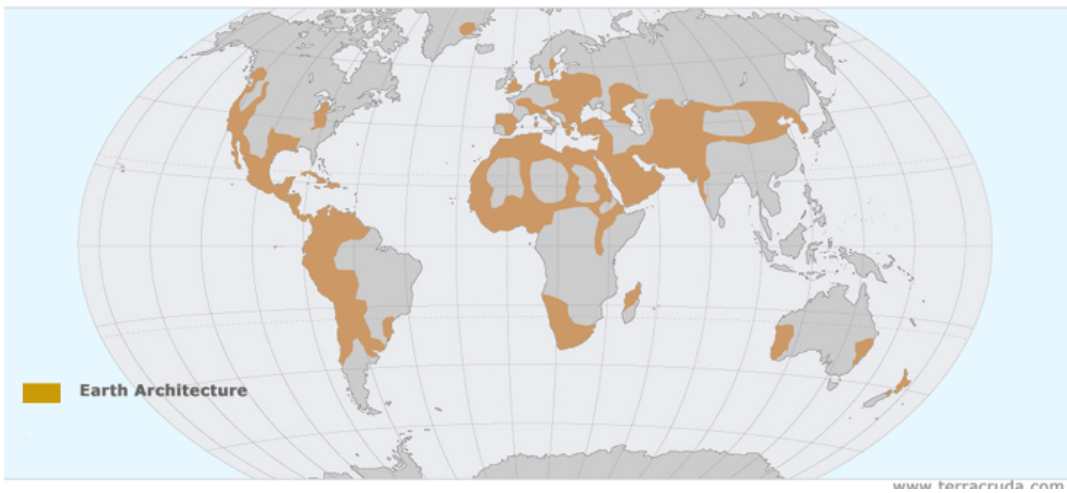

(a) – World Distribution of Earth Architecture

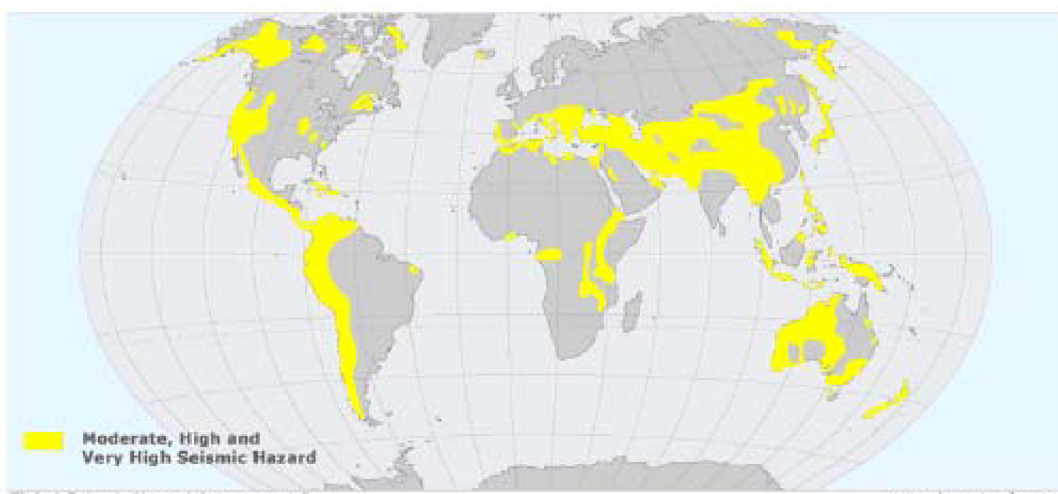

(b) – World Distribution of Moderate and High Seismic Risk

Figure 1.6: World maps of earthen architecture (a) and seismic hazard risk areas(b) from www.terracruda.com (De Sensi 2003).

1.2.2 Historical earthquake damage to conventional adobe buildings

Earthquakes are a natural disaster that have destroyed many seismically unreinforced masonry buildings, especially poorly made adobe houses in earthquake-prone cities in developing countries. In the 20th century four of every five deaths caused by earthquakes were in developing countries. Most vulnerable buildings to earthquake forces are constructed from unreinforced masonry structures, especially *adobe* or sun-baked clay bricks (Smith 2001). Unreinforced adobe buildings, especially those made from poor quality mud mortar had in the past suffered severe damage from seismic forces (Tomaževič 1999). Unreinforced adobe has low material ductility coupled with low strength which is commonly characterised by sudden and dramatic failure. A high likelihood of serious injuries and loss of life usually accompanies local or general collapse of such structures (E. Leroy Tolles 2000).

Adobe construction is still widely used in many seismic hazard regions as shown in figure 1-6. These regions are faced with the loss of lives and properties, especially in developing nations for example Iran, India, China, Peru, Turkey, El Salvador, etc. According to Keith Smith (2001), in Peru, about two-thirds of rural dwellers and over one-third of those in cities live in adobe structures. In May 1970, there was an earthquake in Peru in which over 60,000 adobe buildings collapsed killing about 50,000 people (Figure 1.7). These countries live under the constant threat to large losses of life and property in the event of an earthquake.

There is considerable evidence of the vulnerability of adobe houses in seismic areas. More than one million people living in adobe dwellings were left homeless in EL Salvador in early 2001. Two major earthquakes rocked the small Central American country of El Salvador. The earthquakes happened on the 13th of January and 13th of February, 2001 registering M_w 7.7 (depth 60 km) and M_w 6.6 (depth 10 km), respectively. The earthquakes claimed the life of about 1,100 people and, over 1,600,000 people were affected and more than 150,000 adobe buildings were totally destroyed in EL Salvador (Dowling 2004a). In the south of Peru an earthquake caused the deaths of 81 people, the destruction of almost 25,000 adobe houses, and damage to another 36,000 houses which was a magnitude 8.4 which affected the Peruvian regions of Arequipa, Moquegua and Tacna (Blondet, M. & Brzev 2003). In 2003 and 1997 two earthquakes in Iran resulted in over 40,000 deaths and 1,568 death, respectively. In the

1990 earthquake in Manjil registering M_w 7.4, over 40,000 people died and most of them were killed in adobe structures (Mehrain & Naeim 2004). Recently, thousands of deaths were attributable to vulnerable adobe structures in Bam, Iran (Eeri et al. 2004) (Figure 1.8). Table 1-1 shows a list of major earthquakes in areas where adobe constructions commonly exist which has resulted in widespread damage and loss of life.

Figure 1.7: Earthquake damage to adobe houses
Peru-Aug 16, 2007 (Jean Luis Arce /Reuters).

Figure 1.8: Collapsed Adobe structures by Bam Earthquake
Jan 14, 2004 (World Housing Encyclopedia).

Table 1.1: Major earthquakes in regions where adobe buildings are located

Year	Region	Fatalities	Magnitude
2008	Eastern Sichuan, China	87,587	7.9
2005	Pakistan	86,000	7.6
2003	Southeastern Iran(Bam)	31,000	6.6
2001	Gujarat, India	20,085	7.6
1999	Turkey	17,118	7.6
1990	Western Iran	40,000 – 50,000	7.4
1978	Iran	15,000	7.8
1976	Tangshan, China	255,000	7.5
1976	Guatemala	23,000	7.5
1974	China	20,000	6.8
1970	Tonghai, Yunnan Province, China	10,000	7.5
1968	Dasht-e Bayaz, Iran	7,000 – 12,000	7.5
1962	Bu'in Zahra, Qazvin, Iran	12,225	7.1
1949	Khait, Tajikistan (Tadzhikistan, USSR)	12,000	7.5
1948	Turkmeniya, USSR	110,000	7.3
1939	Erzincan, Turkey	32,700	7.8
1935	Baluchistan, India	30,000	7.6
1934	Bihar, India - Nepal	10,700	8.1
1927	Gansu, China	40,900	7.6
1920	Ningxia, China	200,000	7.8
1905	Kangra, India	19,000	7.5

Source : (USGS 2009a)

Figure 1.9: Losses in the 2001 earthquake in Bhuj, India

© Randolph Langenbach, 2007.

Comprehensive earthquake damage statistics from around the world serve as clear reminders that urgent action on this research is required. On the other hand, there are some historical earthen buildings which withstood several seismic attacks in recent centuries such as the Hakka houses in China, the Bhunga houses in India, the Yomata houses in Malawi, and rammed earth buildings in Argentina. These existing earthen houses used different construction techniques and they were all of a circular shape. It seems that the building proportions may also be a significant determining factor for the seismic resistance of a building.

1.2.3 Factors affecting building damage

According to Minke (2006), the quality of an earthquake-resistant structure depends on their structural resistance and ductility which can be expressed in the following formula:

Structural quality = Resistance x Ductility

This means that the higher ductility of a given structure, the lower the required resistance, while the lower its resistance, the higher its ductility must be (Grohmann, 1998 as cited in Minke 2001).

Because adobe structure is a brittle material and has a completely different behaviour to a ductile structure when subjected to earthquake forces (E. Leroy Tolles 2000). These horizontal forces may cause adobe walls to lose their tensile strength which leads to destabilisation of the structures such as overturning, out-of-plane failure, etc.(see more details in Section 3.3 of Chapter 3). In the meantime, most of the adobe research only focus on the ductility factor and on how to give higher flexibility within the structures by using various local material reinforcement. There are some existing circular earthen buildings that had performed very well in seismic events as presented in Chapter 4. These circular earthen houses had enough resistance to withstand earthquakes without the need for any ductile reinforcement. Therefore, the resistance factors of all these houses may come from the building proportions or their construction details.

1.3 Effect of shape on earthquake resistance

The behaviour of a building during an earthquake depends critically on its overall shape, as well as on how the earthquake forces are transmitted from the ground (Murty 2008). Ambrose and Vergun (1985) cited that the building configuration was an important factor in determining the fundamental period of the building which also affected the amount of seismic forces. Arbabian (2000) states that overall layout of the building is one of the most important elements in building design. Earthquake damage in buildings with significant irregularity are found to be five to ten times worse than buildings with essentially regular layout (Booth, Arup & Partners 1994). The shape determines the magnitude of the seismic forces which act on the building and their distribution: distribution is important in the vertical direction in section as well as the horizontal direction in plan. Therefore in the planning stage it is very important that architects and engineers work together to ensure that a good building configuration has been designed and unsuitable features are avoided (NICEE 2002b).

Although traditional rectangular adobe buildings are often damaged in even moderate earthquakes, some shapes of buildings show superior performance even when located in regions of high seismic risk such as India, etc. Their improved performance is due to the local people having learned the principles of seismic resistant construction by a " trial and error" process which has led to suitable construction methods for seismic areas.

Norton (1986) stated that the dimensional proportion of the building is one of the factors likely to lead to building damage during an earthquake. A building of wrong size or shape can be easily damaged by lateral and adulatory motions. Tomaževič (1999) also states that a regular layout in plan is preferred when building adobe buildings in seismic areas.

> "…*The behaviour of a building during earthquakes depends critically on its overall shape, size and geometry, in addition to how the earthquake forces are carried to the ground....The shape of the building has significant bearing on the performance of the building during strong earthquakes*..."(NICEE 2002b)

BRE 1972; Matsushita 1970 and National Research Council 1973 cited in Christie (1990) that "…*unsymmetrical buildings subjected to seismic loads experience increased shearing forces due to twisting and warping, and should be avoided. Because of this, floor plans and elevations should be as symmetrical as possible, ensuring that the centers of rigidity and mass are close together. It is recognized that builders should start-off with a good configuration and reasonable planning in order to avoid serious damage to their buildings".*

It has been noted in "*The construction manual for earthquake-resistant houses built of earth*" by Minke (2001) that the shape of the plan might have an influence on its stability in seismic areas and the more compact a plan, the better the stability. In 1985, a study on effect of shape of earthen buildings on earthquake forces was done at *University of Kassel* in Germany (more details in Section 2.8). The results of this research indicated that a square plan had better seismic performance than a rectangular one, and the circular plan had better seismic resistance than the square one (Minke 2001).

Mauro Sassu (n.d.) states that the circular floor plan of vernacular buildings offers the best resistance to seismic forces, however, a box shaped building creates troubles with out-of-plane forces and separation at the wall corners. Circular earthen houses had been built in many regions of high seismic risk such as India, Malawi and China. These houses have all shown good seismic performance. Sufficient seismic behaviour of these existing houses confirmed that it is possible to improve the seismic resistance by considering simple factors such as the architectural configuration.

Figure 1.10: The quake-safe circular Adobe houses in India.(swissinfo.ch).

At the present time, there is considerable amount of literature, documentation and manuals which contain construction details and recommendations for the configurations of unreinforced adobe houses in earthquake prone areas. However, these guidelines and manuals concentrate only on <u>square</u> and <u>rectangular</u> plan buildings which may not be suitable for circular adobe buildings' construction. A discussion of some of these - *The Australia earth building handbook* (Walker & Standards Australia 2002), *Earthquake – Resistant Construction of Adobe Buildings: A Tutorial (Blondet, M. & Brzev 2003), Construction manual for earthquake-resistant houses built of earth (Minke 2001)*, are presented and discussed in Chapter 2. Therefore, it should be valuable to explore the seismic resistance of circular adobe structures to gain useful information and recommendations on their suitable configurations which can be applied to circular structures located in seismic hazard areas. This research contributes to reducing the vulnerability of adobe houses to earthquake hazards.

In order to explore this issue, there are some existing procedures which can be performed by mathematics or by physical testing and can be utilized to investigate and extract informative data for circular adobe structures. However, these methods may be too complicated and expensive to apply to many example tests or may not be available in some cases. There may be another simple method of using a static tilt test to collect data and develop research methodologies (see Chapter 5). Consequently, this study focuses on exploring the seismic resistance of circular adobe buildings by developing a simple methodology to confirm their suitability.

1.4 Aim of thesis

The main aim of this thesis is:

<u>To develop a simple design methodology using static tilt table for the evaluation of existing and design of new circular adobe buildings under seismic hazard.</u>

1.5 Scope of the study

In order to achieve the research aim, the following relationships relating to circular adobe buildings will be investigated by both static and dynamic testing:

1. The relationship between the following parameters and failure load of buildings.
    - Diameter of building
    - Wall thickness
    - Wall height
    - Roof dead load
2. The relationship between failure loads and shear and bending strength of wall specimens.
3. The relationship between static and dynamic testing.

The research will also include:

1. A study of existing circular shaped adobe houses located in seismic areas to understand their seismic resistance.
2. Review of current literature on adobe model testing using both static and dynamic methods, and also the existing guidelines and manuals for adobe design and construction for earthquake resistance.

1.6 Limitations

This investigation will not investigate the influence of soil composition on earthquake resistance, but will adopt the shear and bending capacities of soils as tested. The bricks will be fabricated by trial and error to meet the drop test requirement as described in Standards New Zealand: Earth brick drop test (NSW 4298: 1998).

The thesis will focus on the behaviour and interaction of circular adobe walls under lateral forces. The effectiveness of roof diaphragms will not be examined.

1.7 Research methodology

The research methodology is based upon:

1. Studying all available literature on how seismic activity affects adobe house construction and subsequent wall failure.
2. Review of current literature covering previous adobe research, especially in relation to the simulation of seismic shocks in both static and dynamic tests and also an investigation of the existing guidelines and manuals for constructing adobe buildings for seismic resistance.
3. Studying existing circular shaped adobe houses located in seismic areas with a focus on the relationship between their configuration, functional usage and construction techniques and their seismic resistance performance (Fujian Province in China, Gujarat state in India and Malawi).
4. Studying static design methods used in different earthquake regions.
5. Testing of adobe prisms to find out key structural properties such as compressive strength.
6. Perform simple tilt table tests on square and circular adobe models to confirm the superior performance of circular adobe buildings.
7. Conduct extensive tilt table testing of circular adobe models to identify failure mode with the following varying parameters (see more details in Section 8.3):

    a. Roof loads (2, 3 and 4 kN/m^2).

   b. Wall thicknesses (33, 50 and 67 mm).
   c. Diameters (1.2, 1.4 and 1.0 m).
   d. Heights (0.8, 1.02 and 0.67 m).
8. Develop a theoretical model based on tilt table tests.
9. Conduct static pushover and shake table tests to confirm validity of circular adobe models with and without openings.
10. Illustrate by means of a case study how design method can be applied to real buildings.
11. Prepare a thesis and identify further research needs.

1.8 Thesis layout

The report is organized in the following manner:

Chapter 1 is the introductory chapter which provides the background, circumstance and justification of the research. It also provides the evidences of the impact on adobe structures when facing earthquake actions, this leads to the aim of the research program, scope of the study and the methodology of the research.

Chapter 2 is a literature review of research related to evaluating the seismic performance of adobe structures and circular shaped structures, undertaken using both static and dynamic methodologies. The chapter includes review of existing improved adobe design and construction guidelines and manuals.

Chapter 3 provides the information about the damage patterns and failure mechanisms of adobe houses subjected to earthquakes. It also provides the fundamentals of static and dynamic methods to evaluating and improving the seismic performance of adobe structures.

Chapter 4 contains details of three case studies of circular earthen structures which located in high seismic risk areas. This chapter describes each house and their effectiveness in relation to seismic resistance.

Chapter 5 explains the simple static design method for determining earthquake loads according to Australian Standard AS 1170.4. As part of this it includes the theory of reduced model testing and the calculation of static design loads of the existing houses.

Chapter 6 describes the fabrication of the adobe bricks used in the tilt-table-testing, and presents the material property testing of adobe prisms.

Chapter 7 presents the seismic capacity comparison between square and circular plan unreinforced adobe buildings using the tilt-table-testing. The chapter also provides a discussion on the social aspects of the circular adobe building.

Chapter 8 details the core component of this research: tilt table tests of 1:3 scale circular wall units. This chapter describes the failure mechanisms and cracking patterns of the circular adobe specimens. It also provides an analysis of the predictive formula which is used to predict the seismic resistance of adobe circular structures.

Chapter 9 presents the details of a static pushover test and two shake table tests of circular adobe models to evaluate the reliability of the tilt-table-testing's outcome. The chapter also contains the fabrication of the adobe bricks used in this research section, and a series of compressive tests of adobe prisms.

Chapter 10 contains the application of the proposed design methodology by applying it to a case study of the documented building.

Chapter 11 describes conclusions from the research and suggests areas for future study.

Chapter 2 Previous Research into the Seismic Resistance of Earth Buildings

2.1 Introduction

Previous research into the seismic resistance of adobe buildings has concentrated on the following four areas:

1. Research related to evaluating and improving the seismic performance of adobe structures or other circular (non adobe) features by using the static tilt-table testing methods.
    a. Static tilt-table tests of adobe models research conducted by the Pontificia University in Peru (PUCP).
    b. Static tilt tests of a tall cylindrical liquid storage tank investigated by the University of California.
    c. Adobe research conducted in El Salvador by the Salvadoran Foundation for Development and Minimum Housing (FUNDASAL).
    d. Static test of scaled geogrid-reinforced adobe models research conducted by the University of Auckland.
2. Research related to studying and improving the seismic performance of adobe buildings using shake testing machine.
    a. Dynamic testing of adobe structures conducted by the Pontificia University in Peru (PUCP).
    b. Seismic strengthening of adobe-mud brick houses research conducted by the University of Technology Sydney.
    c. Small-scale adobe research conducted by the Stanford University.
    d. Dynamic testing of scaled geogrid-reinforced adobe models research conducted by the University of Auckland.
3. The development of the test methods investigating the influence of the architectural aspects of the earthen buildings on their seismic performance.

a. A study into the seismic resistance of small-scale rammed earth walls conducted by the Kassel University.

4. Review of existing adobe construction guidelines and manuals which presented suitable configurations and or/and improving the earthquake performance of adobe structures.

    a. The guidelines for earthquake resistant non-engineered construction have been developed by IAEE (1986). It has been used in post-earthquake rehabilitation efforts after earthquakes and translated in several languages such as Hindi in India, Bangali in Bangladesh, and Spanish.

    b. The Australian Earth Building Handbook was published by Standards Australia in 2002. It provided guidance on material selection and recommendations for design, construction and maintenance details of earthen structures. It also described a number of standard test procedures for earthen buildings.

    c. The Earthquake Tips is developed by the Indian Institute of Technology at Kanpur. It contains basic concepts of earthquake-resistant construction with simple language and drawings. It consists of 24 tips ranging from a basic introduction to earthquakes to aspects of seismic design and detailing of reinforced concrete and masonry buildings. This publication is also placed at the web site of the National Information Centre of Earthquake Engineering (www.nicee.org) and Building Materials & Technology Promotion Council (www.bmtpc.org).

    d. The Earthquake –Resistant Construction of Adobe Buildings: A Tutorial has been developed by World Housing Encyclopedia (WHE). The tutorial gives simple instructions for improving the performance of new adobe buildings and for the earthquake protection of existing adobe buildings. It is clearly explained with simple drawings and diagrams.

This chapter describes these research projects and guidelines, and analyse the data given by other researchers in order to gain an insight into the various methods that are relevant to the test methods of the seismic performance of adobe structures.

2.2 Adobe research at the Catholic University of Peru

There are several research studies into the earthquake resistance of adobe buildings conducted by the Catholic University of Peru (PUCP) , Lima, Peru.

In 1972, the first simple experiment was undertaken at PUCP. A number of 1:1 scale model adobe houses were constructed using the same materials available in rural regions of Peru. These models incorporated various types of structural reinforcement (Blondet, Torrealva & Garcia 2002). The research carried out by them included material property testing, assembly testing, static tests on wall elements, static testing of wall panels, and model houses using a reaction frame and tilt table, and dynamic testing of wall panels and model houses.

Eight full-size model adobe houses were subjected to a constant acceleration (due to gravity) on a tilt table (Figure 2.1). The lateral component of the models' weight was used as a parameter to quantify the maximum seismic force for each model (Vargas & Ottazzi 1981). The research methodology for this static test is as follows:

- A 4x4 metre reinforced concrete tilting platform was built.
- Full-scales of eight adobe-housing models with several reinforcement procedures using wood, bamboo cane, and steel wire were built on top of the platform. The dimensions of models were (W) 4 m x (L) 4 m x (H) 2.4 m.
- Testing consisted of slowly tilting the platform and measuring the tilt angle at models' collapse.
- The inertial earthquake force with the inclined component of its own weight was used as a parameter to quantify the maximum seismic force for each module.

	
(a) Unreinforced specimen (tensile failure in corners)	(b) Test specimen strengthened with cane reinforcement

Figure 2.1: Seismic Performance of an Unreinforced and a Strengthened Adobe Building in PUCP (Blondet, Garcia & Loaiza 2003).

Various static tests of adobe walls have been undertaken, including the out-of-plane flexural tests and in-plane shear tests with different reinforcement. This initial work obtained the basic information about the elastic parameters of the adobe masonry (Vargas & Ottazzi 1981). The most efficient reinforcement procedure was using bamboo canes placement in the interior adobe walls. Figure 2.2 shows the effect of cane reinforcement on the strength of adobe wall panels.

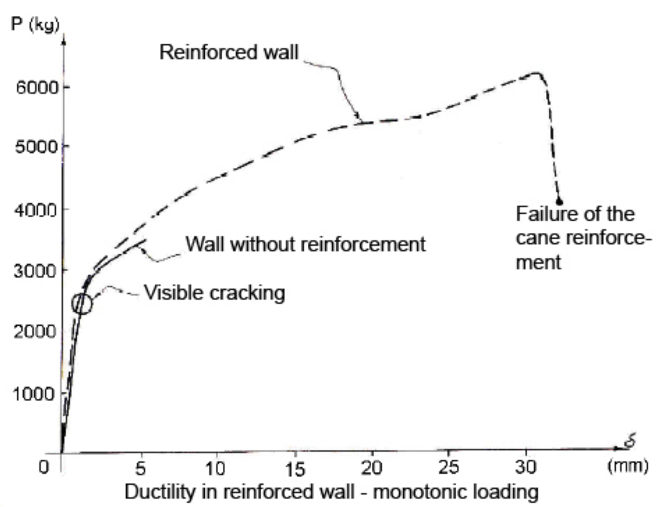

Figure 2.2: Lateral load deformation of static test of unreinforced and reinforced adobe wall's panels in PUCP (Blondet, Garcia & Loaiza 2003).

The main conclusion of the research from these static tests was that a vertical interior reinforcement made of cane, combined with the placement of horizontal crushed cane every fourth row of adobe blocks outstandingly increased the seismic strength of the house models. The cane reinforcement almost doubled the maximum horizontal load capacity and about six times the lateral deformation of the reinforced walls when compared to the unreinforced walls. With the improvement proposed, an increase of the static seismic coefficients from 0.23 g to 0.42 g was achieved. This research provided data on the wall's ability to retain its stability even after suffering a major crack when reinforced with mesh interior of cane (Blondet, Garcia & Loaiza 2003). This was also verified through the monotonic lateral load tests of full-scale walls (Blondet, Torrealva & Garcia 2002).

In 1984 the full-scale adobe models were subjected to the seismic simulation tests using the uni-directional shake table at PUCP (Torrealva, Vargas & Blondet (n.d.)). Full-scale models with and without internal cane reinforcement were tested by subjecting the models to seismic motions of increasing amplitude. The tests were performed using the time history from the May 31, 1970, Huaraz earthquake. The main result of these tests indicated that the internal cane reinforcement with a wooden ring beam prevented wall separation and the out-of-plane failure.

The next research project on adobe masonry was developed through the cooperation of the PUCP and the National Autonomous University of Mexico (UNAM) in 1979 (Figure 2-3). The 4 m x 4 m uni-axial shake table was used to simulate an earthquake for dynamic testing of wall panels and model houses. The time history of Huaraz earthquake of 1970 with intensity scaling of ground motion was used for most simulations to assess the behaviour of the structures under dynamic load conditions. There were also property tests of adobe specimens. Adobe specimens were tested in axial compression, indirect tension, diagonal compression and full-scale shear tests (Figure 2.3) (Blondet, Torrealva & Garcia 2002). The soils were gathered from six zones in Peru in order to correlate their physical, chemical, and mineralogical characteristics with the strength of adobe brick constructed with each soil. The field tests were conducted to determine the most adequate quality of soil for construction of adobe bricks and mortar to build the adobe walls. The test result showed that the clay was the most significant component of soil as it provided the dry strength of adobe bricks. However, a high content of clay also increased drying shrinkage, which caused cracking in the walls (Blondet, Torrealva & Garcia 2002). However, it has been noted by Dowling (2006) that varying the test sequence and parameters in PUCP research makes it complicated to make comprehensive comparisons between the test specimens while the dynamic similitude has not been considered.

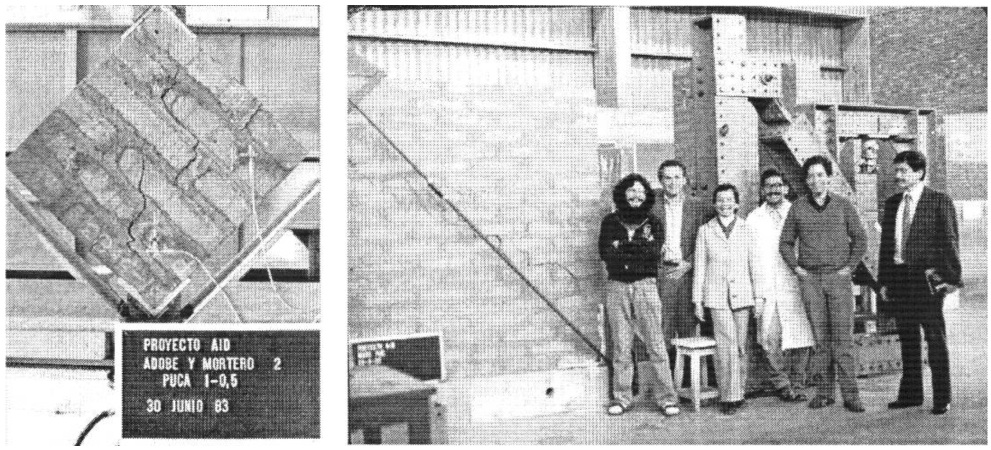

(a) Diagonal compression test (b) Full scale of adobe wall test

Figure 2.3: Adobe research at PUCP in 1979(Blondet, Garcia & Loaiza 2003).

In 1992, the adobe research team conducted a dynamic testing of full-scale adobe models in order to improve adobe constructions at PUCP (Figure 2.4). Eight full-size models of a one room single-storey building were tested on a shaking table with variations in construction technique. Each model was tested with shake increasing intensity to represent a series of shaking events. The main conclusions drawn were that improvement in the adobe construction technique by itself increased the wall resistance and stiffness. The results have shown that reinforcement which the horizontal and vertical cane reinforcement, integrated with a solid ring beam, can avoid the separation of walls in the corners and can also maintain the structure's integrity even after the walls are significantly damaged (Blondet, M. & Brzev 2003).

Figure 2.4: Dynamic test of adobe model with cane reinforcement in PUCP(Blondet, Garcia & Loaiza 2003).

The research team at PUCP devised an important experiment in both static and dynamic procedures to understand adobe structures performance when subjected to seismic forces. These experiments have qualitative outcomes. However, the research report has limited quantitative information on pre-test processes and post-test analysis which are valuable for further study in the research methodology and the behaviours of adobe structures. Furthermore, the main limitation of PUCP research of static testing was the lack of quantitative information of the specifications of all models and tilt test table set up. Such information would be a very useful resource for developing the static and dynamic testing methods for further seismic studies.

2.3 Static tilt tests of a tall cylindrical liquid storage tank

In 1979, the University of California conducted an earthquake simulation of shell cylindrical liquid storage tanks by using static tilt test, in which a liquid filled tank was subjected to a lateral force simply by tilting it from its normal vertical position with a crane (Clough & Niwa 1979). The main reasons for using a static tilt test in the research were that the dynamic response instrumentation can measure the tank behaviour during the tests and also the cost of time and money was quite low. The test parameters considered were the tilt angle, water level (0, 7, $10^1/_2$, 13 ft.) base stability condition (free or fixed base), roof condition (open or closed) and the tilt direction (North or East). The test measurements included membrane stresses and deformation behaviour of the tanks. A results of these tests have provided a great amount of detailed information and have contributed to a general understanding of the behaviour of circular thin shells and the tilt test.

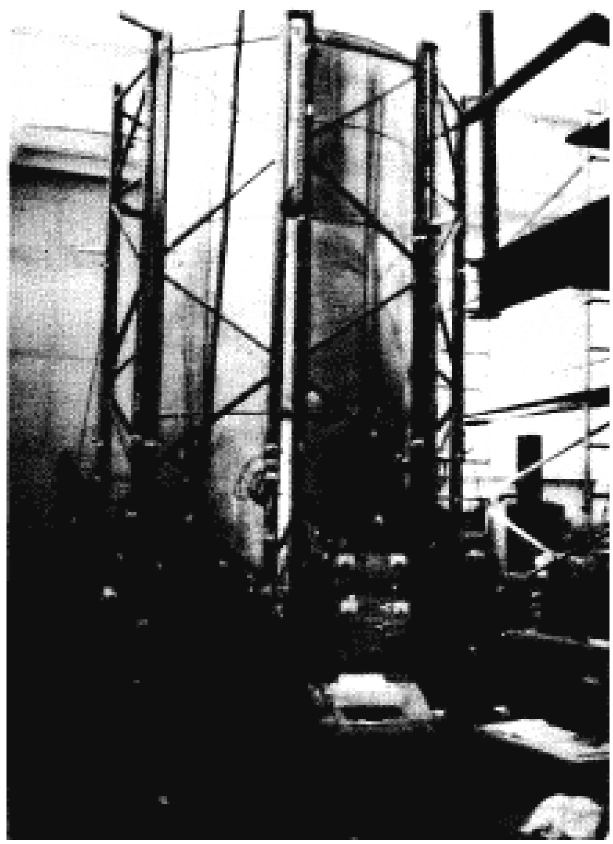

Figure 2.5: View of the tilt test facilities (Clough & Niwa 1979).

Test procedure

Tilt testing at the University of California was undertaken on a 10 ft. (3.05m.) square tilt platform (see Figure 2.7). A potentiometer and a simple tilt angle indicator were attached for visual monitoring of the tilt angle during the tests (see Figure 2.8). The model tanks were a one – third scale representation of a steel tank which one with free base condition and the other with fixed base condition. The tanks' specifications were 7 ¾ ft. (2.36m.) in diameter, 15 ft. (4.50m.) in height and welded from sheet aluminium in three courses-0.090 in. (2.3mm.), 0.090 in. (2.3mm.) and 0.063 in. (1.6mm.) in thickness. At the bottom of the free base case, the tank had been attached by a central bolt through the steel base to prevent sliding. For the fixed base case, the tank was attached by anchored clamps around the circumference to prevent uplift. The aluminium flat roofs were installed for a closed top situation braced by cross beams. Then the tank was filled with water to reach the required level and tilted up the platform for a tilt test by lifting one side with a laboratory crane. The observed results were compared with the predicted results from typical design calculations.

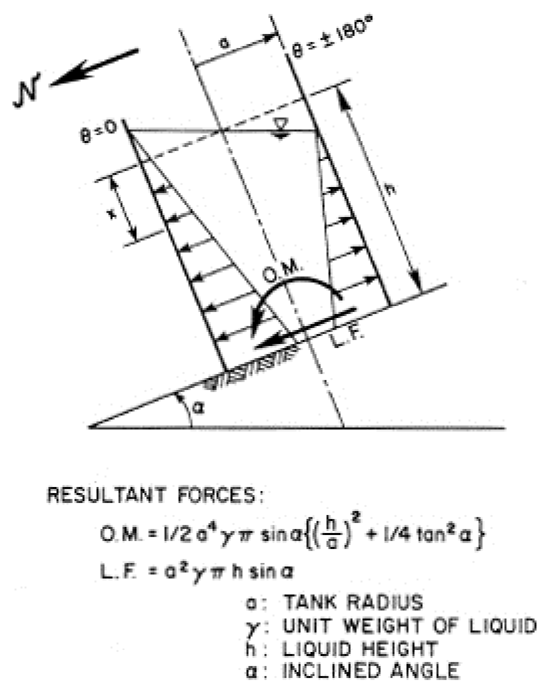

Figure 2.6: Resultant Forces on Inclined Cylinder (Clough & Niwa 1979).

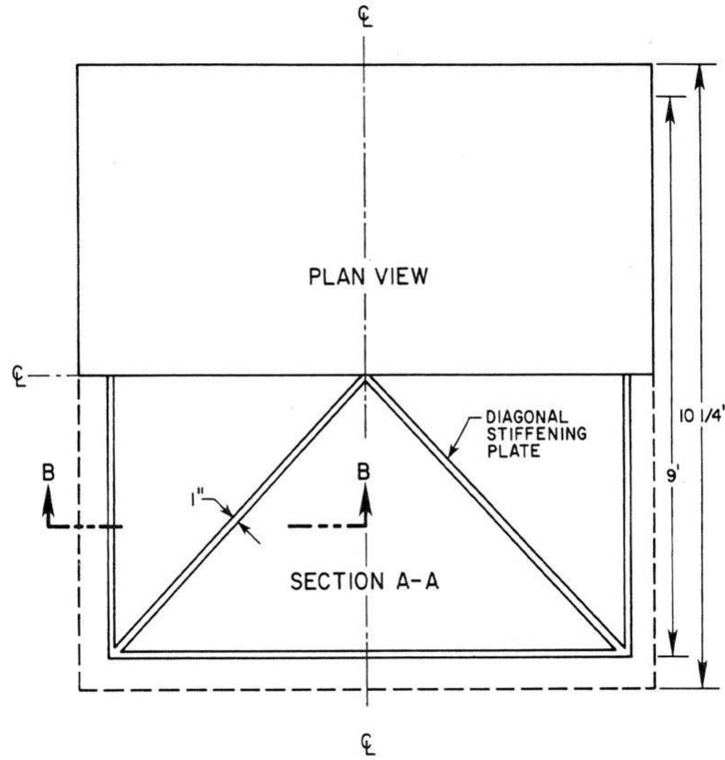

Figure 2.7: The plan of the tilt table (Clough & Niwa 1979).

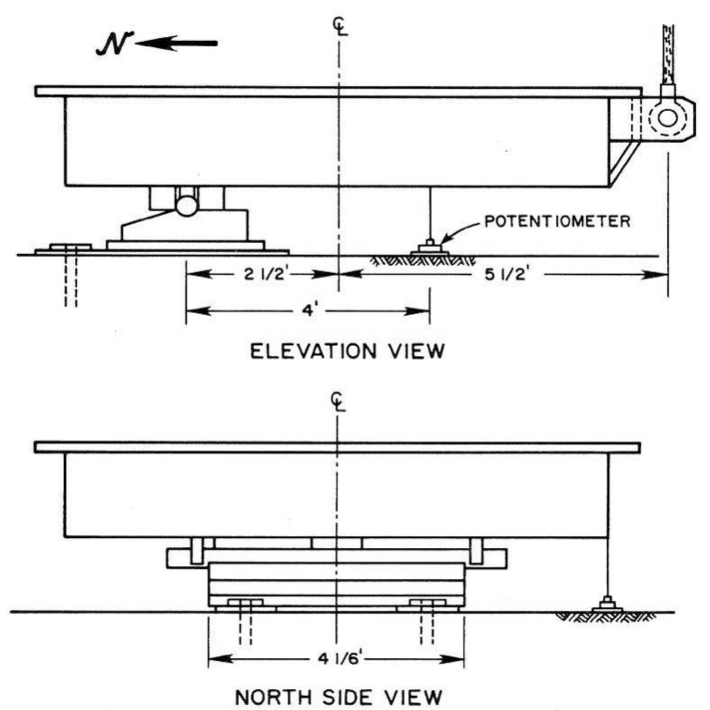

Figure 2.8: The elevations of the tilt table (Clough & Niwa 1979).

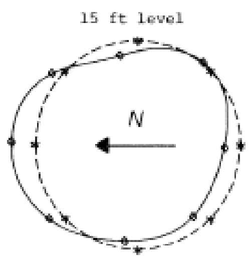

(a) Fixed base case.

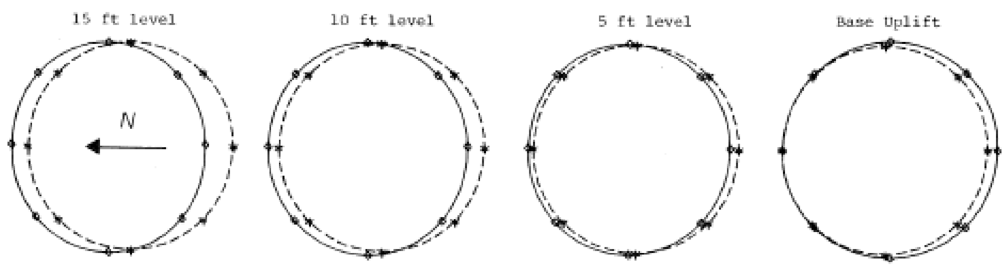

(b) Standard free base case.

Figure 2.9: Deflected shapes of the model tanks with different base conditions. (Clough & Niwa 1979).

The key outcomes of the research at the University of California included:

- *The relative amplitudes of the out-of-round response components of displacement and stress were not as great in these static tests as in the previously reported dynamic shaking table tests.*
- *Initial imperfections of the tank are seen to have an effect on both stress and displacement response, as evidenced by changes in response as the tilt direction was changed. However, it is significant that higher harmonics of displacement were not influenced greatly by changing the tilt direction.*

Clough and Niwa (1979) noted that the tilting test provided a great amount of detailed information on the behaviour of thin shell tanks at little cost of time and funds. It directly corresponds to the static design process that is used in the industry, leading to more effective correlation with the design assumptions.

The research showed a significant improvement in earthquake performance can be achieved by using the tilting tests. Such data from these tests were useful resources for the development of a simple static method in this research.

2.4 Tilt-table-testing of the FUNDASAL, El Salvador

In 2007 two model adobe houses were built on a tilt table to evaluated their seismic resistance by a static method (Pena & Lopez 2007). These tests were conducted by the Salvadoran Foundation for Development and Minimum Housing (FUNDASAL). The models were built entirely solid (no doors and windows), one was unreinforced adobe house and another with bamboo reinforcement and wall buttresses. Both houses used similar materials in both bricks and mortar with a 1:4 mixture (a clay by four of sand). Each model house was 6.00m long, 3.00m wide and 2.28m high. The dimensions of adobe bricks of each model were 0.40m x 0.25m x 0.10m. The objective of this research was to determine the different behaviours of walls when faced with the lateral forces. The application of lateral loads of models was a function of its own weight and the tilting angle (see Figure 2.10). The results of these experiments led to improvements in the technology of construction of traditional houses.

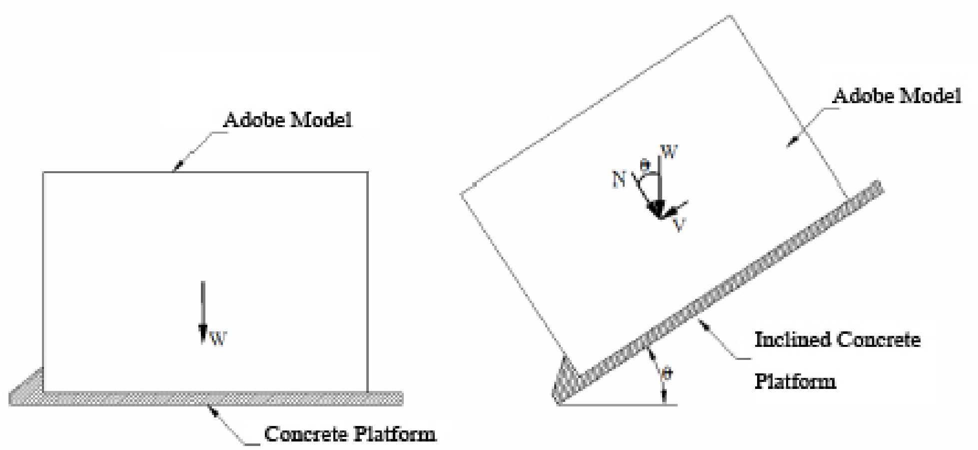

$$V = W \sin \theta$$

$$N = W \cos \theta$$

Figure 2.10: Basic concept of the static tilt testing (Pena & Lopez 2007).

The value of V represents the value of the lateral force which depends on the tilt angle and the weight of the model. The value of N represents the load of the model mass. Two models were tested, one of traditional construction (Figure 2.12), the other reinforced with buttresses and bamboo reinforcement (Figure 2.13).

Figure 2.11: Tilt table with 40 degrees as maximum angle(Pena & Lopez 2007).

Figure 2.12: The collapses of the front wall of traditional adobe house when tilting reach 14 degrees (Pena & Lopez 2007).

Figure 2.13: Commencement of cracking of reinforced house in the side wall at 30 degrees and cracking in the front and rear walls at 34 degrees (Pena & Lopez 2007).

For the research project, a specific value of 1600 kg/m^3 was applied for an average unit weight of adobe structure to calculate the total weight of the house models. Therefore, total weights of two experimental houses were:

- Traditional house: 17.66 ton
- Improved house: 26.16 ton

Based on these weights, the traditional house had V = 4.27 ton and N = 17.14 ton at the critical point and the improved house had V = 13.08 ton and N = 22.65 ton at the first cracking.

The results showed that a significant improvement in seismic capacity was achieved for the adobe house with buttresses and reinforcement elements installations. The traditional adobe house collapsed when the horizontal force equivalent was 24% of its own weight, whilst the reinforced house collapsed at around 50%. The traditional house failed by tension in the corners of the out of plane wall, whilst the strengthened house exhibited flexural cracking in the out of plane walls. The researchers concluded that the construction of adobe buttresses and strengthening with internal rods of bamboo, gave the earthen houses a greater capacity during seismic events.

The research in El Salvador presented successful outcomes by using the static tilt tests. The main limitation of the *FUNDASAL* research was the lack of quantitative data obtained for the material property tests for adobe bricks.

2.5 Seismic strengthening of adobe-mud brick houses

Dominic Dowling completed a PhD research project titled "*Seismic strengthening of adobe-mud brick houses*" at the University Technology of Sydney (UTS) in 2006 (Dowling 2006). The main purpose of his research was to develop a low cost and low-tech reinforcement system to improve the seismic resistance of new and existing adobe houses in developing regions. This research included extensive experimental testing such as compressive strength, shear strength and flexural bond strength of adobe prisms. The dynamic testing of eleven u-shaped wall units with scale 1:2 and a 3.5m x 1.8m x 1.2m retrofit-strengthened model house was undertaken on a uni-axial shake table with an input time history taken from the EL Salvador earthquake of January 13, 2001.

U-shaped wall units testing were subjected to dynamic loading, and the focus was on observing behaviour and recording responses of each individual specimen against out-of-plane seismic forces. The configuration and dimensions of test structures are shown in Figure 2.14. Test results showed significant improvement in both newly-built and existing adobe houses for earthquake resistance by using external vertical and/or horizontal bamboo reinforcement, external horizontal wire and/or internal horizontal chicken wire mesh reinforcement and ring beam. Table 2-1 shows the specimens and reported results for each wall panels tested at UTS.

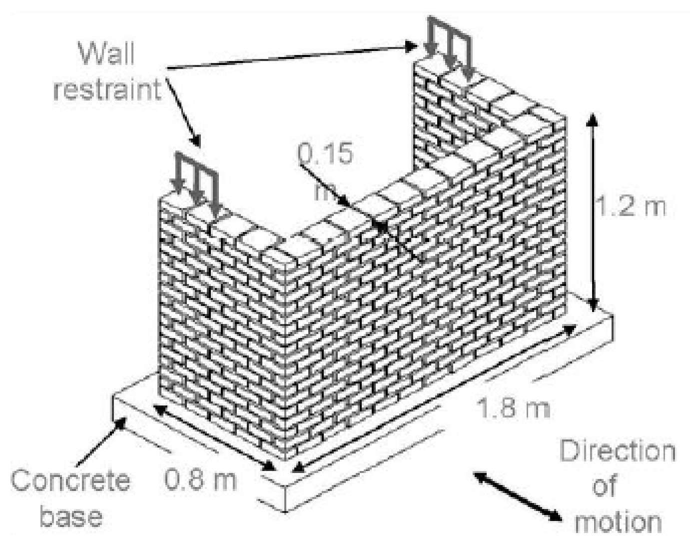

Figure 2.14: Specimen configuration and dimensions of u-shaped wall unit (Dowling 2006).

Figure 2.15: Vertical corner cracking of unreinforced u-shaped adobe wall testing at UTS, Sydney (Dowling 2006).

Figure 2.16 Preparation of reinforced u-shaped adobe wall unit at UTS (Dowling 2006).

Table 2.1: U-shaped adobe wall units testing at UTS: specifications and results (Dowling 2006)

Specimen	Horizontal Reinforcement	Vertical Reinforcement	Ring Beam	Notes	Intensity* (Displacement)	Damage Grades
3A	(None)	(None)	(None)	Traditional, Unreinforced	75%	4
3B	(None)	Corner pilasters	(None)		100%	4
3C	Chicken wire mesh (internal)	(None)	(None)		100%	4
3D	Chicken wire mesh (external wrapping)	Chicken wire mesh (external wrapping)	Timber		100%	3
3E	Chicken wire mesh (internal)	Bamboo (external)*	Timber		125%	3-4
3G	Chicken wire mesh (internal)	Bamboo (external)*	Timber		100%(x2)	3
3I	Chicken wire mesh (internal) Bamboo (external)	Bamboo (external)*	Timber		100%(x2)	3

Table 2.1: (continued) U-shaped adobe wall units testing at UTS: specifications and results (Dowling 2006)

Specimen	Horizontal Reinforcement	Vertical Reinforcement	Ring Beam	Notes	Intensity* (Displacement)	Damage Grades
3H	Chicken wire mesh (internal)	Bamboo (external)	Timber**	Thin wall (100mm)	100%(x2)	3
3F	Fencing wire (external)	Bamboo (external)	Timber**	Retrofit	100%(x2)	3
3J	Chicken wire mesh (internal) Fencing wire (external)	Bamboo (external)	Timber**	Optimised	100%(x2)	2-3
3K	Chicken wire mesh (internal)	Timber poles (internal)*	Timber**		100%(x2)	3-4

Notes:

Damage grades: 0 – no damage; 1 – slight damage (fine cracks); 2 – moderate damage (small cracks, spalling); 3 – heavy damage (large + deep cracks); 4 – destruction (gaps in walls, separation of components); 5 – total collapse.

* Vertical reinforcement connected to concrete foundation of test frame

** Timber ring beam connected to wall restraint.

Model house (1:2 scale) was tested, which was retrofitted with external vertical bamboo, external horizontal wire and a timber ring beam. The results showed that an improvement in seismic capacity was achieved in the reinforced model. Though the unreinforced u-shaped wall unit totally failed during 75% intensity simulation, reinforced model house got only first minor cracking at 75% intensity. Model house had progressive damage from 100% intensity simulation, but collapse was prevented even with repeated 100% intensity simulation test.

Figure 2.17: Detail of reinforcement of model adobe house at UTS (Dowling 2006).

Figure 2.18: Damaged model adobe house retrofitted with string, bamboo, wire and timber ring beam at UTS (Dowling 2006).

Experimental Modal Testing and Analysis (EMTA) were undertaken both prior to, and during dynamic testing to determine the mode shapes and natural frequencies of each test specimen, in order to subject each specimen to scaled earthquakes and allow reliable comparisons between the structural response and overall performance. The test results showed the importance of time scaling the input motion to induce damaging near-resonance conditions which were achieved when the natural frequency of each specimen is matched with the dominant frequency range of the input spectrum.

The key outcomes of the research at UTS related to this research include (Dowling 2006):

- *Significant improvement in shear and flexural bond strength of adobe masonry can be achieved by: (i) wetting the surface of each brick prior to laying; (ii) using a thin mortar joint; and/or (iii) applying a modest compressive load during drying.*
- *Test results confirm the importance of appropriate time scaling of input shake table motion to induce damaging conditions in a structure. Even an unreinforced adobe wall unit was undamaged during a 200% intensity simulation using the raw, unscaled (with respect to time) input motion.*
- *U-shaped adobe wall panels (with appropriate 'wing' wall restraint) exhibit classic failure patterns when subjected to shake table testing using a suitable input time history. Damages were consistent with damaged patterns observed in real structures subjected to real earthquakes.*
- *The main crack patterns in damaged adobe structures (vertical corner cracking, vertical mid-span cracking, and horizontal and diagonal cracking) are due to combinations of overturning, vertical flexure and horizontal flexure. The most effective improvement systems reduce movement in the wall, which minimise these stresses, and thus delay the onset of initial cracking and the loss of strength of the structure.*

The UTS research has made a major contribution to the study of the seismic capacity of adobe structures. The results showed a significant improvement of adobe model structures by using low-cost and low-tech reinforcement systems.

In addition, the research has added a significant amount of detailed quantitative data, i.e., static testing data of adobe prisms to determine characteristic material properties, shake table testing, review and comparative analysis of the dynamic test results. In particular, the research had made a distinguished research on specimen-specific time scaling of input shake table motion and Experimental Modal Testing and Analysis (EMTA) which were useful tools to reflect the physical response and changes in dynamic characteristics of adobe buildings.

2.6 Getty Seismic Adobe Project, U.S.A.

In 1990, the adobe research project entitled 'Seismic Stabilization of Historic Adobe Structures' was initiated by the Getty Conservation Institute for the purpose of developing technical procedures for improving the earthquake performance of historic adobe buildings with minimal impact on component of their structures (Leroy Tolles et al 2000). The goals of the research were (1) seismic retrofitting to provide sufficient life-safety defense and (2) preserving the architectural aspect of the adobe house. The main component of this research was the shaking-table tests on both 9 small-scale (1:5) models and 2 large-scale models (Leroy Tolles et al 2000).

The purpose on small-scale tests of 1:5 scale was to study the performance of adobe walls to include the effect of wall thickness. Six of the models were built with rectangular plan without roof and floor system. The others were constructed to simulate the global behaviour of complete building system. The design of the adobe models was based on the typical *tapanco*-style houses of California. The other two large-scale models were constructed on 1:2 scale having both roof and floor systems. The objective of these large model's tests was to establish if gravity loads had influence over the nature of the in-plane and out-of-plane wall motions and to evaluate the effectiveness of the retrofits in minimizing damage (Leroy Tolles et al 2000).

Material property tests were also done to determine the flexure, compressive strength and diagonal tension. The results showed that the compressive strength of adobe prisms was less when compared to the prototype; however the flexural and diagonal tension properties had nearly the same values as the prototype.

Model construction procedure

The models were constructed on concrete bases with a running bond. These models were different in the thickness of walls, but had the same length of bricks. The mortar was made of the same mixture as the adobe bricks. After drying for a minimum of 30 days, each model was transported to the shaking table before the testing began. Then, steel dowels were installed into the concrete base in order to limit slipping of the model along the base. Wood lintels were also used over all the model's openings.

Test Procedure

The 1:5 scale models were tested on the uni-axial shaking table at the John A. Blume Earthquake Engineering Centre at Stanford University. The earthquake motion was using the N21E of the 1952 Taft earthquake in Kern County, California. Each model was subjected to ten intensity simulations and the subsequent displacement motion was increased by 20%-30% for each test. The maximum intensity simulation was about 6-7 times larger than the original earthquake. The input time history was based on the N21E component of the 1952 Taft Earthquake in California. Each model house was subjected to ten series of displacement earthquake motions which increased by 20-30% for each series (see Table 2-2). The specifications and results of 1:5 scale models testing are presented in Table 2-3 (Leroy Tolles et al 2000).

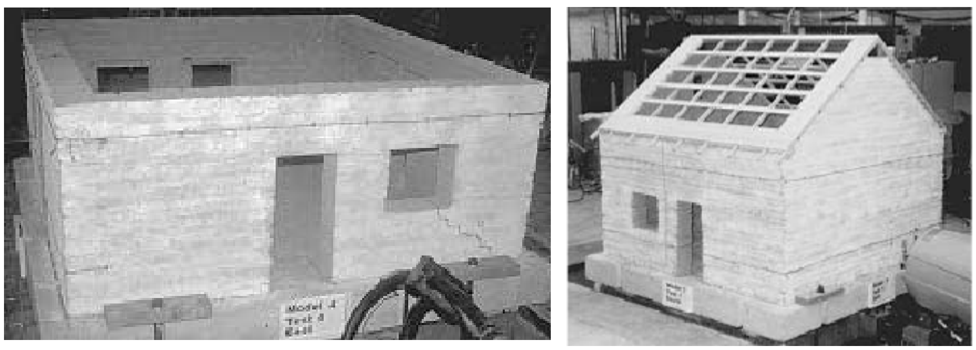

(a) (b)

Figure 2.19: Model house 4 (a) and model house 7 (b) prior to testing (Leroy Tolles et al 2000).

The test on 1:2 scale model houses, model 10 and model 11, were performed on a shaking table at the institute of Earthquake Engineering and engineering Seismology (IZIIS) of University "SS. Cyril and Methodius" in Skopje, Republic of Macedonia. The methodology of the large-scale testing was mostly the same as 1:5 scale model testing with the addition of measurement instruments of the acceleration and displacement of the structure and stresses in the reinforced straps installed. The quantitative data of testing was reported for each model. The specifications and results of 1:2 scale models testing are presented in Table 2-3.

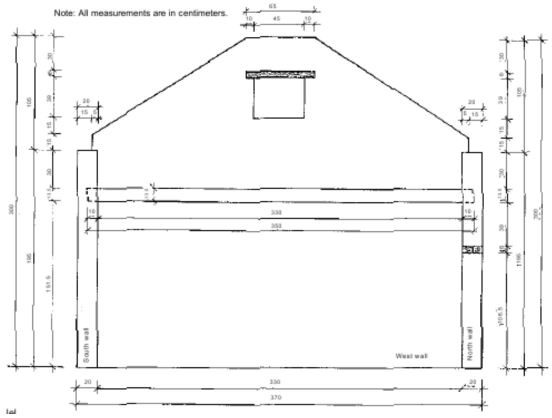

(b)

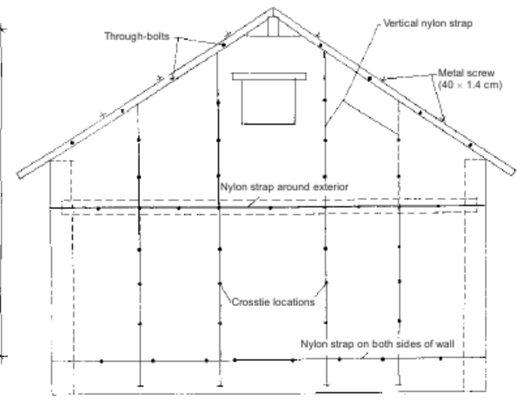

(b)

Figure 2.20: Model house 10 (a) and model house 11 (b) configuration (Leroy Tolles et al 2000).

Table 2.2: Simulated seismic motions for GSAP testing

Test Level	**Maximum EPGA*** (g)	**Maximum displacement** (cm)		
		Full scale	**1:5 scale**	**1:2 scale**
I	0.12	2.54	0.51	1.27
II	0.18	5.08	1.02	2.54
III	0.23	7.62	1.52	3.81
IV	0.28	10.16	2.03	5.08
V	0.32	12.70	2.54	6.35
VI	0.40	15.88	3.18	7.94
VII	0.44	19.05	3.81	9.53
VIII	0.48	25.40	5.08	Not available**
IX	0.54	31.75	6.35	Not available**
X	0.58	38.10	7.62	Not available**

Note: EPGA* = Estimated peak ground acceleration (Leroy Tolles et al 2000).
Not available**- Due to the capacity of IZIIS shaking table

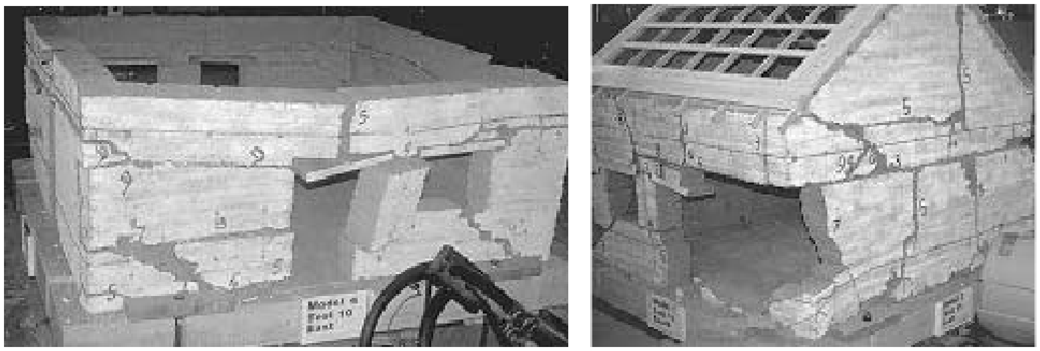

(a) (b)

Figure 2.21: East wall of Model house 4 (a) after test level X and east wall of model house 7 (b) after test level X(2) (Leroy Tolles et al 2000).

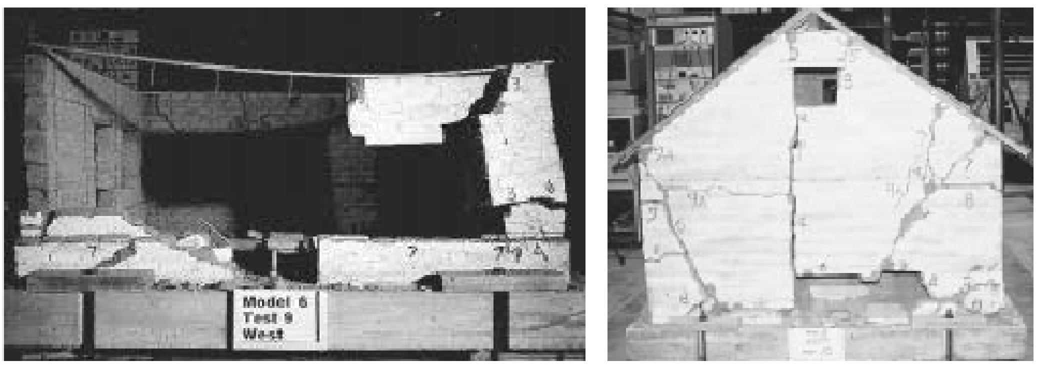

(a) (b)

Figure 2.22: West wall of Model house 6 (a) after test level VIII and west wall of model house 8 (b) after test level X (Leroy Tolles et al 2000).

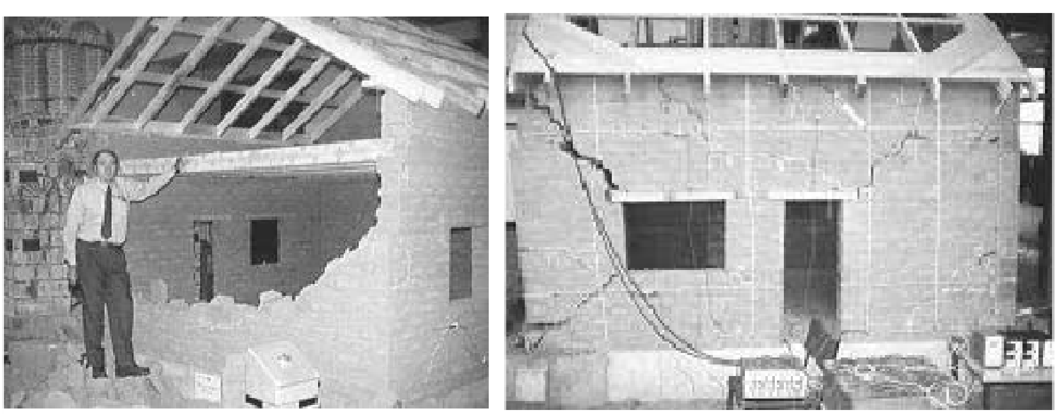

(a) (b)

Figure 2.23: Out-of-plane failure of Model house 10 (a) after test level VIII and north wall of model house 11 (b) after test level VIII (Leroy Tolles et al 2000).

Table 2.3: Specifications and results of adobe model testing at GSAP *(Leroy Tolles et al 2000)*

Model	Scale	h/t ratio	Type and location of retrofit	Walls	Results
1	1:5	7.5	Upper horizontal strap Upper and lower horizontal straps	NE SW	Out-of-plane collapse that may have been more closely spaced crossties
2	1:5	7.5	Bond beam and centre cores Bond beam plus vertical and horizontal straps	NE SW	Near to collapse of east wall at the final test
3	1:5	7.5	Bond beam, centre cores, and saw cuts; lower horizontal strap only in west pier of north wall Bond beam, centre cores, and internal lower horizontal strap	NE SW	Stable behaviour in all tests
4	1:5	5	Upper strap Upper and lower straps	NE SW	Near to collapse of east wall at the final test; substantial permanent displacements throughout the model
5	1:5	11	Unreinforced (traditional)	NE+SW	Collapse of 75% of the walls; complete collapse of out of plane walls in test level VII
6	1.5	11	Bond beam, lower horizontal and vertical straps Bond beam, lower horizontal strap and local ties	NE SW	Partial collapse of south and each wall in test level IX and X respectively

Table 2.3 (continued): Specifications and results of adobe model testing at GSAP *(Leroy Tolles et al 2000)*

Model	Scale	h/t ratio	Type and location of retrofit	Walls	Results
7	1:5	5	Partial diaphragms on attic-floor and roof framing, upper and lower horizontal and vertical straps	NW	Crack pattern nearing full development in testing level VI, offsets in the in-plane and out-of-plane walls in testing level VIII, Collapse of lower section of south wall in testing level X
			Partial diaphragms on attic-floor and roof framing, upper and lower horizontal	SE	
8	1:5	7.5	Partial diaphragms on attic-floor and roof framing, upper and lower horizontal and vertical straps	NE	Model performing well with offsets in each wall up to 1 in. in testing level X
			Partial diaphragms on attic-floor and roof framing, upper and lower horizontal and vertical straps; no lower strap on west wall	SW	
9	1:5	7.5	Unreinforced (traditional)	All	Collapsed during test level VI
10	1:2	7.5	Unreinforced (traditional)	All	Out-of-plane of east wall collapsed during test level VIII
11	1:2	7.5	Partial diaphragms on attic-floor and roof framing, upper and lower horizontal and vertical straps	NE	Stable in all test level
			Partial diaphragms on attic-floor and roof framing, upper and lower horizontal and vertical straps; no lower strap on west wall	SW	

The GSAP research has made a major contribution to small-scale models testing by using the dynamic method. The outcomes of this research are as follows (Leroy Tolles et al 2000):

- *The performance between the small and large-scale buildings was very similar in several way. For the most part, the behaviour of the small-scale models was an acceptable predictor of large scale model performance.*
- *The retrofit systems involved horizontal and vertical straps, ties, vertical centre-core rods, and improvements in the anchoring of the roof to the walls, proved to be successful in reducing the model walls to collapse.*
- *The retrofit tool using vertical straps was most effective in providing life safety of the out-of-plane wall collapse. They also had little effect on the initiation and early development of crack damage.*
- *A set of retrofit tools can be applied on historic adobe buildings.*
- *Vertical centre-core rods were found to be mostly effective in delaying and limiting the damage to in-plane and out-of-plane walls.*

This research had provided significant information for the reinforced systems of the adobe structures. However, there is some limitation of GSAP research such as the lack of quantitative information and specification for all the models.

2.7 Shake table testing of scaled geogrid-reinforced adobe models

In recent years, the static and dynamic adobe research has been undertaken at the *University of Auckland* (Tipler et al. 2010). The research has included:

- Shake table testing of two U-shaped adobe model (1:3 scale) with different amount of reinforcement systems in order to comply with the requirements of *NZS 4299:1988 Earth Buildings Not Requiring Specific Design* which focus on geogrid reinforcement system.
- A series of static tilt testing of two U-shaped adobe walls using the same reinforcement configurations as the dynamic testing.

Dynamic testing was undertaken at the *Department of Civil Engineering*, *University of Auckland*. Two U-shaped adobe test walls (1:3 scale) were built with different amount of reinforcement configurations. The tests were to confirm that the use of geogrid as recommended by NZS4299 provided suitable seismic reinforcement for adobe structures. The first model was an ordinary reinforcement which had 4mm vertical steel bars at the intersection of orthogonal walls and a bond beam system. The other was a full reinforcement system with additional vertical steel reinforcement and polysynthetic geogrid in every third course of mortar layer. The two wing walls were anchored by steel rods and a wooden beam. The configuration of adobe walls are shown in Figure 2.24. Each wall was initially subjected to a number of sine sweep waves between 1 and 50 Hz in order to gauge the pre-cracked dynamic behaviour of the walls. The PGA of the three selected earthquake records were scaled based on the worst-case situation (see Table 2-4).

Table 2.4: Earthquake scale factors for the research at University of Auckland

Earthquake record	k(SLS)	k(ULS)
El Centro, California, 1940	0.1242	0.3549
Northridge, California, 1994	0.4648	1.3279
Llolleo, Chile, 1985	0.5675	1.6213

Note: SLS- run at the serviceability limit state.
ULS- run at the ultimate limit state.

Static test was undertaken in order to gain comparative displacement information from both models under an identified acceleration. The models were tilted by the gantry crane to lift one side of the model base in order to gain the gravitational accelerations. The results were recorded by displacement gauges and calculated using gravitational accelerations from the tilt angle. Figure 2-25 shows the tilt test process.

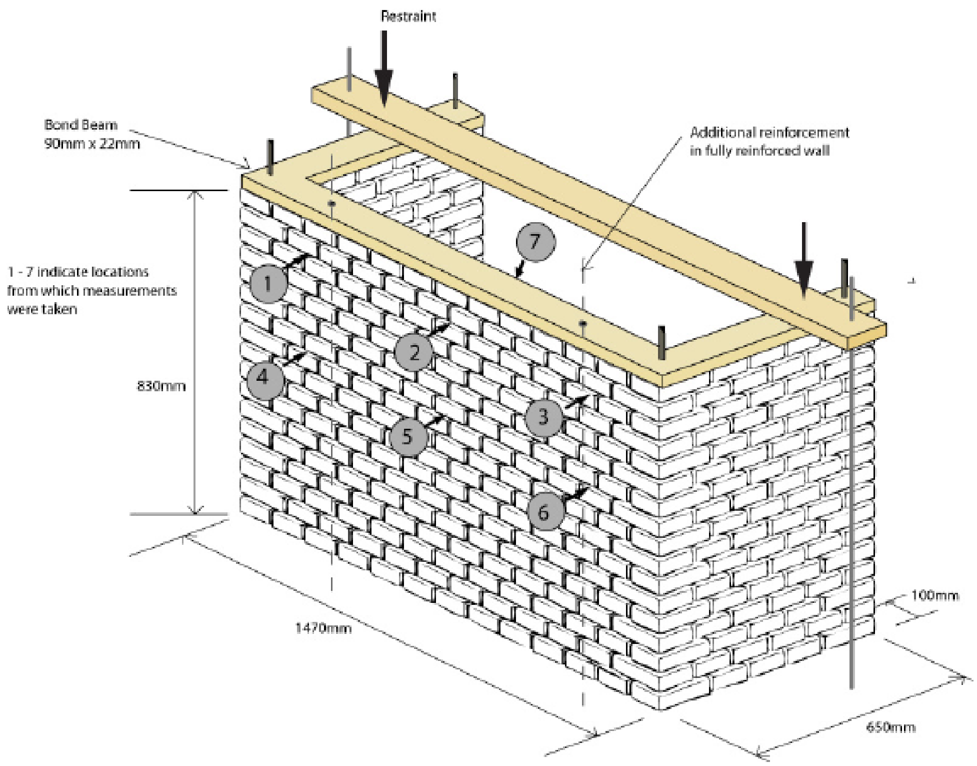

Figure 2.24: U-shaped adobe wall configuration (Tipler et al. 2010).

Figure 2.25: Tilt testing of the U-shaped adobe wall (Tipler et al. 2010).

The dynamic test results showed that the geogrid reinforcement improved the seismic resistance of adobe walls more than the nominal one.

The result from the static testing indicated that the fully reinforced wall with additional steel and polysynthetic geogrid provided more stiffness to the post-cracked adobe model than the nominally reinforced model. Figure 2-26 shows the comparative results of two models in static tilt testing.

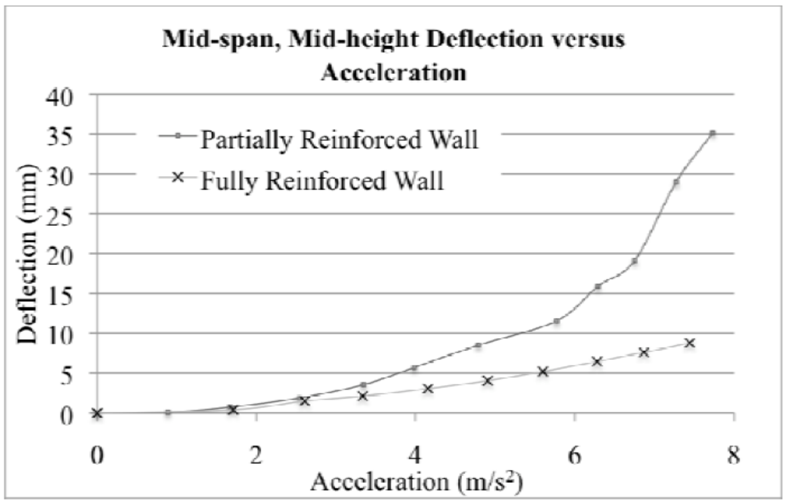

Figure 2.26: Tilt testing of the U-shaped adobe wall (Tipler et al. 2010).

The main limitations of the research at *University of Auckland* include:

- Limited technical depth and detail, particularly in the static testing section.
- There was no discussion on detailed comparative analysis of the behaviour between static and dynamic tests' results. Such data would be a very useful resource for the development of both static and dynamic tests.
- There was the lack of quantitative data and details of construction of all specimens. Furthermore, the lack of information on the material property testing of masonry prisms was noted.

2.8 Adobe models testing at the University of Kassel, Germany

In 1985, seismic earthen building's research had been conducted by H. Yazdani, the PhD student of the University of Kassel, Germany (Minke 2001). The research was to investigate the influence of the rammed earth wall shapes on the resistance to seismic forces with simple methods. Two walls of the small-scale (1:5) model with square and circular plan were constructed. A weight of 40 kg at the end of a 5.5 m long pendulum was allowed to swing and impact against the housing models in order to simulate the earthquake forces (see Figure 2-27). The results were compared by the failure behaviours of models in each stroke.

Figure 2.27: Simulation of seismic shocks (Minke 2000).

The earthen house with square plan showed the first large cracks after the second stroke. After three strokes one part of the wall became separated and after four strokes the box house collapsed. On the other hand, the circular earthen model showed the first cracks after three strokes and after six strokes had only one small part of the wall separated. The circular model did not collapse even after seven strokes.

The results showed that the circular earthen structure had better performance against the lateral loads than the rectangular earthen structure.

Figure 2.28 : Earthquake resistance of earthen buildings in circular shape (left) and square shape (right)(Minke 2001).

The research presented a simple method to evaluate the seismic resistance of two different wall shapes which provided valuable insight. Unfortunately, this doctoral thesis was not published. The main limitation of this research was the lack of quantitative data and details of experiment and specifications of all specimens.

2.9 Adobe guidelines and manuals

There is a large number of manuals and guidelines that have been produced in order to give information on how to build safer adobe constructions which are located in seismic areas. This section focuses on four guidelines and manuals for unreinforced adobe construction that provide the information relevant to this thesis:

- Guidelines for earthquake resistance non-engineered construction (1986) published by IAEE, International Association for Earthquake Engineering, Tokyo.
- The Australia Earth Building Handbook (2002) published by Standards Australia International Ltd.
- Earthquake Tips (2005) developed by the Indian Institute of Technology at Kanpur explaining basic concepts of earthquake-resistant construction in simple language.
- Earthquake-Resistant Construction of Adobe Buildings: A Tutorial (2003) published by the World Housing Encyclopedia (WHE) to cite an interactive web-based encyclopedia of housing construction types in earthquake hazard areas of the world.

There are a number of other manuals and guidelines reviewed which were not described in this section. These cover the same general information with different approaches and emphases. These include:

- Earth Construction Handbook by Gernot Minke (2000) published by WIT press.
- Building with Earth (Doat et al. 1991) translated by Asha Puri in collaboration with Manu Bhatnagar.
- The three New Zealand Standards for earth building, NZS 4297, NZS 4298 and NZS 4299, which are focussed on seismic resistance with a strong adobe consideration.

2.9.1 International Association for Earthquake Engineering (IAEE)

The International Association for Earthquake Engineering (IAEE) was established in February 1963 with its Central Office in Tokyo. The IAEE published the first *Guidelines for earthquake resistant non-engineered construction* in 1986. The objective of these guidelines was improving the earthquake safety for non-engineering dwelling constructions. The guidelines offered basic concepts and construction techniques in traditional materials such as stone, brick, adobe, wood and non-engineered reinforced concrete buildings to understand the earthquake resistant features of these building types' construction, while these kinds of structures contribute the majority of the damage or collapse of buildings in past earthquake disasters. The IAEE guidelines provide the following chapters:

1. The problem, objective and scope.
2. Structural performance during earthquakes.
3. General concepts of earthquake resisting design.
4. Buildings in fired-brick and other masonry units.
5. Stone buildings.
6. Wooden buildings.
7. Earthen buildings.
8. Non-engineered reinforced concrete buildings.
9. Repair, restoration and strengthening of buildings.

The detailed information of the IAEE guidelines are of particular relevance to this research's issues, especially chapter 7. This chapter provides the information on failure mechanisms of free standing walls which have been adopted to describe the failure patterns of the testing models in this research (Chapter 3). The general details for improved unreinforced adobe constructions are summarized in Table 2.5.

Table 2.5: Recommendations from IAEE guidelines (1986)

Topics	**Recommendation**
Building configuration	One floor construction. Regularity and symmetry in the overall shape of a building; box shape as rectangular both in plan and elevation.
Opening size	The fewer the openings the less the damage. Width of opening: 1.20 m for maximum opening. The sum of the widths of openings: not exceed one-third of the total wall length.
Adobe soil	Dry strength test should be done to verify the soil (Figure 2.29). Soils with low clay content should not be used. Sand and straw needs to be added to avoid fissures.
Mortar joints	Same materials used to manufacture the block; Some straw and sand added to control fissure; the adequate proportion verified by the fissuring control test.
Adobe blocks	Well dried to avoid cracking; different sizes in various regions; Strength test should be done to ensure the block strength (minimum value = 1.2 N/mm^2).
Walls	The length of wall should not be greater than 10 times the wall thickness (t) or greater than 64 t^2/h, where h is the height of the wall. The height of a wall should be less than 8 times its thickness.
Roof	Light roof structures, well connected, and adequately tied to the walls. Rain protection overhang about 500 mm.

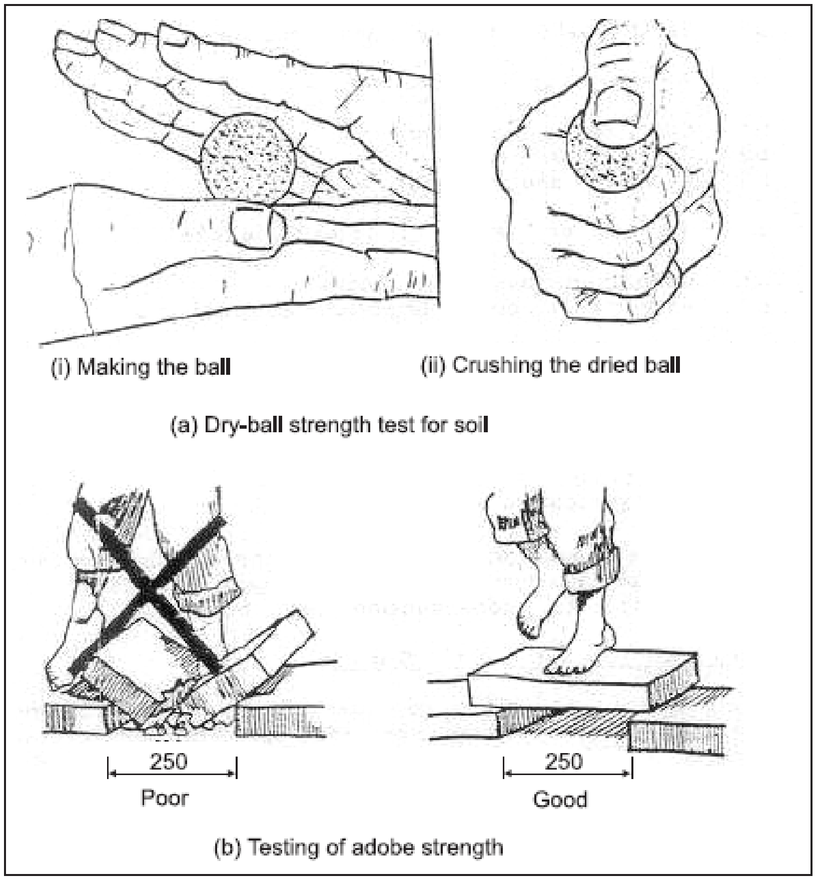

Figure 2.29: Field strength test of soil (a) and adobe block (b)(IAEE 1986).

Many of the practical and effective suggestions in the IAEE guidelines are beneficial for this research project for strength test of adobe and block construction. The guidelines are presented in a very visual manual, containing clear drawings which are both attractive and informative (Figure 2.29).

2.9.2 The Australia Earth Building Handbook

This standard was published by Standards Australia in 2002 (Walker & Standards Australia 2002). It provides guidance on material selection and recommendations for construction detail for design and maintenance, as well as setting out standard test procedures for earth building materials such as soil characterization tests, simple field tests for soil analysis and laboratory tests for earthen blocks. Some useful information on soil tests are described below.

- Sensory testing undertaken during on site inspection for the presence of organic matter (smell test) and to assess grading (touch test).
- Ribbon test was used to determine relative grading of a soil and its suitability for mud brick where the length of ribbon should achieve between 60mm -120mm before breaking.

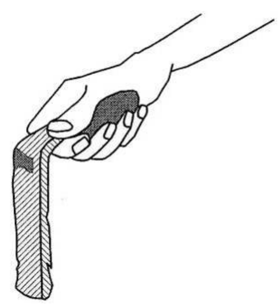

Figure 2.30: Ribbon test (Walker & Standards Australia 2002).

- Dry strength test should be done to check the plasticity of soil. The earth ball should be difficult to crush if has adequate fines for mud brick.
- Sedimentation test was used to determine the soil ingredients such as fine gravel, sand, silt and clay fractions.

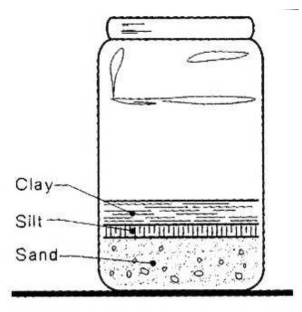

Figure 2.31: Sedimentation test (Walker & Standards Australia 2002).

This handbook recommends some laboratory tests which should be conducted to determine the material property of the adobe bricks as follows:

- Compressive strength is used to determine unconfined compressive strength of adobe blocks.
- Bending strength is determined from specimen dimensions, span and load to cause fracture.
- The accelerated erosion test determined relative erosion resistance of adobe blocks.
- The earth masonry bending strength by bond wrench test is used to determine out-of-plane bending strength of earth masonry bond.

There is also stated statistical analysis method used to determine mean, unbiased standard deviation, coefficient of variation, and characteristic value from a series of test results.

The handbook gives principles of accepted good practice and recommended design guidelines especially for unreinforced earthen walls and floors. Source material for the handbook has been taken from results of recent research and a variety of publications. Whilst some information of this handbook is derived from the work of Standards Australia Committee BD-083 and extracts taken from AS 2870 and AS 3700 are included. The useful recommendations for adobe constructions from this handbook relating to this research are described in Table 2.6.

Table 2.6: Recommendations from the Australia Earth Building Handbook (Walker & Standards Australia 2002)

Topics	Recommendation
Building configuration	One floor construction. Symmetry in the overall layout and building length should not exceed 3 times the building width.
Opening size	The widths of openings: not exceed 3 m in height and total combined horizontal length of all openings in a wall should not exceed one-third of the total wall length. The minimum distance between openings should normally not be less than 1 m and openings should be inset at least 0.75 m from the corner of the wall. Total area of openings should normally not exceed 20% of the wall's area in seismic risk areas.
Adobe soil	Soil for mud bricks should contain 30% to 75% of sand, 10% to 30% of silt and 10% to 40% of clay. Straw should be added to reduce shrinkage cracking when dry.
Mortar joints	Same materials used to manufacture the block. Sand could be added to reduce high shrinkage.
Adobe blocks	Bricks should have no cracks longer than 75 mm and wider than 3 mm. Robustness assessment should be undertaken to determine overall suitability and handling qualities of adobe blocks. Typical physical characteristics of mud bricks should be as follows; • Dry density : 1200 to 2000 kg/m^3 • Dry compressive strength : 1 to 5 MPa • Bending strength: 0 to 0.5 MPa • Thermal resistance (250mm thickness): 0.25 to 0.60 m^2 K/W
Walls	The height of walls laterally retained top and bottom should not exceed 15 times the minimum wall thickness.
Roof	Light roof structures and appropriately tied into the earth building.

2.9.3 Earthquake Tips

In 2002, the Indian Institute of Technology at Kanpur (IITK) and the Building Materials and Technology Promotion Council (BMTPC) developed the IITK-BMTPC Series on Earthquake Tips explaining the basic concepts of earthquake-resistant construction in simple language and very clear graphics (Murty 2005). The project consists of developing 24 tips ranging from a basic introduction to earthquakes and terminology, concepts of earthquake resistant design, and aspects of seismic design and detailing of reinforced concrete and masonry buildings. The Tips are also published at the web sites of the Building Materials & Technology Promotion Council (BMTPC) and the National Information Centre of Earthquake Engineering (NICEE).

The chapters which are useful to this research included:

1. Tip 01: What causes earthquake?
2. Tip 02: How the ground shakes?
3. Tip 03: What are magnitude and intensity?
4. Tip 05: What are the seismic effects on structure?
5. Tip 06: How architectural features affect buildings during earthquakes?
6. Tip 08: What is the seismic design philosophy for buildings?
7. Tip 12: How do brick masonry houses behave during earthquake?
8. Tip 13: Why should masonry houses behave in simple structural configuration?

Tips 01, 02 and 03 give the basic knowledge on earthquake phenomenon, about its causes and effects. The performance of buildings during earthquake activities presented in Tip 05 which explains effect of deformations in structures and flow of inertia forces to foundation. Tip 06 discusses about the importance of the configuration of a building which has significant effect on building performance during earthquake shaking. The earthquake design philosophy of buildings is summarized in Tip 08 which aims to avoid a disaster. Tips 12 and 13 are of particular relevance to the issue of earthquake safety of adobe buildings. They give useful information about earthquake performance of masonry walls and recommendations on how to improve their seismic performance.

The guideline contains both technique discussion and clear graphics for understanding building behaviours under seismic forces which are appealing to a broad audience.

2.9.4 Earthquake-Resistant Construction of Adobe Buildings: A Tutorial

World Housing Encyclopedia (WHE) project was established by cooperation between the Earthquake Engineering Research institute (EERI) and the International Association for Earthquake Engineering (IAEE) to build an interactive web-based encyclopedia of housing construction types in earthquake hazard areas of the world. It also includes documents on earthquake-resistant construction of adobe buildings, confined masonry dwellings and reinforced concrete frame building. These tutorials and guides have outlined key factors affecting seismic performance and recommendations for improved earthquake-resistant construction practices for new buildings and for strengthening the existing at-risk buildings. For adobe wall constructions, the recommendations of new buildings are as follows (Blondet, M. & Brzev 2003):

The tutorial gives recommendations for adobe brick construction as follows (Blondet, M. & Brzev 2003):

- *Clay: Perform the "dry strength test"—making at least three mud balls of about 2 cm diameter from the selected soil. Once dry (after at least 24 hours), crush each ball between the thumb and the index finger. If none of the balls can be broken, the soil contains enough clay to be used for adobe construction, provided that micro cracking of the mortar due to drying shrinkage is controlled. If some of the balls can be crushed, the soil is inadequate, since it lacks clay and should be discarded.*

- *Roll test: field alternative for choosing the soil; using both hands, make a little mud roll. If the unbroken length of the roll is between 5 to 15 cm, the soil is adequate. If the roll breaks with less than 5 cm, the soil must not be used. If the unbroken roll is longer than 15 cm, coarse sand must be added.*

- *Additives: straw; add to the mud, especially when preparing the mortar, the maximum amount of straw that still allows for adequate workability. If straw is not available, perform the "micro cracking control test"…if the mortar does not show visible cracking, the soil is adequate for adobe construction.*

- *Additives: course sand; the most adequate soil-coarse sand proportion is determined by performing the micro cracking control test with at least eight sandwiches made using mortars with different proportions of soil and coarse sand. It is recommended that the soil: coarse sand proportions vary between 1:0 (no sand) to 1:3 in volume.*

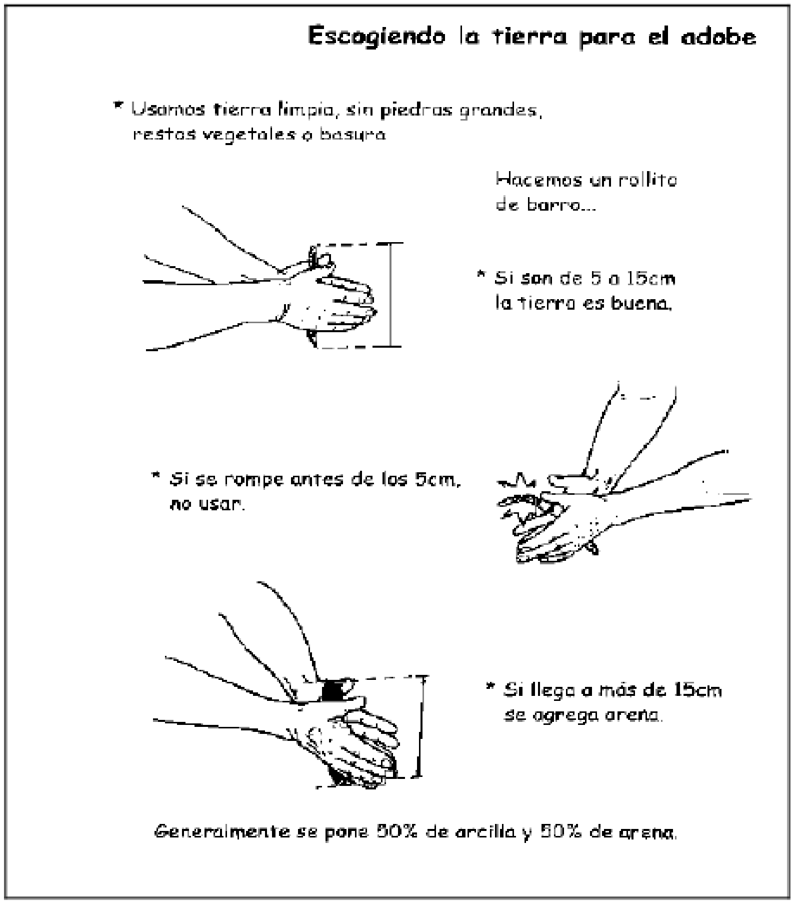

Figure 2.32: Roll Test (CTAR/COPASA,2002 cited in Blondet, M. & Brzev 2003).

The tutorial suggestions for the construction of adobe walls are as follows (Blondet, M. & Brzev 2003):

- The adobe bricks should be wet before laying. All adobe faces that are to be in contact with mortar should be wetted superficially which can be achieved by spraying water.
- The adobe wall height should not exceed more than eight times the wall thickness at its base, and in any case should not be greater than 3.5 m.

- The unsupported length of an adobe wall between cross walls should not exceed ten times the wall thickness, with maximum length of 7 m.
- Wall openings should not exceed one-third of the total wall length.
- The openings should not exceed 1.2 m width.
- A wall space of at least 1.2 m width between openings should be provided.

The recommendations of the wall length and sizes and distribution of openings in adobe house are illustrated in Figure 2.33.

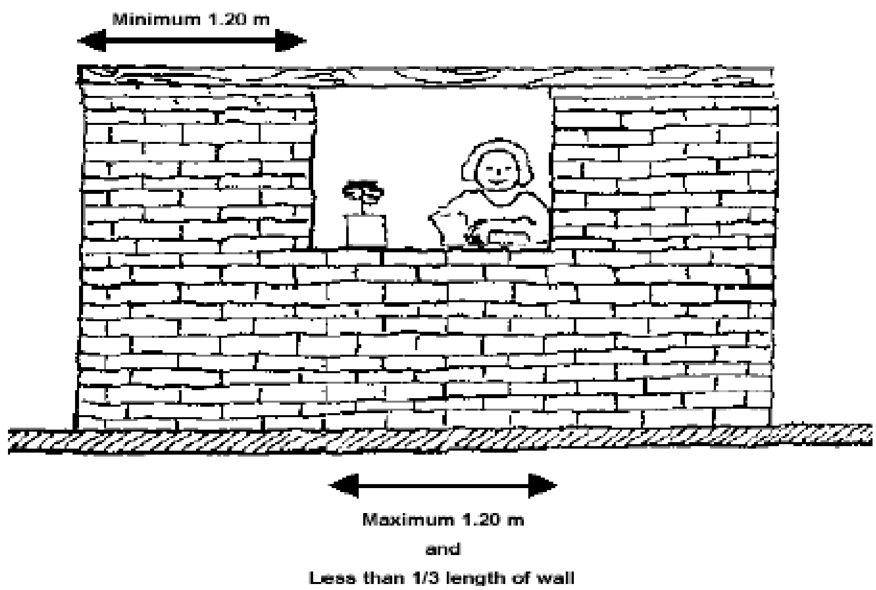

Figure 2.33: Configuration of opening guideline (RESESCO, 1997 from WHE).

The tutorial presents simple instructions for improving the performance of new adobe construction and for the earthquake protection of existing adobe dwellings. The instructions are clearly explained with simple illustrations. It also includs identification of the specific issues and recommendations for buildings made of fired-brick, stone, timber, earth and reinforced concrete.

2.10 Summary

This chapter presents research methods and dissemination techniques on how to improve adobe structures' seismic performance. The literature review has provided two key components which are research methodology on the experimental adobe structure testing and adobe construction techniques presented as guidelines and manuals.

The works undertaken to date have made a significant contribution to the body of knowledge relating to the seismic resistance research of adobe structures. These include:

- A tilt table test could be an appropriate alternative for a dynamic test. Because it is easy to perform and observe, and gives reasonable test results.
- Most of the experimental adobe testing and guidelines for adobe construction techniques have focused on box layout only. Even though, the circular shape has performed better under seismicity and should be recommended for –at-risk areas.
- The scaling of house model had a significant effect when compared to full-scale model. It appears to decrease the nature and amount of failure patterns and to increase the strength of model walls when compared to the prototype structure. In addition, the frequency scaling also had a significant effect on dynamic tests. Therefore, the effects of model scaling should be investigated in details to ensure accurate results.
- Adequate attention should be given to adobe brick fabrication and construction techniques, as it will lead to less variability in structural properties, and improve overall structural performance. There are some simple field tests, such as ribbon test, sedimentation test and drop test, which give guidance on material selection.
- This research should be conducted using both static and dynamic tests; therefore comparisons can be done between the test results. Dynamic tests can provide information that static tests cannot achieve, such as model displacement and peak ground acceleration by simulated ground motion.

In addition, various resources were reviewed to support this PhD research. These include:

- Examining existing circular shape adobe houses located in seismic areas with a focus on the relationship between their configurations, functional usage and construction techniques and their seismic resistance performance which are presented in Chapter 4.
- Study on typical damage patterns and failure mechanisms of adobe structures presented in Chapter 3.
- Investigate material properties of adobe prisms presented in Chapter 6 and Chapter 9.

Chapter 3 Seismic Performance of Adobe Buildings

3.1 Introduction

The aim of this chapter is to provide a basic understanding of the behaviour of adobe structures under the damaging effect and influence of seismic activities. A brief description of each damage pattern of adobe structures is given.

3.2 Earthquake Definition

An earthquake is a shaking movement of the ground that creates seismic waves. They are caused by natural phenomena, such as tectonic movements, volcanic eruptions or sudden failure of parts of the ground (Tomaževič 1999).

The most common cause of earthquakes is tectonic plate movement along active faults (Tomaževič 1999). These lead to two types of earthquakes.

1. Inter-plate Earthquakes – These earthquakes occur along the boundaries of the tectonic plates.
2. Intra-plate Earthquakes – These earthquakes occur within the plate itself away from the plate boundaries.

The slip of the earth plates which occurs in both types of earthquakes is also of two types (NICEE 2002a).

1. *Dip slip* is the slip generated at the fault during the earthquakes which is along both the vertical and horizontal directions.
2. *Strike slip* is the slip generated at the fault during the earthquakes which is along the lateral directions.

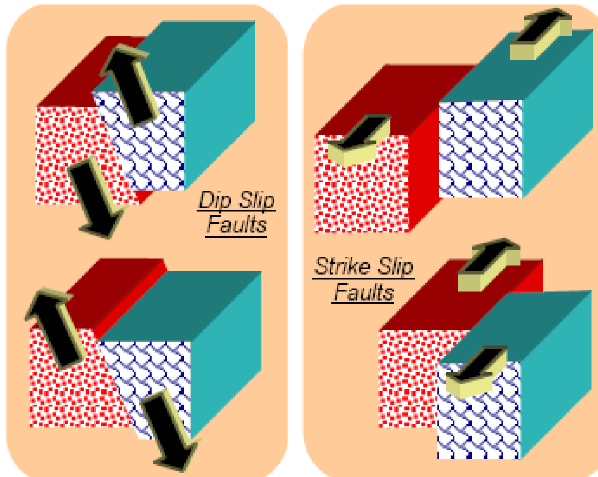

Figure 3.1: Types of Fault (NICEE 2002a).

There are 2 types of seismic waves which are released in all directions through the Earth's layers. These waves are *Body waves* (Primary waves and Secondary waves) which travel through the earth's interior and *Surface waves* (Love waves and Rayleigh waves) which travel along or near the earth's surface (NICEE 2002a; Tomaževič 1999; USGS 2009b). The seismic waves are filtered and attenuated when travelling through various layers of sub-soil and finally reach the ground surface with different amplitudes and energy levels at various instants of time. Therefore, the ground motions carry characteristic data such as *peak ground acceleration* (PGA), *duration of strong shaking*, *frequency content* and *energy content* (NICEE 2002a). The design parameter to determine the intensity of the ground shakings is the peak ground acceleration (PGA) and is often given in terms of acceleration of gravity (Tomaževič 1999).

Dynamic response of buildings

During an earthquake, the ground surface moves in all directions caused by seismic waves. These dynamic forces are not life-threatening on their own but when they are transmitted to structures through their foundations can result in significant collapse of buildings which is the main cause of death, injury and economic loss (Booth, Arup & Partners 1994). The inertia of the building's mass resists the motion applied to its base which affects the building in the way indicated in Figure 3.2. The most damaging effects on buildings are caused by horizontal inertial forces which disturb the stability of the structure, causing it to topple or to collapse sideways. Since buildings are normally constructed to resist gravity, many conventional systems of construction are not inherently resistant to horizontal forces, especially adobe structures (Ghaidan & R.I.B.A. 2002).

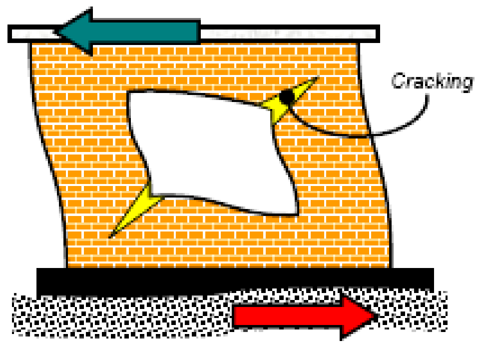

Figure 3.2: Earthquake-induced inertia force of masonry houses.
(Source: IITK-Earthquake Tips)

Shock-waves are transmitted to the ground and the resulting phenomenon can be schematically represented as two main types of motion, which can occur simultaneously (Norton & Intermediate Technology Development Group. 1986).

a) Lateral motion: the earth moves (the impression is of being pulled and pushed), which in construction terms means that the foundation moves while the rest of the building is left behind.

b) Undulatory motion: (a pitching sensation). In building terms this can lift the building up.

3.3 Typical damage patterns and failure mechanisms

There are a great number of vulnerable masonry buildings subjected to strong earthquakes. Masonry buildings are brittle structures which are considered unsuitable for in seismic zones, especially in cases of adobe and stone-masonry (Tomaževič 1999).

Adobe structures may undergo failure in earthquakes due to their low tensile strength and brittle properties (Virdi & Rashkoff 2007). Adobe structures subjected to ground vibrations may undergo failure by in-plane shear, out of plane flexure, tension (in corners) or a combination of these. The most common failure was flexure (Christie 1990). Typical failure modes during earthquakes are severe cracking and disintegration of walls, separation of walls at the corners, and separation of roofs from the walls, which can lead to collapse (Christie 1990).

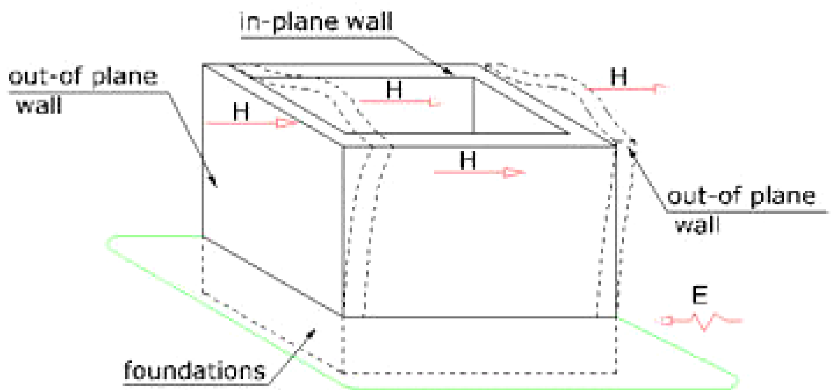

Figure 3.3: Definition of In-plane and Out-of-plane walls.
(Source: City University, London)

The following brief description of each damage pattern is based on a review by Blondet, M. & Brzev 2003; Christie 1990; Dowling 2006; McHenry 1983; Minke 2001; NICEE 2002a; Virdi & Rashkoff 2007.

1. **In plane shear**

   This type of failure usually occurs in walls parallel to the ground vibrations. The in-plane forces cause a wall to rack in shear. The racking load is the dead load of wall itself as well as the weight of the roof. These loads cause the wall to be stressed in shear. If the shear stress exceeds the shear strength of the wall, diagonal cracking occurs. It becomes significant when these cracks propagate to the plane corner. This situation can lead to the collapse of the walls. Large roof mass or heavy dead load above the wall, poor roof anchoring, large or numerous openings (windows and doors), poor block arrangement and walls that are too thin and slender walls can all lead to this type of cracking.

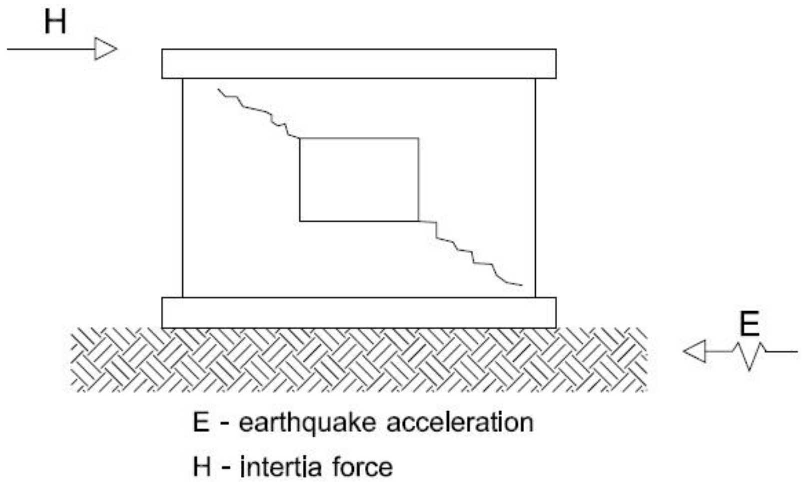

Figure 3.4: In-plane crack pattern.

Figure 3.5: Inclined cracking in the wall in Pinarkaya.
(Source: GFZ-German Research Centre for Geosciences)

2. Out of plane flexure

According to Christie (1990), out of plane bending flexure is the most common cause of failure. The out-of-plane forces due to the self-weight of the wall leads to failure patterns similar to those observed in brick walls subjected to wind loading.

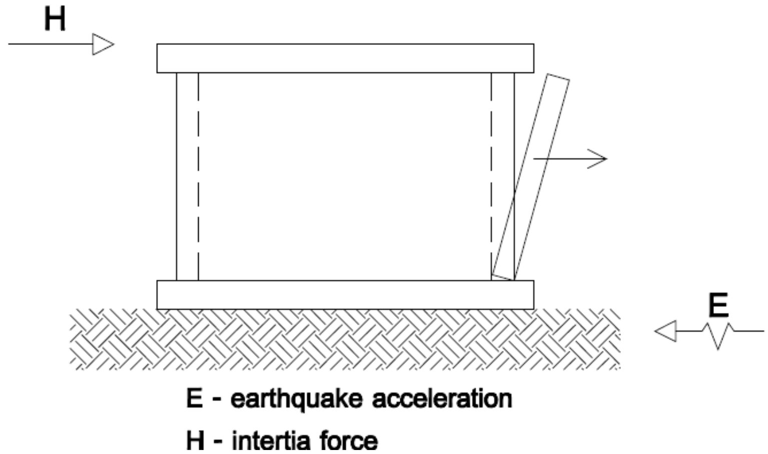

Figure 3.6: Out-of-plane flexural crack pattern.

Figure 3.7: Cracking and separation of walls in 1997 Jabalpur Earthquake (Source: World housing Encyclopedia, reports # 23).

This type of failure occurs in walls perpendicular to the ground vibrations. The out-of-plane forces lead to flexural stresses in the wall and where these exceed the capacity of the material, cracking results. Flexural failure most frequently occurs in long non-load-bearing walls. Load-bearing walls are to some extent restrained by the roof beams, and the higher initial compression stress means that flexure is less likely to result in the development of tensile stresses. Typically vertical cracks begin in the upper corners and are propagated downwards by continued shaking. As the crack length increases in both ends where the wall is unrestrained, the wall begins to form a hinge from the swaying and acts like a cantilever. Finally, the out-of-plane failure on adobe walls usually causes walls to fall away from a building.

3. **In-plane failure**

In-plane failure can occur in the corners of walls normal to the ground vibration as expressed by double-diagonal (X) shear cracking (Figure 3.8).

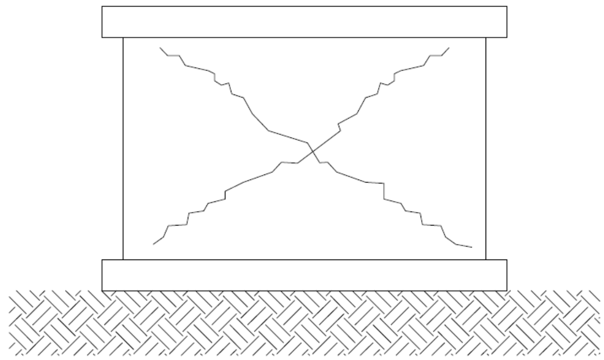

Figure 3.8: In-plane failure pattern.

Excessive bending may produce in-plane shear failures, depending on the aspect ratios of the wall. Slender walls are more subjected to greater shear stresses, as well as greater compressive stresses due to its weight. Openings (door and windows) induced high stress concentrations when they are located close to other openings or corners (Figure 3.9).

Figure 3.9: In-plane shear failure – San Giuliano (Marrow).
(Source: Conservationtech.com)

However, the damage patterns of adobe buildings vary in different regions, shapes of floor plan, and details of construction may be classified in an identical way. The summarized typical failure modes of adobe structures are shown in Figure 3-10.

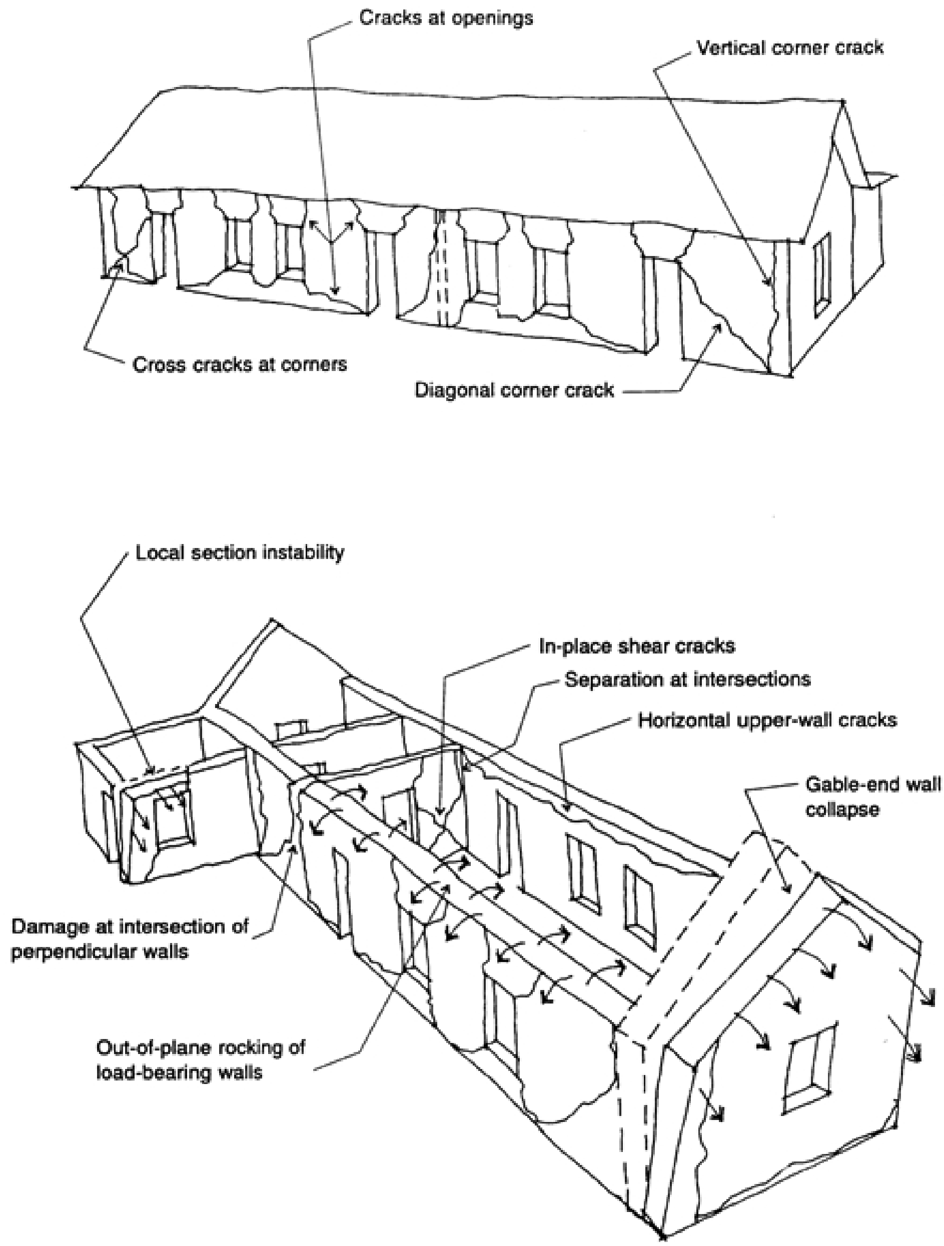

Figure 3.10: Various types of failure in adobe structures under seismic excitation (GINELL & Tolles (n.d.)).

3.4 Static and Dynamic Analysis

In order to design a seismic-resistant structure, the forces on the structure must be specified and rely on a realistic estimate (Naeim 1989). There are a number of factors that should be integrated with the seismic design forces, such as the earthquake characteristics, the distance from the fault, the site sub-soil, the type of lateral-load-resisting system, and also the importance value of the structure (Naeim 1989). There are two procedures for specifying seismic design forces which are the *equivalent-static-force analysis* and *dynamic analysis (Jr 2003)*. These methods are used according to what considerations are taken into account in the design (United Nations 1975). Arros (2003) commented about the variation of these two methods that "*Static studies systems in static equilibrium, i.e., in a state where the system internal forces counterbalance external forces do not vary in times; they are time-independent. Dynamics is the study of systems subject to time-varying applied force….While a static problem has a single time-independent solution, the solution of a dynamic problem involves a description of the system's state at every time point within the period of study*".

The detailed analysis of these two methods are described below.

3.4.1 Static method

Static method is permitted in most Codes of Practice for low to medium-rise buildings (Booth, Arup & Partners 1994). The codes allow the results obtained from a dynamic analysis to be normalized so that the maximum dynamic base shear is equal to the base shear. The static equilibrium equation is expressed in term of the balance between the external forces and the structure's internal forces (Arros 2003).

This static method defines as a base shear coefficient, which is multiplied by the total weight of the building to define the lateral forces that the building must sustain at its base. This base shear coefficient depends on factors such as:

a. The effect of the subsoil on the ground shaking which depends on historical records of the earthquakes in each region.

b. Probability factor for the annual probability of exceedance.

c. Spectral shape factor dependent on sub soil and period of vibration.

d. The ductility factor of the earthquake-resistant the building.

e. Structural performance factor.

Mario Paz (1994a) cited that the equivalent static method is applicable only to regular structures which should have an orthogonal layout, not to be unbalanced in its distribution of mass or stiffness, should not exhibit large variations in mass in elevation and should be constructed as rigid diaphragms. Roger and Di Julio (2003) claimed that irregular structures which are not related to the above categories should be analysed using dynamic method to specify and distribute the seismic design forces. The detailed analysis used in static method in the earthquake codes were described in Section 3.5. However, it is found that the calculated earthquake forces using static equilibrium equation are significantly less than those that actually happen in larger earthquakes likely in the area concerned (Dowrick 1977). The forces calculated using dynamic analysis can be as great as ten times those calculated from the static seismic codes (Dowrick 1977).

3.4.2 Dynamic method

In dynamic method, the linear dynamic properties of structure are considered more precisely than in the static method. The structures are considered with due regards to the dynamic equilibrium through the governing equation of motion. The equation of motion states the equilibrium of internal and external forces, same as the static equilibrium equation, with the addition of and the inertia forces and damping effects (Arros 2003). This implies taking into account the small displacements and the distribution of stresses in the structure.

There are three techniques normally used for dynamic analysis, and they are (Dowrick 1977);

1. Direct integration of the equations of motion which provides the most accurate and informative for dynamic analysis but it is computationally very expensive.
2. Normal mode analysis which is a more limited technique compared to the direct integration. This analysis is limited to linear material performance where the modes cannot be truly separated.

3. The response spectrum technique which is a simpler case of modal analysis. It is suited for basic structures such as a single-degree-of-freedom system but would not be good enough to generate informative output for other complicated systems.

Dowrick (1977) also suggested the selection of method of seismic analysis in Table 3.1 with one condition being that the appropriate load input was used.

Table 3.1: Selection of method of seismic analysis (Dowrick 1977)

Type of structure	Method of analysis
Small simple structures	1) Equivalent static analysis (appropriate code)
↓	2) Response spectra (appropriate spectrum)
Progressively more demanding structures	3) Modal analysis (appropriate dynamic input)
↓	4) Non-linear plane frame (appropriate dynamic input)
Large complex structures	5) Non-linear 3-D frame (appropriate dynamic input)

Duggal (2007) commented about the selection of analysis method and the fact that the method of seismic analysis can be classified as linear static analysis, linear dynamic analysis, non-linear static analysis, or non-linear dynamic analysis. Linear static analysis or equivalent static analysis can be used for ordinary structures with limited height. Linear dynamic analysis can be used in the same type of structures as linear static analysis but had differences in the level of forces and their distribution along the height of building. Non-linear static analysis was an improvement over linear static or dynamic analysis in that it allows for the inelastic-structures performance. A non-linear dynamic analysis can be used to gain informative data of the actual seismic behaviour of the structure.

It is clear that for adobe structures as low-rise buildings with orthogonal layouts, the static method can be applied for this research project to assess their seismic resistance.

3.5 Seismic Design Codes for Earth Building Regions

This section explores the general concept of seismic design codes used in earthquake regions. In order to understand the equivalent static analysis, it also examines the various parameters of the static base shear equation by using the UBC-97 code for the study model. In addition, the details of provisions used in the three case studies including regions in China, India and Malawi were also studied and discussed in relation to the earthen building type.

3.5.1 Concept of seismic code

Earthquake codes have been developed over the years in order to deal with earthquake disasters (Sen 2009). Coburn and Spence (2002) claimed that the best way to protect buildings against the earthquake actions is to ensure that the building is strong enough for the lateral forces. Some of the earthquake risk areas such as Japan, USA and New Zealand have developed codes of practice for the design of new buildings for most of the last century in order to design structures to withstand earthquake forces. The formal study of earthquake-resistant design started after the 1906 San Francisco earthquake (Lindeburg & Baradar 2001). These primary codes became the models for seismic codes used in other countries today (Coburn & Spence 1992). The theme of the early codes was that the buildings must be *strong* enough to resist a static lateral force or the base shear (V) of some fraction of the weight (W) in order to protect the human lives and the buildings. Seismic codes were proposed to prevent total failures of buildings. However, it allowed for the damage of noncritical sections (Department of Urban and Regional Planning 1998). The response of the structures during the ground motion may be determined by considering the site hazard and the dynamic characteristic and configuration of the building (Weller 2005). The lateral forces produced by the ground motion can be estimated by the equivalent lateral force which is represented by the Newton’s second law (Williams 2004), as:

$$F = ma \tag{3.1}$$

where

F = force

m = mass of structure

a = acceleration

The lateral force concept was introduced through the simple equation (Sen 2009):

$$V = \frac{W}{g} a_{\max} = kW \tag{3.2}$$

where

V = lateral force

W = total weight of structure

$a_{\max}$ = the earthquake horizontal acceleration generally in the range of 0.05g to 0.20g (Dowrick 1977)

$k = \dfrac{a_{\max}}{g}$ = seismic coefficient

This equation gives the total design lateral force that acts on the building structures or shears at the structure's floor levels.

Now a days, the base shear coefficient has been modified many times based on the building period and/or the height of a building but the basic concept is still the same.

The objectives of equivalent static load requirements in most seismic codes are as following:

1. Define the earthquake loads to be used in the structural design of buildings.
2. Define the criteria for overall structural performance.
3. Provide the detailed guidelines of the building constructions that are suitable for the materials and structural systems in use.

Furthermore, there are many differences in the details of seismic codes used in each region with earthquake hazard. Some regions have their own code, but most of them use Uniform Building Code (UBC) for design purposes or as a reference in drawing up earthquake regulations where they do not exist which includes China, India and Malawi (MCEER 2007).

The Uniform Building Code (UBC) is published by the International Conference of Building Officials (ICBO) in the United States. Many of seismic provisions of UBC have been influenced by the Recommended Lateral Force Requirements and commentary published by the Seismology Committee of the Structural Engineers

Association of California (SEAOC) (Jr 2003). The UBC code is dedicated to the development of better building construction and greater safety to the public. The horizontal equivalent force from UBC 1997 code is described as follows (Jr 2003):

$$\begin{array}{c} (0.11C_a I)W \\ and \\ \left(\dfrac{0.8ZN_v I}{R}\right)W \end{array} \leq V = \frac{C_v I}{RT} W \leq \left(\frac{2.5C_a I}{R}\right) W \tag{3.3}$$

where

Z = Seismic zone factor which is given as a percentage of acceleration due to gravity. It was presented in the seismic zone map

T = Fundamental period of the structure is the length of time, in seconds; it takes a structure to move through one complete cycle of free vibration in the first mode. There are two methods in UBC-97 to estimate T:

(1): $$T = C_t (h_n)^{3/4} \tag{3.4}$$

where

C_t = Seismic dynamic response spectrum values

h_n = Height of the structure in feet

(2): $$T = 2\pi \sqrt{\frac{\sum W_i \delta_i}{g \sum f_i \delta_i}} \quad \text{(not generally used in regular structures)} \tag{3.5}$$

where

W_i = Weight of structure of level i

δ_i = Elastic deflection of level i relative to base

f_i = Force at level i

I = Structure importance factor for the building occupancy (I =1.25 for essential and hazardous facilities, and I =1.0 for all others)

C_v = A numerical coefficient, dependent on the soil conditions at site and the seismicity of region

C_a = Another seismic coefficient, dependent on the soil conditions at site and regional seismicity

W = Structure total seismic gravity load

R = Response modification factor related to the inherent ductility, damping, and over-strength of structure

N_v = A near-source factor that depends on the proximity to activity of known faults near the structure (applicable in only seismic zone 4 which account for the very large ground accelerations near the seismic source). This factor is also used to determine the seismic co-efficient, C_v.

The UBC code provides for the use of the equivalent static and dynamic procedures for ordinary buildings less than 240 feet in height and asymmetrical buildings less than 65 feet in height, and buildings that are located on poor soil and have a building period greater than 0.7 seconds (Jr 2003).

According to this static equation adobe structures should have a low value for T due to its low-rise nature (better seismic performance) and a low amount of R due to its brittle material nature (worse seismic performance). From this, most of the seismic research on of adobe structures have tried to investigate the ductility factor and how to provide a higher flexibility into its walls by using various local material reinforcement. While there are some unreinforced earthen buildings which had performed very well in seismic events and had no ductile reinforcement in their earthen walls.

Further details of the equivalent static procedures used for the three case studies' regions are presented in the next section.

3.5.2 The earthquake codes of case studies' regions

The static equations used in the three case studies' regions in Chapter 4 are described in this section.

3.5.2.1 Chinese earthquake code

In 1974, the first official seismic code of China was published by the Ministry of Construction as a trial version with the title: *Seismic Design Code for Industrial and Civil Buildings - TJ11-74*. The revision of the first version was undertaken after two strong earthquakes in 1975 and 1976 with 242,829 people killed in total and was published in 1978 (TJ11-78). A further revision was published in 1989 named *Seismic Design Code for Buildings and Structures - GBJ11-89*. The update version was issued on 20th July 2001 and actualized on 1st January 2002 named *The Code for Seismic Design of Buildings – GB50011-2001* (National Standards of the People's Republic of China 2001). China was divided into seven zones with the highest ground acceleration equal to or greater than 0.4g (Burton & Cole (n.d.)). The Seismic zoning map of China presented the expected ground acceleration with 10% probability of exceedance in 50 years (see Figure 3.11).

This code classifies buildings and structures into four types as following (Paz 1994b):

- Type A. Building and structures that should not fail beyond repair during an earthquake because of their important functional usage and the severe consequences of their failure.
- Type B. Buildings and structures of lifeline systems in main cities of the country.
- Type C. Buildings and structures not included under Type A, B and D.
- Type D. Buildings and structures of less importance where damages are not likely to cause deaths or injury to people and/or considerable economic losses.

The sites categories are based on the characteristics of the soil at the site of the structure for example:

Site Category I.is a soil profile with either (a) a rock-like material or (b) a stiff or dense soil condition or (c) other soil condition where the soil depth is less than 10 feet.

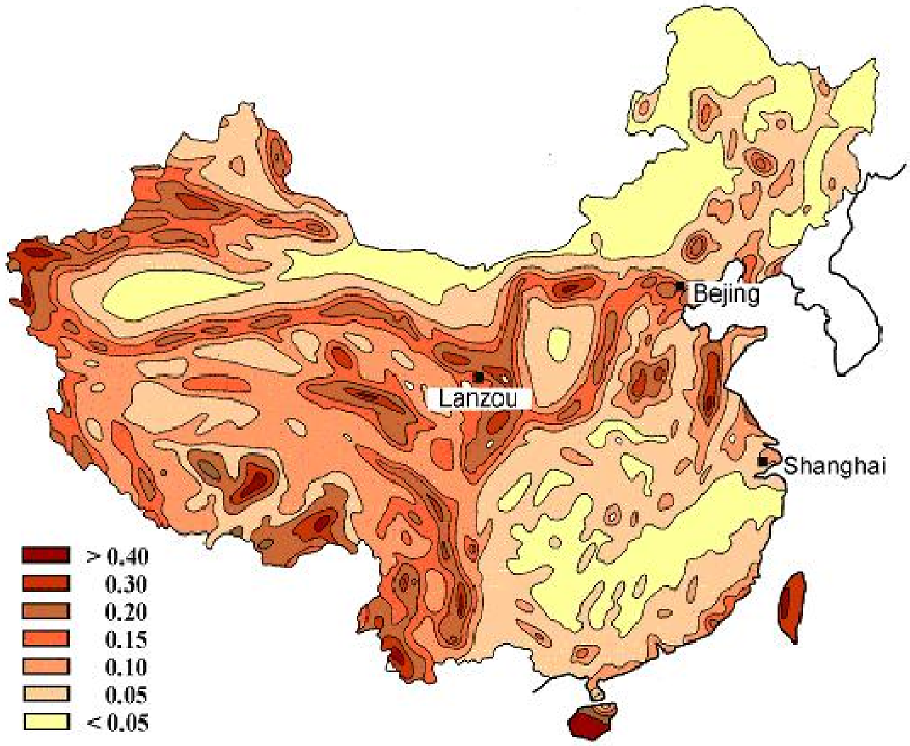

Figure 3.11: Seismic zoning map of peak ground acceleration (PGA) of China (RP = 475 years; PE = 10%/50 years) (GB 18306 – 2001 – A1)

The total horizontal seismic force using base shear method was calculated using the following equation form the Chinese seismic design code GB50011-2001.

The base shear equation was:

$$F_{EK} = \alpha_1 G_{eq} \tag{3.6}$$

where

F_{EK} = Standard value of the total horizontal seismic action on the structure.

G_{eq} = Total equivalent seismic weight of a building.

α_1 = The horizontal seismic effective coefficient corresponding to the fundamental period of the structure (T) (see Figure 3.12).

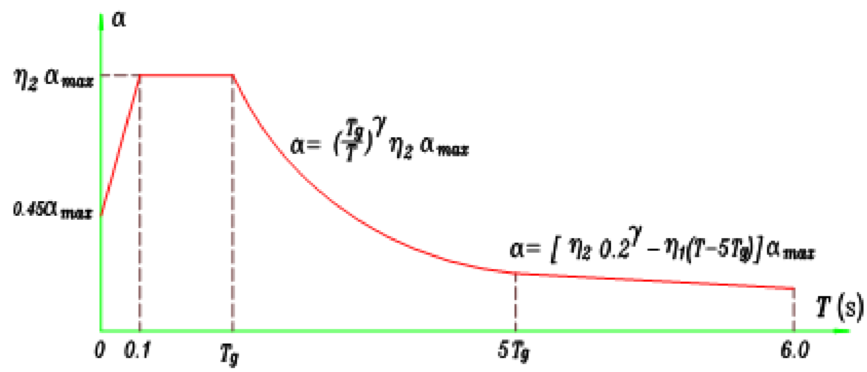

Figure 3.12: Seismic effective coefficient curve of GB50011-2001(IISEE 2002).

T_g = Design characteristic period of ground motion (see Table 3.2).

Table 3.2: Design characteristic period of ground motion

Design Earthquake Groups	**Site Category**			
	I	II	III	IV
First Group	0.25	0.35	0.45	0.65
Second Group	0.30	0.40	0.55	0.75
Third Group	0.35	0.45	0.65	0.90

The characteristic parameters of response spectra and modification with different damping are:

$$\gamma = 0.9 + \frac{0.05-\xi}{0.5+5\xi} \text{ for } 0.1 < T < T_g \tag{3.7}$$

$$\eta_1 = 0.02 + (0.05-\xi)/8 \text{ for } T_g < T < 5T_g \tag{3.8}$$

$$\eta_2 = 1 + \frac{0.05-\xi}{0.06+1.7\xi} \text{ for } 5T_g < T < 6.0 \tag{3.9}$$

3.5.2.2 Indian earthquake code

In 1962, the first official earthquake code in India was published and it has been revised 5 times in 1966, 1970, 1975, 1984 and 2002 (Jain (n.d.)-b; NICEE 2002d). The new release was *IS 1893:2002, Indian Standard Criteria for Earthquake Resistant Design of Structure*. It provided the seismic zone map and specifies design force (NICEE 2002d). According to the zoning map, Zone II is associated with the lowest level of seismicity whereas zone V expects the highest level of seismicity.

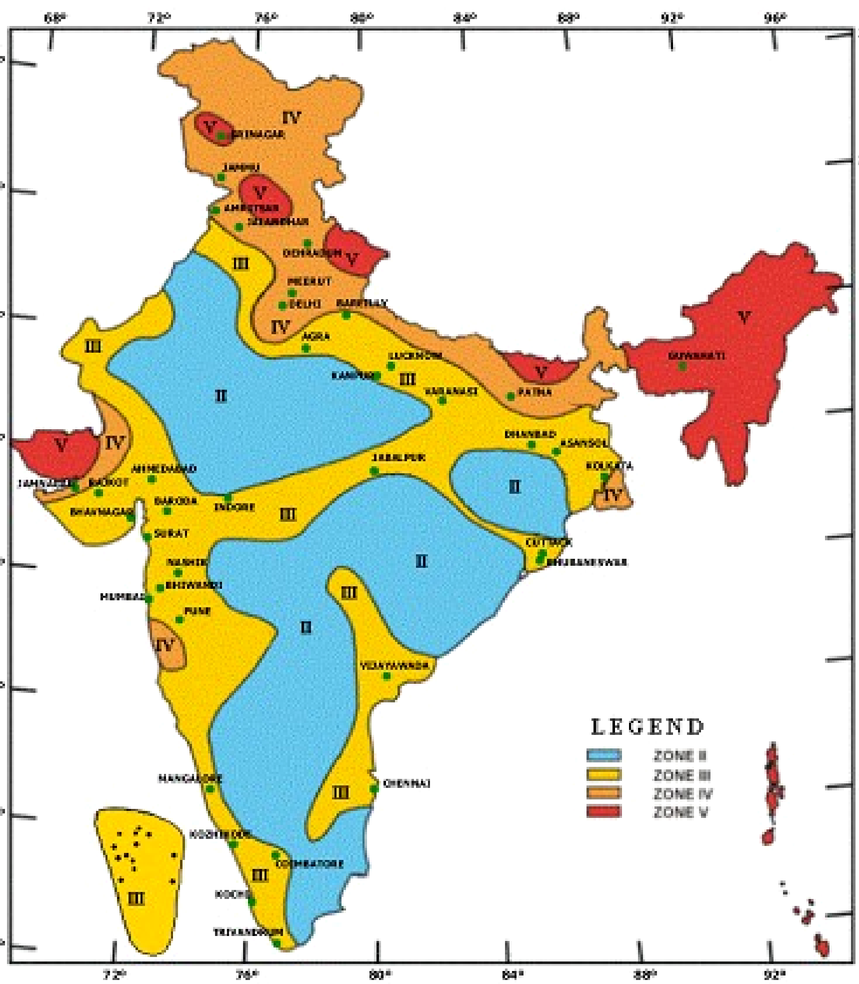

Figure 3.13: Seismic zoning map of India (IS 1893:2002) (Source: The Institute of Seismological Research (ISR)).

Design base shear is given by (Clause 7.5.3 of IS:1893 Part 1)(Jain (n.d.)-a):

$$V_B = A_h W \tag{3.10}$$

where

$$A_h = \frac{ZI}{2R} \times \frac{S_a}{g} \tag{3.11}$$

Fundamental period (Clause 7.6.2 of IS:1893 Part 1) (Jain (n.d.)-a):

$$T = 0.09h\sqrt{d} \tag{3.12}$$

where

d = Length of the building

3.5.2.3 Malawi earthquake code

Unfortunately, there is no consideration of earthquake ground motion in the building code of Malawi. Although it is located on the most seismically active belt of the East African Rift System (EARS) (Chapola 2001). Therefore, the seismic hazard map of Africa was used to estimate the peak ground acceleration of Malawi (see Figure 3.14). An estimation of seismic hazard indicated that the peak ground acceleration (PGA) for a 10% probability of exceedance in 50 years (475 years return period) for the entire country ranges from 0.8-1.6 m/s^2.

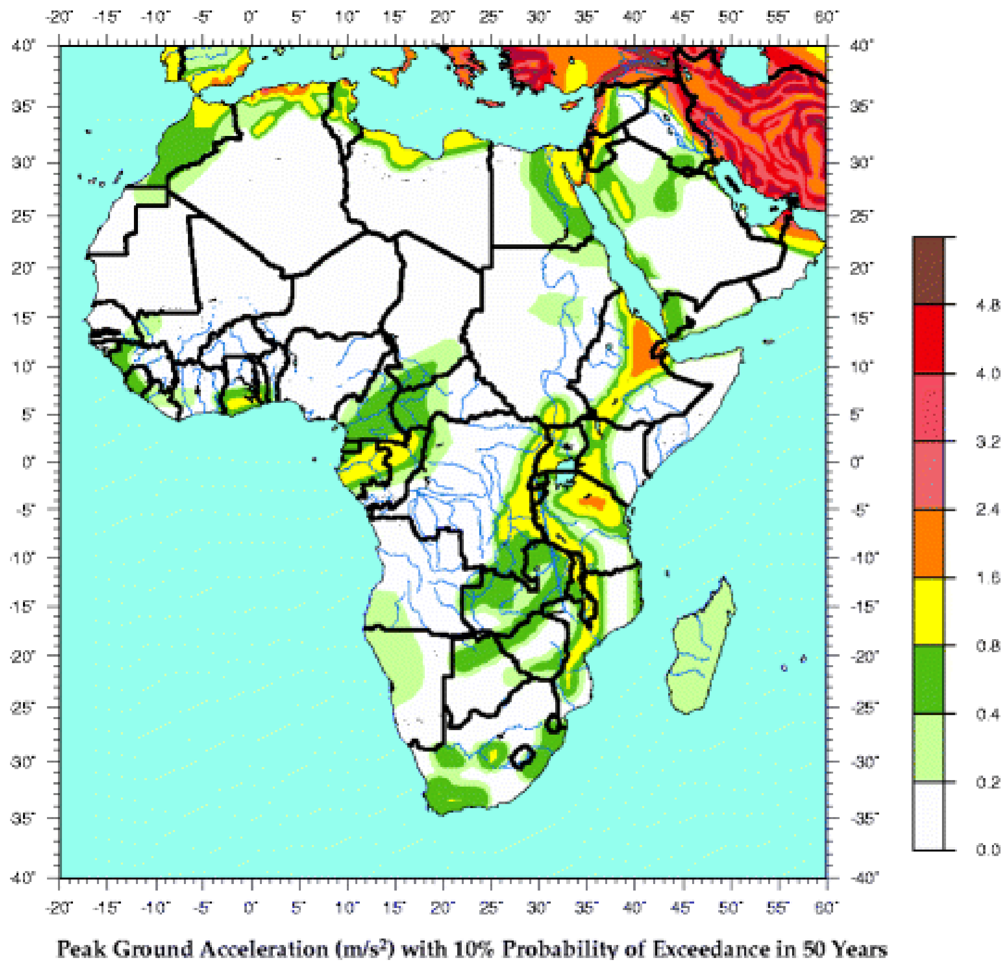

Figure 3.14: Seismic hazard map of Africa

(Source: GSHAP-Global Seismic Hazard Assessment Project).

As presented, there are a variety of seismic codes used in different seismic regions which may use different parameters or values, depending on the seismic hazard factor in each area. Most earthquake codes provided information on how to calculate a minimum lateral force requirement and details of construction for each building type. The consensus is that the existing equivalent lateral force formula is appropriate for designing most structures (Krinitzsky, Gould & Edinger 1993). Fred Webster (2002) cited that the UBC-97 code for earthen structures was limited in addressing specific materials and construction techniques, e.g. there is no reduction factor listed for unreinforced or even reinforced adobe construction which restricted people to use these types of buildings. Therefore, it may not be suitable to use UBC-97 earthquake code in this research project. While the Australian earthquake code (AS1170.4) contains much more information and factors which are specific to the earthen construction. Therefore author decided to use AS1170.4 as the standard static equilibrium equation which would be applied for all cases in this research project. The detailed analyses of the static equation of AS1170.4 are described in Chapter 5.

3.6 Summary

This chapter presented a basic understanding of adobe structures, their behaviour under seismic activities, and their effects on structures. It also analysed both static and dynamic methods used for earthquake research. These included:

- Typical damage patterns and failure mechanisms of adobe structures, which described the common damages to structures when subjected to seismic forces.

- Study on both static and dynamic procedures to specify seismic design forces, which presented some key differences between these two procedures.

- Study on the seismic design code for earthquake regions, which described a concept of seismic code and some earthquake codes used in the case studies' regions.

- The analysis result from the earthquake codes shows that there are a variety of seismic codes used in different seismic regions. Therefore, AS 1170.4 was applied as the standard static equilibrium equation used in this research project.

Chapter 4 Performance of Existing Circular Earthen Houses located in Seismic Regions

4.1 Introduction

Earthquakes are natural disasters that have destroyed many seismically unreinforced masonry buildings, especially poorly made adobe houses in earthquake-prone regions in developing countries. In the 20th century four of every five deaths caused by earthquakes were in developing countries. More than one million people living in adobe dwellings were left homeless in El Salvador and Peru after earthquakes struck these two countries in 2001. Recently thousands of deaths were attributable to vulnerable adobe structures in Bam, Iran (Eeri et al. 2004).

Earthen construction is still widely used in many seismic hazardous countries, especially in developing nations, for example Iran, India, China, Peru, Turkey, El Salvador, etc. These countries live with the constant threat of large losses of lives and properties should an earthquake occur. Figure 4.1 and 4.2 show the location of seismic risk regions.

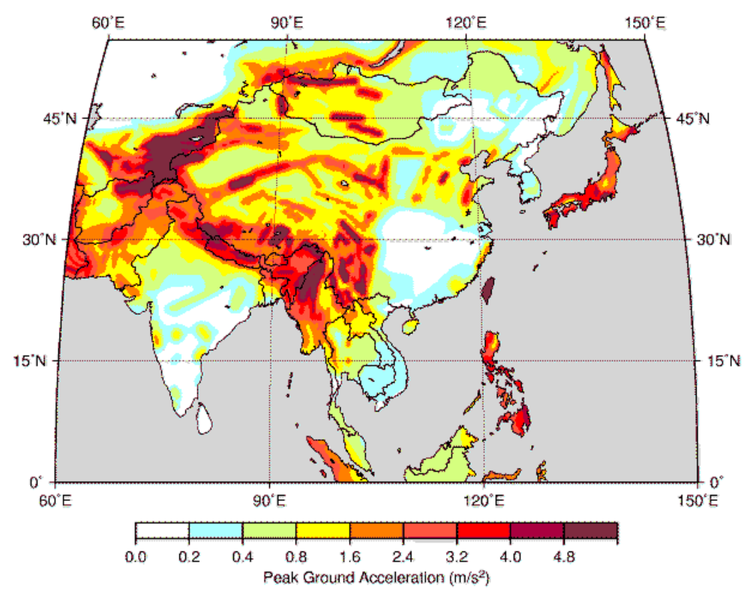

Figure 4.1: Seismic Hazard map of Asia

(Source: Global Seismic Hazard Assessment Program, Switzerland).

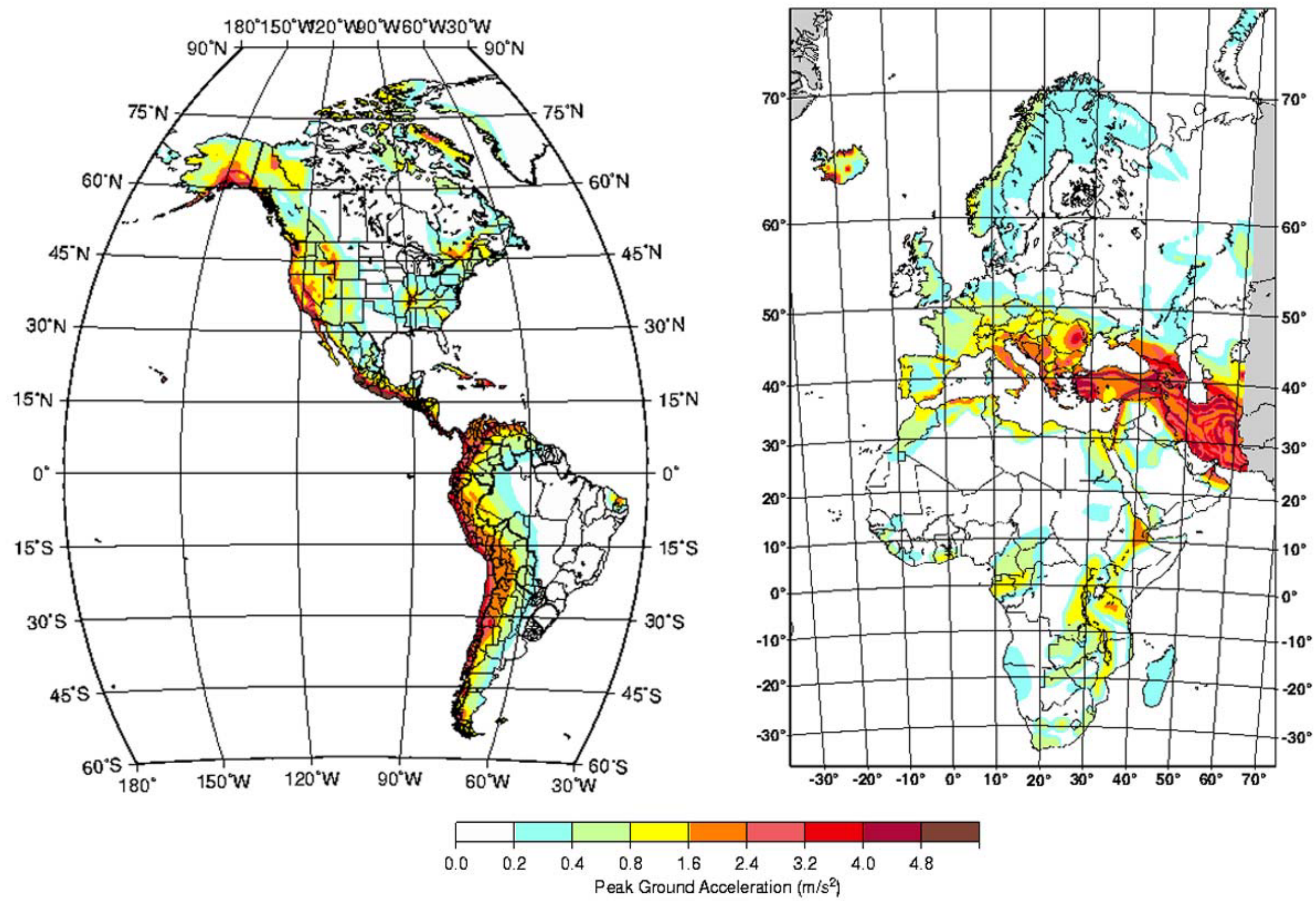

Figure 4.2: Seismic Hazard map of the Western Hemisphere (left) and Europe, Africa and the Middle East (right)

***(Source: Global Seismic Hazard Assessment Program, Switzerland)*.**

On the other hand, while this type of construction has performed poorly under seismic impact, there are some existing traditional earthen houses which had shown good seismic resistance in high risk regions such as China, India, Malawi (Minke 2001; Sassu n.d.). Most of these surviving houses have a circular plan. These earthen houses have been built without specific material or construction knowledge, but the local people have learned how to resist the earthquake force through a "*trial and error*" process.

This chapter will explore the performance of three case studies of circular earthen structures in seismic prone areas such as China, India and Malawi. It describes the general context of each site, their architectural features and discusses their effectiveness.

Exploring to these case-study aspects has been fundamental to understanding the general issues of circular earthen structures, and realization of the objective of this research project.

4.2 Hakka earth buildings in China

Location: Yongding County (永定县) in Fujian Province (福建), southern China (中國)

4.2.1 Background

As the world's most populated country and being subjected to frequent earthquakes, it is not surprising that China has been the site of four of the ten most devastating earthquakes in history. The deadliest earthquake in history with an estimated magnitude of between 8.0 and 8.3 occurred on the 23rd January 1556 in the Chinese province of Shaanxi causing damage in 100 counties in 10 provinces. The death toll was estimated at 830,000 with 60% of the population dying in the hardest hit areas. Large aftershocks occurred regularly for 6 months following the initial quake.

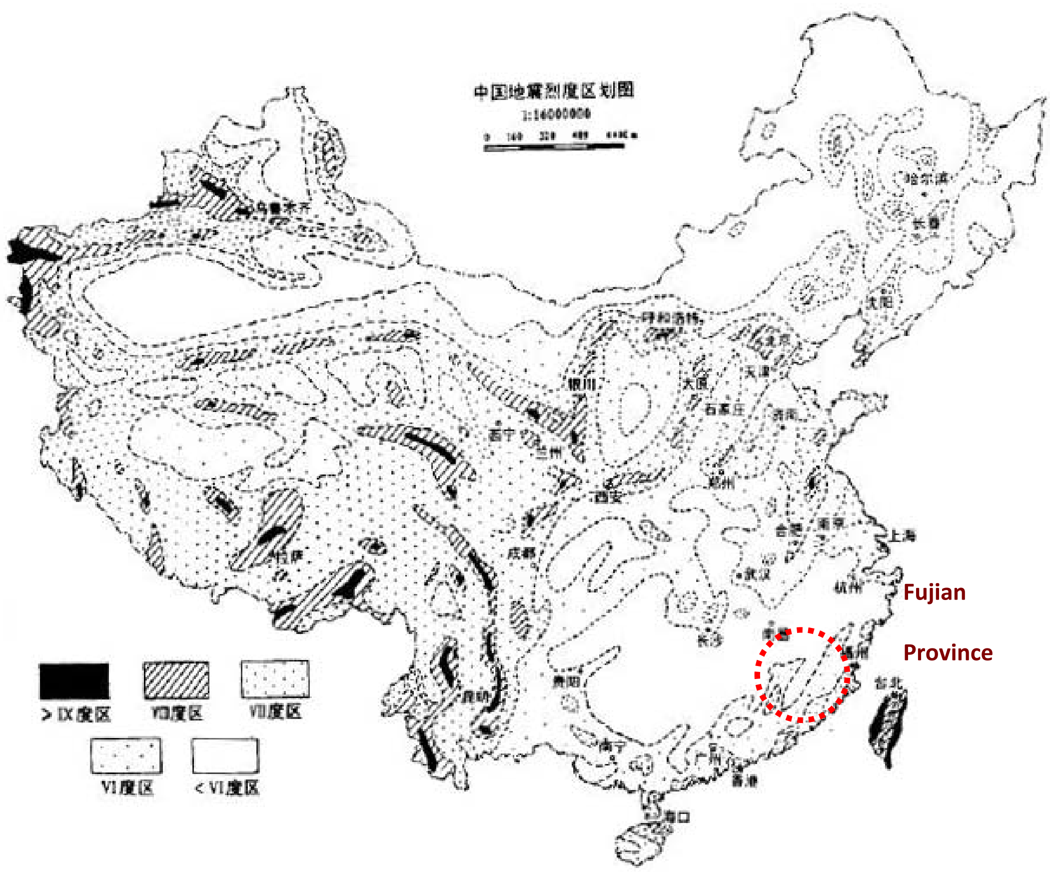

Figure 4.3 : Seismic intensity zoning map in China.

There are about 30,000 earth buildings that have been built in China, mostly completed in the Ming (1368-1644) and Qing (1644-1911) dynasties, in the south and east China provinces. Over 23,000 of them are in the mountainous Yongding County of Fujian (Xinhua 2004). They appeared in China and Central Asia about 5,000 years ago. Over twenty thousand of these historic houses are still standing today, ten of which are over 600 years old. The oldest one, "*Fu Xing Lou*" in Hu Le town, was constructed over 1,200 years ago and is regarded as a "living fossil" of the construction style of central China. In 2008, Fujian's "earthen buildings" (Hakka houses) were given as the World Heritage status for the history of Asian clay culture and uniquely embody the highest artistic skill in rammed-earth construction (Liming & Baoguo 2009).

Earthen houses represent a vernacular architecture specific to Jiangxi, Fujian and Guangdong provinces following the flow of the Hakka people from central China to the South. As most Hakka resided in mountains, communal houses made of compacted earth were built to provide protection against bandits and wild animals. The older examples of this style of construction consist of interior buildings enclosed by huge peripheral ones holding hundreds of rooms and dwellers. With all the halls, storehouses, wells and bedrooms inside, the huge tower like building functions almost as a small fortified city. Earthen houses are made of earth, stone, bamboo and wood, all readily available materials. After constructing the walls with rammed earth, branches, wood, strips and bamboo chips were laid in the wall as "bones" to reinforce it. The end result is a well-lit, well-ventilated, windproof building that is warm in winter and cool in summer (Cultural Institute of Macao 2007).

Circular earth buildings are found in the southern and western part of the Fujian Province. The *Hakka* were originally immigrants who built these architectural types. These buildings are typically designed for protective purposes and consist of a single doorway and no exterior windows at the ground floor. They were often round in shape and internally divided into many compartments for food storage, residence, ancestral temple, weapon storage, etc. The exact period in which they first appeared is not known, but it is believed that they originated from the 13th or 14th century or even earlier. Some were built as late as the late 1900's.

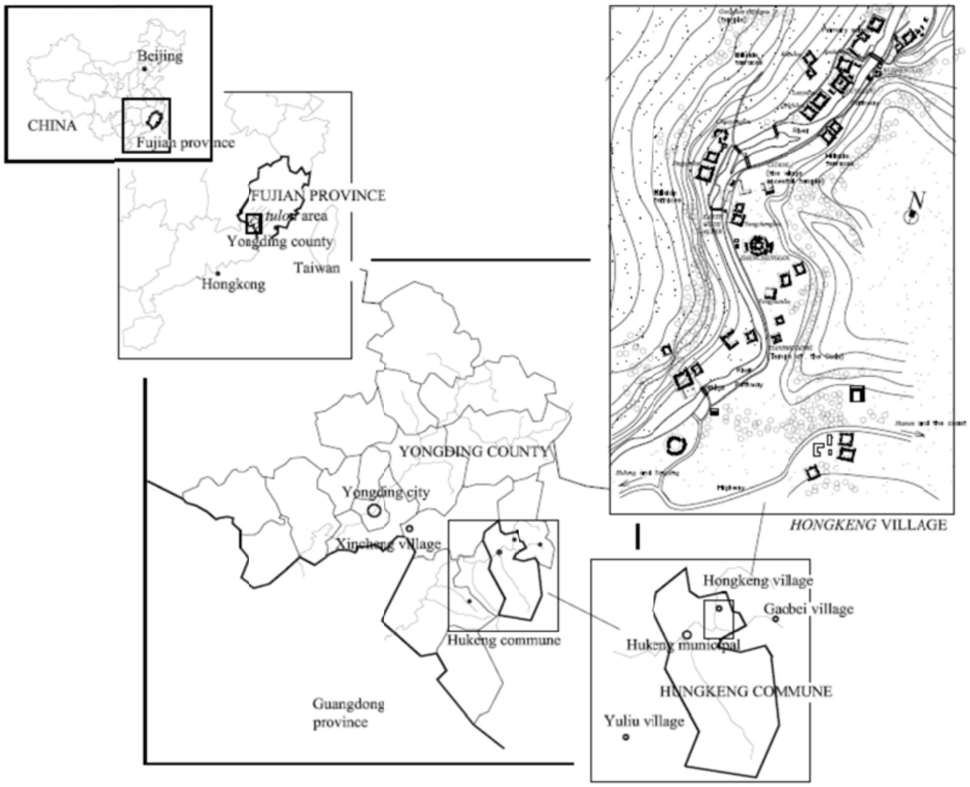

Figure 4.4: The map showing the location of Hongkeng village.

4.2.2 Architectural and structural features

There are perhaps a thousand of these round earth buildings (*Yuanlou*) left today (Aaberg-Jørgensen 2003-04). The largest concentration of these is found in Hongkeng village covering over 40,000 m² (see Figure 4.6). They vary in size, having diameters ranging from 17 to 91 meters. This type of building can be divided into three classes as small, medium and large. The small round building has about 12 to 18 rooms and usually has 2 stories with a single ring. The buildings are made of earth, stone, bamboo and wood. After constructing the walls with rammed earth, branches, wood strips and bamboo chips are laid in the wall to reinforce it. The older earth houses normally consist of an interior ring enclosed by a huge peripheral ring. The main entrance door is padded with an iron sheet. The wall is around one meter thick, with observation holes above the entrance for look out and shooting to prevent attack from bandits and marauders.

Construction details of this circular earthen house are as follows:

1. The foundations of the houses are made of large rounded stones from the local river and filled out with smaller stones. The foundation base is approximately 0.60-0.90 metres high, and large stones are used, the largest of which are placed at the core of the wall. Both sides of the foundation are plastered with clay.
2. The outer wall, constructed by the rammed earth technique, is approximately 1 metre in thickness at the ground floor and the thickness of the wall is reduced as the floor level is rising. This is filled with mud, sand and lime called *sanhetu*, and then pounded with a stone. The outer wall leans inward to resist the outward forces and support of the cantilevered wooden construction. The pressure also increases the wall's resistance to erosion. John Lagerwey (1997) noted that in the past all the earth houses were whitewashed to protect the façade from rain. This protected the facade against rain and also reflected solar heat to reduce overheating in summer time. Nowadays, whitewash was applied only to the window frames.
3. The wooden structure includes all decks and columns and is built in parallel with each floor level, with the outer wall and columns bearing the beams. Almost every construction element except the outer wall and roof cladding is constructed of pine wood. The wooden flooring is fastened with wooden pegs, immersed in hot sand to increase durability. The fire wall stabilizes the earth building and in some cases is used to subdivide the building (Aaberg-Jørgensen 2003-04).
4. There was no window in the thick circular wall for the first two floors, and windows for rooms in the upper floor were very small.
5. The roof construction is built with wooden frame and completed with a slightly downward-curving cladding of grey locally fired tile.

Figure 4.5: The view of Hongkeng village where most earth buildings are located.

Figure 4.6: The Zhencheng Buidling was built in 1912 is the biggest circular earthen form at Hongkeng village(source: www. painaima.com).

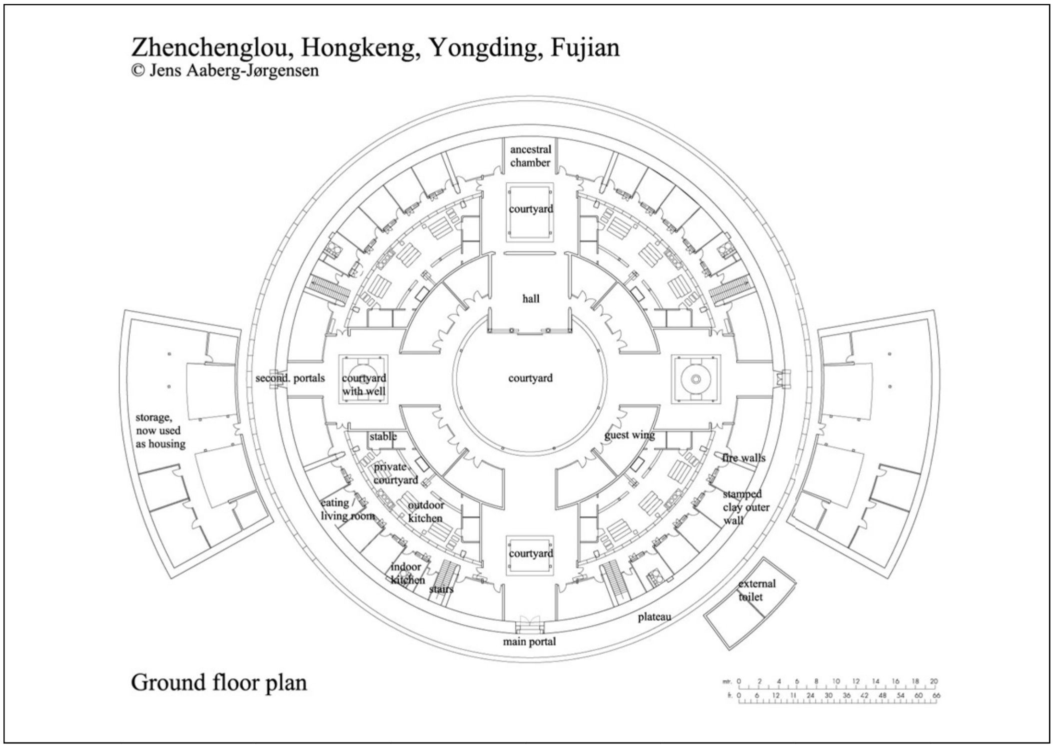

Figure 4.7: Ground floor plan of the circular earthen form.

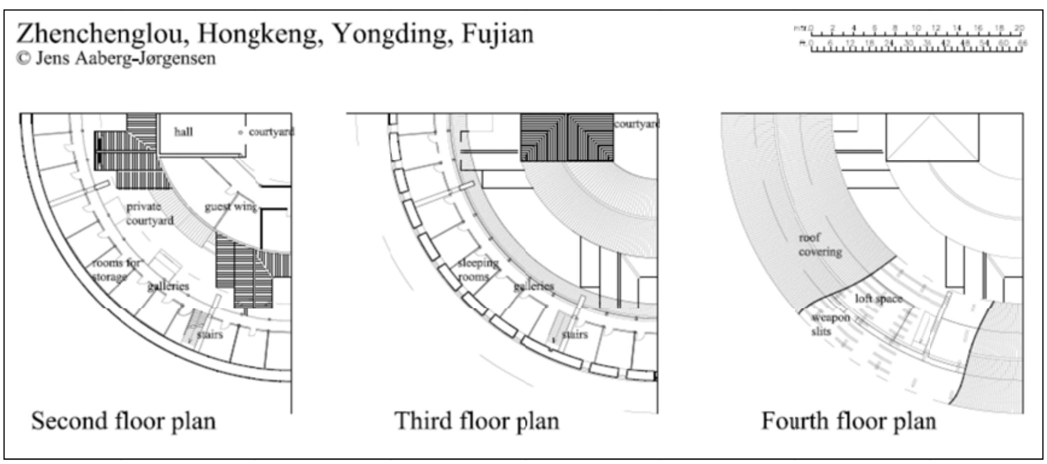

Figure 4.8: The 2nd- 4th floor plans of the circular earthen form.

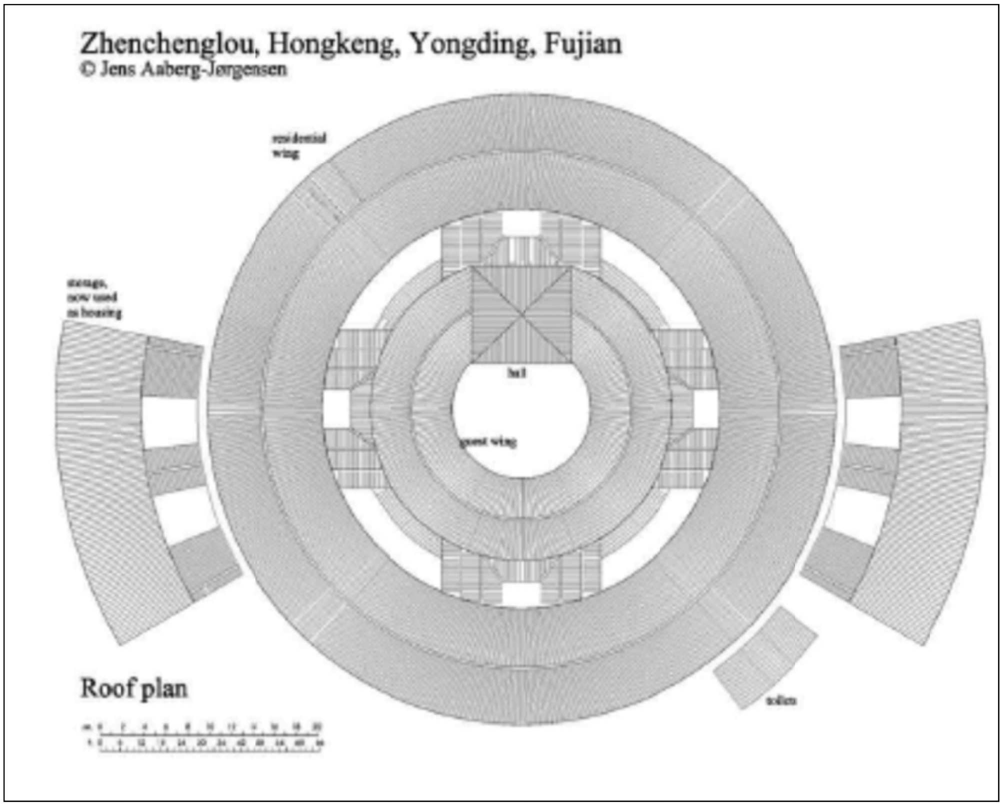

Figure 4.9: The roof plans of the circular earthen form.

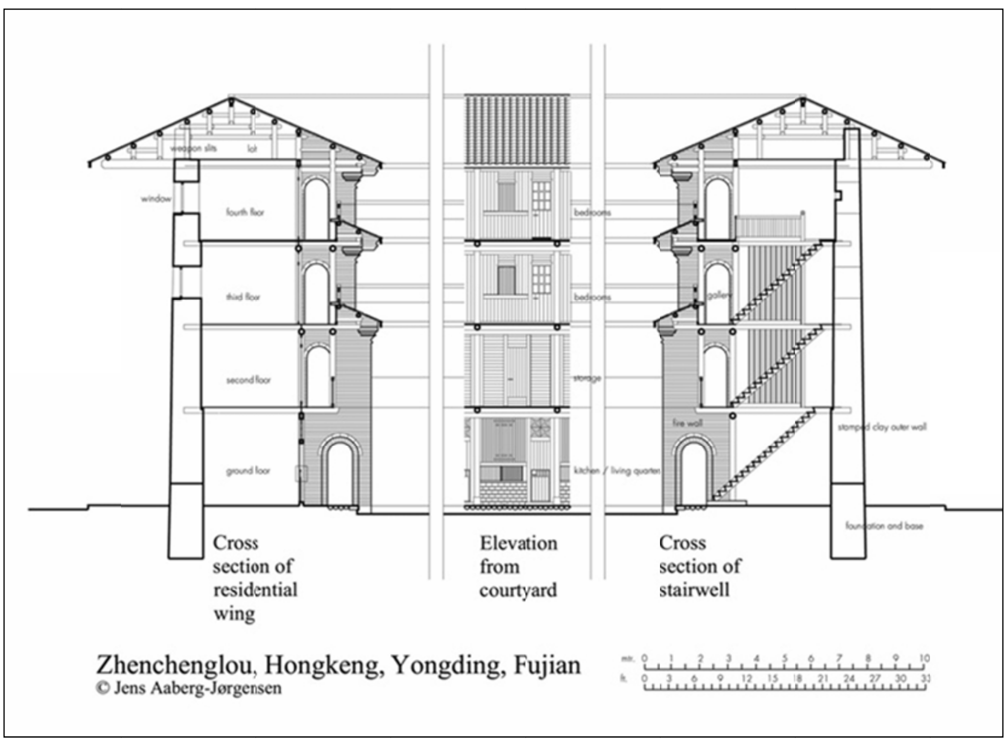

Figure 4.10: The cross section of the circular earthen form.

Figure 4.11: The wooden frame supported the inner earthen wall (Sunny Cai, 2008).

Figure 4.12: Earthen wall with small openings (Sunny Cai, 2008).

4.2.3 Building performance in earthquake

These types of buildings are located in earthquake active zones, zone VI-VII, which are indicated in Figure 4.3 (peak ground acceleration = 0.4-0.8 m/s^2). Fujian province has had a total of 52 earthquakes over time, with the most severe one measuring 4.9 on the Richter scale. In 1918 it withstood an earthquake measuring 6.2 on the Richter scale. Recently, on 13th March 2007, 2 earthquakes measuring 4.9 and 4.7 on the Richter scale struck northern Fujian province. These earthquakes had affected 457,000 people and 5,969 houses in Fujian (FMG 2007).

Ole Vanggaard (2003) noted that a circular building, *Tulou,* has greater static stability due to the shell action of cylindrical walls. The cylindrical shell is further strengthened considerably by the rigid, horizontal and circular decks of each floor (membrane forces). The outer wall construction using rammed earth has excellent static stability for the compression force and for transferring the lateral force. The inner wall construction of timber-frame adds further rigidity and strength and being fixed in four directions the timber-frame creates an integrated matrix which restrains movement and enhances the overall strength of the structure.

4.3 Bhunga houses in India

4.3.1 Background

The *Bhunga* house is a traditional construction type of Kutch district of Gujarat state in India, with a very high seismic hazard. More than 50 percent of the area in the country is considered prone to damage by seismic forces. For instance the Koyna earthquake in 1967 (magnitude 6.6), the Latur earthquake in 1993 (magnitude 6.4), and the Jabalpur earthquake in 1997 (magnitude 6.0) (Jain 1998). Kutch also has experienced more than 90 earthquakes in the past 185 years (Wikimedia Foundation 2009b). It is the largest district in the state of Gujarat covering an area of 45,612 km². In 2001, the district had a population of 1,583,225 of which 30% were urban.

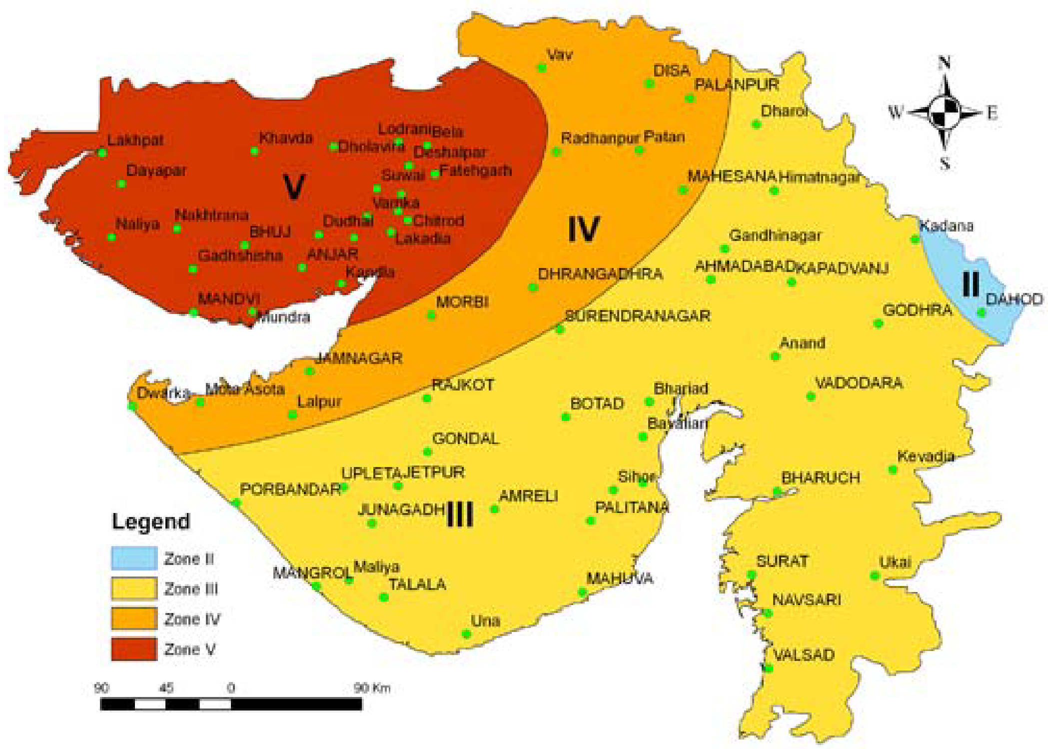

Figure 4.13: Seismic zoning map of Gujarat
(source: The Institute of Seismological Research (ISR)).

Figure 4.14: Map of district of Kutch of Gujarat State (India).

In January 2001, a Richter 7.8 earthquake hit the Kutch district. About 50,000 people were killed and one million people were left homeless. Most of the brick masonry and concrete buildings in the district were destroyed. While the circular adobe-huts were still intact (Amir, January 2005).

Figure 4.15: Typical circular earthen hut of Kutch district (Amir January 2005).

A *Bhunga* house consists of a single cylindrically shaped room and has a conical roof which is supported by cylindrical walls. This type of construction has existed for several hundred years (Sassu 2002). Bhunga is quite durable and suitable for prevalent desert conditions. It also performed very well in the recent earthquake measuring 7.9 on the Richter scale at Bhuj town, on 21 January 2001. About 97 houses in Harijan community were totally collapsed, except for traditional round earthen structures which survived unscathed (Landon 2001). The seismologists and experts associated with the Gujarat state disaster management authority (gsdma) recommended their people to build new earthen houses with typical circular bhunga style in urban, semi-urban and rural areas of quake-devastated kutch (TNN 2001).

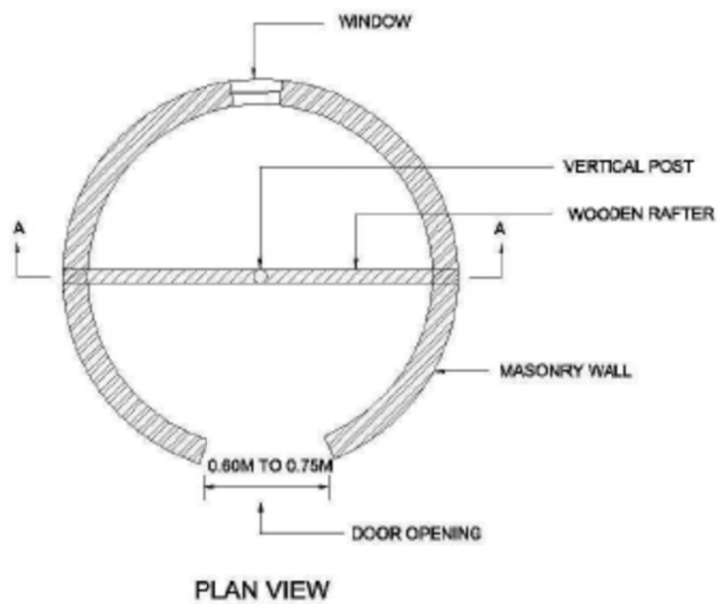

Figure 4.16: Plan of a typical circular building.

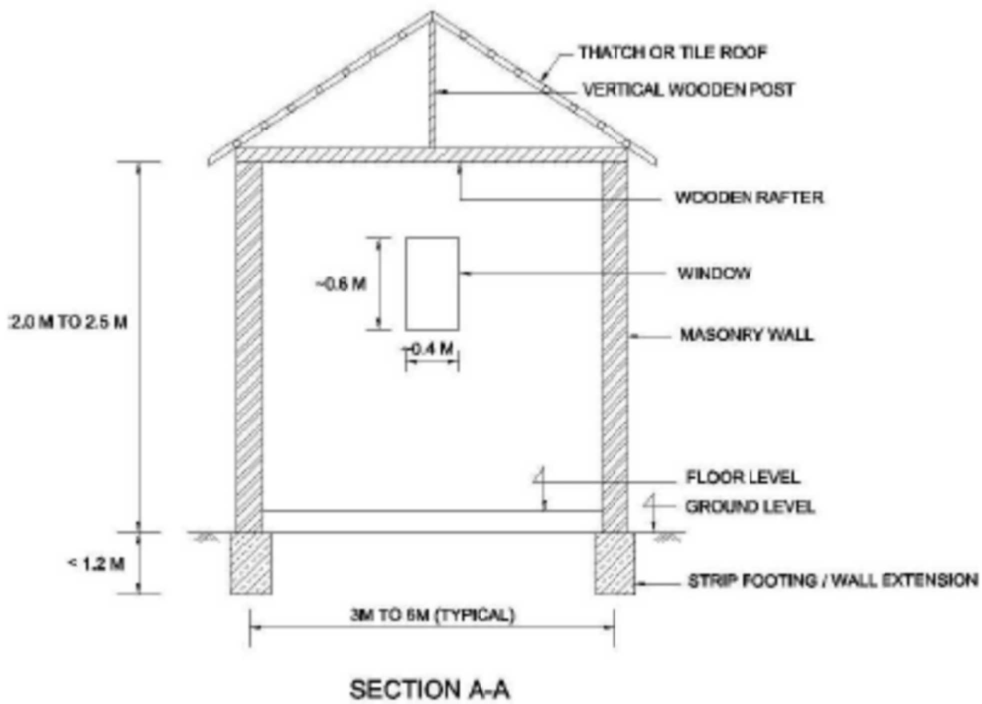

Figure 4.17: Section of the circular house.

Figure 4.18: Light roof structure of Bhunga house.

4.3.2 Architectural and structural features

A Bhunga generally has only three openings, one door and two small windows. This type of construction is usually found on flat terrain. It is circular in plan, with cylindrically shaped walls and topped with conical roof. The internal diameter of the Bhunga is typically between 3m to 6m and the thickness of unreinforced adobe wall is 330 mm (Choudhary, Jaiswal & Sinha 2002). The main function of this type is a single family house and each house also comprises a single room unit. Recent buildings have used a wide variety of construction materials. These include stone or burnt brick masonry either in mud mortar or in cement mortar. Traditional roof consists of light-weight conical roof, while some recent constructions have used heavy tiles on roofs. Some recent constructions have used circular strip footing below the wall, while traditional construction simply extended the walls below ground level.

Figure 4.19: Bhunga houses in India.

4.3.3 Building performance in earthquake

This type of tradition house shows great stability under earthquake situations. This is confirmed by the reports form the World Housing Encyclopaedia by Mauro Sassu (2002). This report also cited its advantages for earthquake resistance as follows:

1. *Due to its circular shape of wall in plan, inertial forces developed in the walls are resisted through shell action providing excellent resistance to lateral forces.*
2. *The thick walls required for thermal insulation have high in-plane stiffness which provides excellent performance under lateral loads.*
3. *The roofing materials, such as bamboo and straw, are generally very light weight and develops low inertia forces. These roofs is usually very robust. Even in situations where the roof collapses, its low weight ensures that the extent of injuries to occupants is very low.*
4. *The roof joist is not directly supported on the cylindrical walls, but is supported by two wooden vertical posts outside the Bhunga, which further improves seismic resistance of the inertia force generated in the roof. In some instances, reinforcing bands at lintel level and collar level have been used to provide additional strength. These bands are constructed from bamboo or from RCC. These increase the lateral load-carrying strength greatly and increase the seismic resistance of the Bhungas.*
5. *Wall layout is suitable for adobe masonry constructions located in seismic areas. The total width of wall openings of Bhunga house is less than 1/3 of the distance between adjacent cross walls and its height-to-thickness ratio of shear wall is less than 13.*

Sussu (2002) also reported that the seismic resistance features of this type of building came from their suitable building configuration and a complete load path for seismic forces effects from any lateral direction serves to transfer inertial forces on the building to the foundation.

4.4 Yomata houses in Malawi

4.4.1 Background

Malawi is located in the most seismically active belt of the East Africa (Lostina 2001). In general, there are higher magnitude earthquakes in the northern part ($M \geq 5.5$) than in the south part ($M<5.0$) of Malawi (Chapola 2000). Historical records show strongly felt earthquakes reported in various parts of the country, but no damage to property or loss of life has been recorded until the 1989 Salima earthquake occurred, which resulted in 9 people being killed and over 50,000 people were left homeless (USGS 2009b). Table 4.1 shows the history of earthquake activities in Malawi. However, the Yomata circular earthen houses performed well even under the worst earthquake activity.

Table 4.1: History of past-earthquakes in Malawi

Year	Epicentre	Magnitude	Intensity
1957	Champira	5	MMI IIIV
1966	Mwanza	5.3	
1967	Thambani in	5.4	
1989	Salima	6	MMI VIII

Figure 4.20, an estimation of seismic hazard for hard rock sites, shows that peak ground acceleration (PGA) for a 10% probability of exceedance in 50 years (475 years return period) for the entire country range from 180-240 gals or about VIII in modified Mercalli Intensity. Lostina serrah Chapola (2000) cited that this intensity would cause damage to ordinary brick buildings and completely destroy clay buildings. And geologists forecasted more intense earthquakes will happen in this region (Sassu & Ngoma 2002). On the other hand, Malawi still has no consideration of earthquake ground motions in its building and seismic design codes.

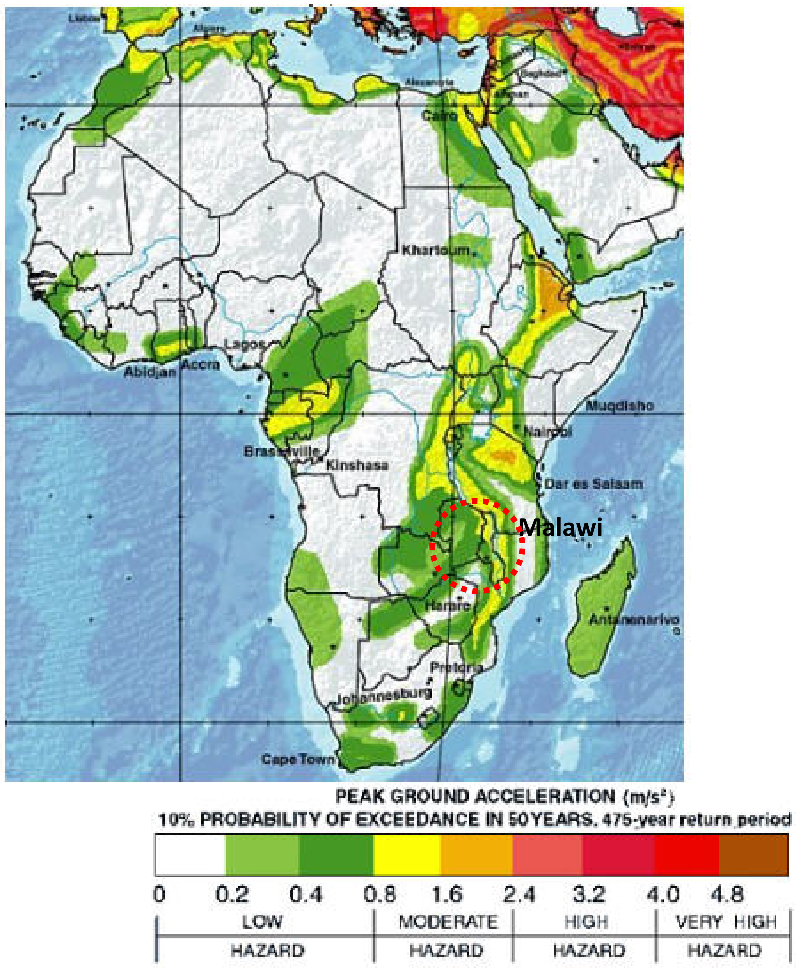

Figure 4.20: Seismic hazard map of Africa.

The Yomata houses are the traditional building of Malawi that can be found in the three areas of Malawi, such as Northern, Central and Southern region. This type of building construction is normally found in rural areas. The building type is a wattle and daub construction. It has been constructed for less than 200 years and more of them are being built currently (Sassu & Ngoma 2002). Such constructions are usually found in flat topography and comprise about 5% of the entire housing stock. This construction type is only built for residential purposes.

Figure 4.21: A traditional Yomata with thatched roof.

4.4.2 Architectural and structural features

A typical Yomata house is constructed generally in a circular shape plan, and it is for single family use. There is no window in this type of circular housing. The space between each house is approximately 3 meters. It has only one door with the size ranging from 1.50 to 1.70 metres in height, and 0.60 to 0.80 metres in width. The diameter of the circular plan is about 3 to 4 meters. The height-to-thickness ratio of wall is about 10/1. The height is generally about 2 metres.

These types of buildings have a shallow foundation. The wall structure is made of mud bricks. However, some houses are constructed with wooden poles reinforcement inside the earthen wall (see Figure 4.21). A thatched roof, a central pole of 0.2 - 0.3 m in diameter is placed in the centre to receive sloping members (60 - 70 mm diameter) acting as rafters spanning to circular walls. The angle of the pitched roof is typically not less than 20 degrees. The grass depth is about 25mm forming a thatched roof. Figure 4.22 shows a typical Yomata houses.

Figure 4.22: Typical Yomata buildings.

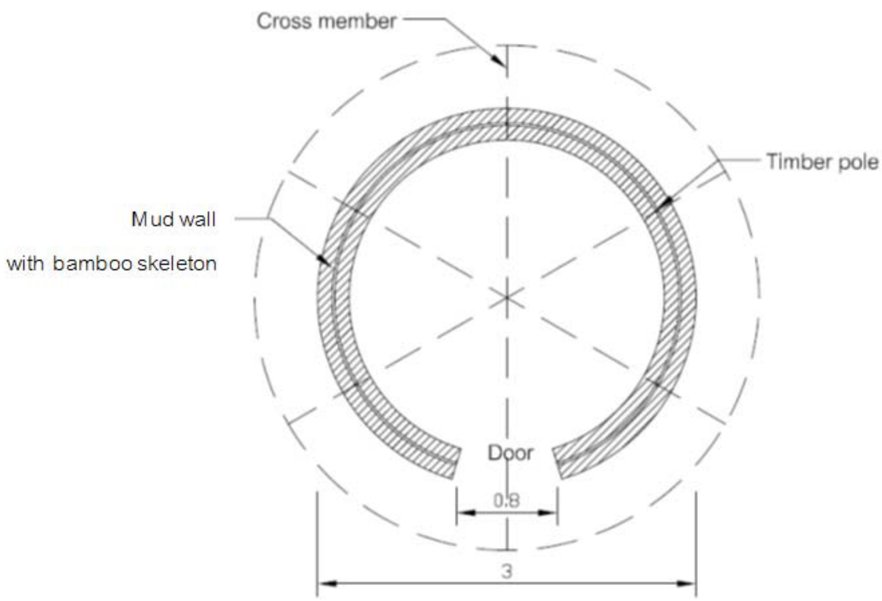

Figure 4.23: The typical plan of Yomata house.

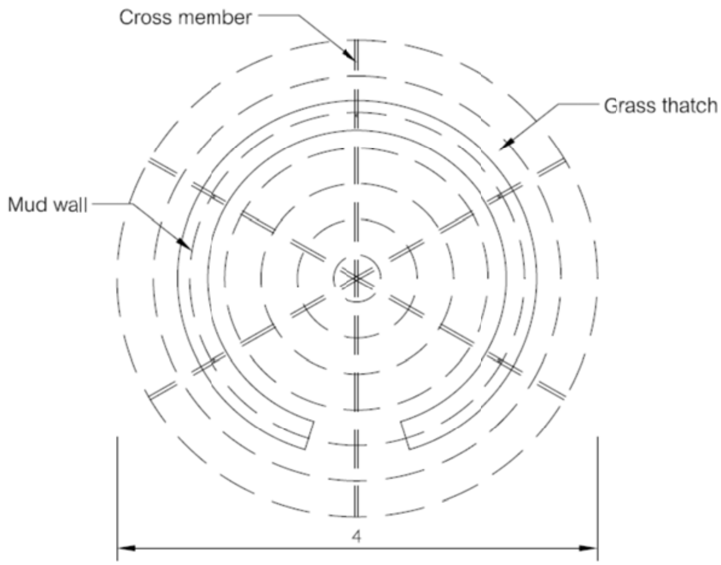

Figure 4.24: A typical roof structure of Yamata house.

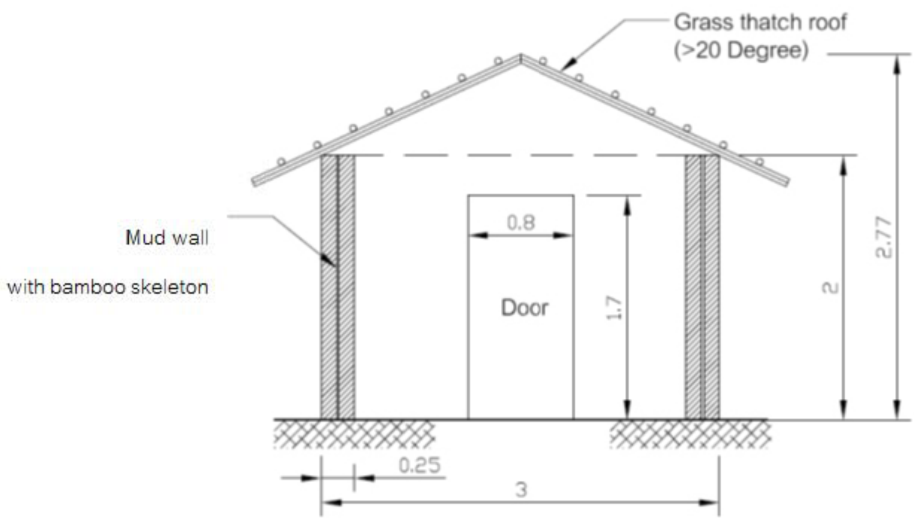

Figure 4.25: A typical section of Yamata house.

4.4.3 Building performance in earthquakes

Mauro S assu (n.d.) not ed t hat typical *Yomata* houses pe rformed well durin g earthquakes, and he pointed out the main reasons as follows:

- *The circular floor plan achieves more desirable seismic performance when compared to rectangular building plan. The latter creates problems with wall separation at the corners and out-of-plane collapse.*

- *Use of timber to reinforce earthen walls can increase ductility and secure the connections, and this ensures a good seismic response.*
- *Lightweight roof structures result in much superior seismic performance when compared to the heavy roofs such as traditional adobe construction in Bam, Iran. Their traditional thatched roof reduces the mass on the top of wall which attracts lower seismic force due to inertia and also makes it safer against falling roof tiles*.

Sassu (n.d.) also noted that the seismic resistance features of this type of building came from their appropriate building configuration and quality of workmanship. However, the seismic vulnerability may increase by poor connections of the wood skeleton and by progressive damage to the natural components.

4.5 Summary

This chapter presented case studies on the existing circular earthen dwellings which have shown good performance in seismic hazard regions in China, India and Malawi, covering the following components:

- General description of region.
- Construction specifications of these earthen structures.
- How do they perform under earthquake forces? What features do they have to resist earthquake?

These studies have provided information for understanding some key aspects of these seismically resistant earthen houses. The most remarkable aspect was that shell action in cylindrical walls provided a great static stability to resist seismic forces. The inertial forces developed in the walls are resisted through shell action providing excellent resistance to seismic forces. Table 4.2 shows the comparison of their configurations which are related to their earthquake resistance effects.

Table 4.2: Comparison of the existing adobe houses' configuration

Building proportions	**Hakka house** (China)	**Bhunga house** (India)	**Yomata house** (Malawi)
Wall height-to-thickness ratio	13/1	13/1	13/1
Height-to-width ratio	3/10	8/10	6/10
Door opening in earthen wall	2.50 x 1.80	2.00 x 0.75	1.70 x 0.80
Window opening in earthen wall	1.00 x 0.60	0.60 x 0.40	-
Total area of openings	Less than 0.3 x area of wall	Less than 0.3 x area of wall	Less than 0.3 x area of wall
Roof structure	Heavy-weight roof	Light-weight roof	Light-weight roof

Table 4.2 shows the important features of these buildings for seismic resistance such as their wall opening and slenderness ratios. All these buildings had small wall openings which contribute to their good seismic performance. Their wall slenderness ratios are higher than the recommendations from the adobe guidelines and manuals presented in Chapter 2, which should be less than 8 (IAEE guidelines). These data show a better performance of circular shapes than square ones and support the thesis statement in

Chapter 1. In addition, it can be noticed that Yomata houses have shown good seismic performances, even when the total width of opening is more than 1/3 the distance between adjacent cross walls.

In conclusion, this chapter investigated the existing circular earthen buildings that have performed well in seismic activities, and noted their features compared with other earthen buildings.

The analysis results of the three case studies are further used in Chapter 5 for the comparison of their seismic resistance by using the static equilibrium equation.

Chapter 5 Simple Static Earthquake Design Method

5.1 Introduction

This chapter describes the simple static design method for determining earthquake loads according to Australia Standard AS 1170.4. It also covers the determination of the scale effects and the calculation of the natural frequencies of circular buildings using the formulas from seismic codes.

5.2 Description of static design method

The equivalent static load method for designing earthquake forces is allowed in many codes (see Section 3.5 in Chapter 3). This method is generally used for the seismic design of building structures to represent their seismic resistance. Structures should be designed to withstand the seismic forces without any considerable losses (NICEE 2002c).

Australian Standard AS 1170.4 (2007) states that the in-plane and out-of-plane earthquake forces can be calculated using an equivalent static method. This method relies on the assumption of an equivalent static analysis. The method replaces dynamic earthquake actions by horizontal equivalent static base shear force (V) given by the following expression, as specified in section 6 of AS 1170.4.

The base shear equation is-

$$V = k_p \times Z \times C_h(T_1) \times (S_p / \mu) \times W_1 \tag{5.1}$$

Where:

k_p = Probability Factor for the annual probability of exceedance

Z = Hazard Factor (Ground acceleration) for specific locations

$C_h(T_1)$ = Spectral shape factor dependent on sub soil and period of vibration

μ = Ductility Factor = 1.25 for unreinforced masonry

S_p = Structural Performance Factor = 0.77 for Unreinforced masonry

W_1 = Seismic weight of the structure taken as the sum of the total weight of the structure as given by the following equation:

$$W_i = G_i + \psi_c Q_i$$

Where:

G_i= permanent action (self-weight or dead load) at level i

ψ_c = earthquake-imposed action combination factor = 0.3

Q_i = imposed action for each occupancy class at level i

The base shear force is distributed amongst the various floors of the building in accordance with Clause 1.2.

$$F_i = \frac{W_i h_i^k}{\sum_{j=1}^{n} \left(W_j h_j^k \right)} \left[k_p Z C_h \left(T_1 \right) \frac{S_p}{\mu} \right] W_t \tag{5.2}$$

where

W_i = seismic weight of the structure at the i^{th} level

h_i = height of level i above the base of the structure, in metres

k = exponent, dependent on the fundamental natural period of the structure (T_1), which is taken as:

1.0 when $T_1 \le 0.5$;

2.0 when $T_1 \ge 2.5$; or

linearly interpolated between 1.0 and 2.0 for $0.5 < T_1 < 2.5$

n = number of levels in a structure

The horizontal equivalent static earthquake shear force at the story i is the sum of all the horizontal forces at and above the i th level (F_i to F_n).

The spectral shape factor depends on the fundamental vibration period of the structure and on the soil type. (See Table 5.1 for shape factors of structures on rock and soft soil.)

Table 5.1: Values for specific shape factors

Fundamental Period of structure (seconds)	Rock Soft	Soil
0	2.94	3.68
0.5	1.76	3.68
1.0	0.88	1.98
1.5	0.59	1.32
2.0	0.33	0.74
2.5	0.21	0.48
3.0	0.15	0.33

AS 1170.4 gives the following expression for the period of vibration of masonry buildings as:

$$T = 0.0625h^{0.75} \tag{5.3}$$

Where:

h = height from the base of the structure to the uppermost seismic weight in metres

For a building less than 8.5 m high the corresponding natural period would be less than 0.3 seconds using the above formula. If one assumes the worst case scenario of soil, this yields a spectral shape factor of 3.68. Substituting this value for $C_h(T_1)$ and values for μ and S_p into formula (5.1) gives:

$$\begin{aligned} V &= 3.68 \times 0.77 / 1.25 k_p Z W \\ &= 2.3 k_p Z W \end{aligned} \tag{5.4}$$

This is equivalent to the simplified formula for unreinforced masonry structures given in appendix A of AS1170.4.

The AS/NZ1170.0 (Australian/Newzealand Standard 2002), requires buildings to be designed for an annual probability of exceedance of 1/500 for earthquakes which gives a k_p of 1.0. The maximum hazard factor (Z) in continental Australia is 0.22 but for example in Macquarie Island it is 0.60.

Using formula (5.4) then:

$$V = 0.5W \text{ (max in Australia)} \tag{5.5}$$

$$= 1.38W \text{ (for Macquarie Island)} \tag{5.6}$$

Note that these assume a worst case scenario in terms of the sub-soil and an approximation for the natural frequency of the structure.

5.3 Relationship between design loads and tilt table performance

5.3.1 Maximum normal stress for design condition

The maximum normal stress theory, in association with Coulomb or Rankine criterion, is often used to predict the failure of brittle materials (Beer, Jr. & DeWolf 1915). It states that the brittle materials generally fail when the maximum normal (principal) stress in that component reaches the ultimate tensile strength (σ_{ut}) obtained from the tensile test of a specimen of the same material. The value of the normal stress that causes a structural element to fail is equal to the ultimate strength of the material. Maximum normal stress could be expressed as:

$$\sigma_{\max} = \frac{(\sigma_x + \sigma_y)}{2} \pm \sqrt{\left(\frac{\sigma_x - \sigma_y}{2}\right)^2 + \tau_{xy}{}^2} \tag{5.7}$$

Where:

$\sigma_{\max}$ = Maximum normal stress

σ_x and σ_y = Normal stresses in X and Y direction

τ_{xy} = Shear stress in XY plane

Therefore, as per maximum normal stress theory/criterion, the structure will be safe if:

$\sigma_{\max} < \sigma_{ut}$

Where:

σ_{ut} = Ultimate tensile strength

According to the theory, the typical ultimate strength of adobe structures can be represented by their maximum normal stresses.

Using either formula (5.1) or (5.4) in Section 5.2 gives a design value of lateral force for a building in a particular hazard zone and for particular ground conditions.

Note that for a single storey building the design horizontal force is applied at roof level. The equilibrium condition is summarised in Figure 5.1, where k is calculated in accordance with formula (5.1) or (5.4).

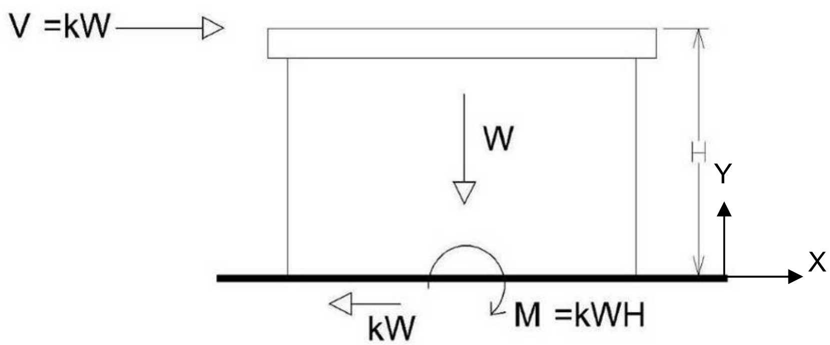

Figure 5.1: Horizontal design earthquake loads for a single story building.

For a circular building of height *H*, diameter *D* and wall thickness *T*.

Compressive stress $(f_c) = \frac{W}{A}(kN/m^2)$ (5.8)

Maximum bending compressive stress $(f_{bc}) = \frac{M}{Z} = \frac{kWH}{\frac{\pi}{32D}\left(D^4 - D_I{}^4\right)}(kN/m^2)$ (5.9)

Average Shear stress $(f'_S) = \frac{kW}{A}(kN/m^2)$ (5.10)

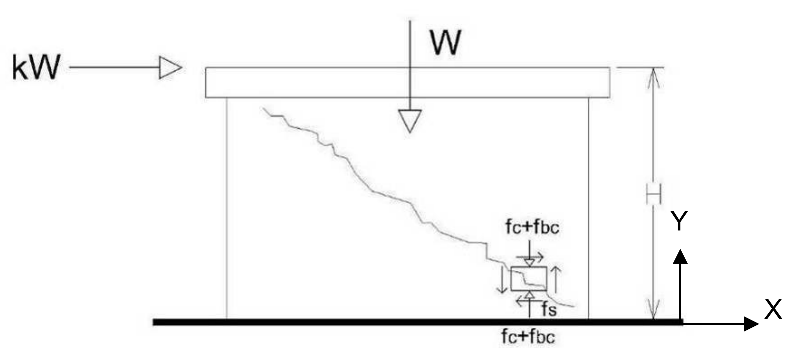

Figure 5.2 : Shear forces on circular adobe building.

Maximum shear stress ($f_{s\,max}$) **=** $\sqrt{\left(\frac{f_c + f_{bc}}{2}\right)^2 + f'^{\,2}_s}$ (5.11)

Maximum normal stress ($\sigma_{\max}$) **=** $\frac{f_c + f_{bc}}{2} + \sqrt{\left(\frac{f_c + f_{bc}}{2}\right)^2 + f'^{\,2}_s}$ (5.12)

Note that there is no normal stress in the X direction.

5.3.2 M aximum normal stress for models

The loads on the models at the failure angle θ are summarised in Figure 5.3 below.

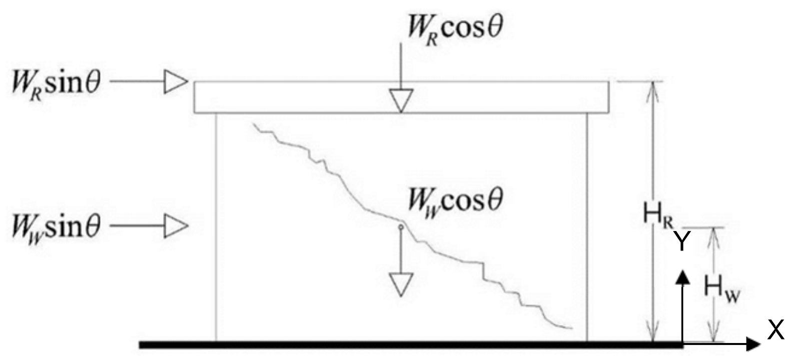

Figure 5.3: Shear forces on circular adobe model at failure angle.

In this case:

Compressive stress $(f_c) = \dfrac{(W_R + W_W)\cos\theta}{\frac{\pi}{4}\left(D^2 - D_I^{\,2}\right)}$ (5.13)

Maximum bending compressive stress $(f_{bc}) = \dfrac{(W_R \sin\theta H_R + W_W \sin\theta H_W)}{\frac{\pi}{32D}\left(D^4 - D_I^{\,4}\right)}$ (5.14)

Average shear stress $(f'_S) = \dfrac{(W_R + W_W)\sin\theta}{\frac{\pi}{4}\left(D^2 - D_I^{\,2}\right)}$ (5.15)

Maximum shear stress ($f_{s\,max}$) **=** $\sqrt{\left(\frac{f_c + f_{bc}}{2}\right)^2 + f'^{\,2}_s}$ (5.16)

Maximum normal stress($\sigma_{\max}$) **=** $\frac{f_c + f_{bc}}{2} + \sqrt{\left(\frac{f_c + f_{bc}}{2}\right)^2 + f'^{\,2}_s}$ (5.17)

5.3.3 Hypothesis of the failure criteria as link between design and model behaviours

Using the formula given in Section 5.3.2, the maximum normal stress at failure for all tests can be worked out as the hypothesis of the failure criteria for all static tests. They should represent the shear capacity of the adobe walls. In the design situation loads are calculated for the appropriate soil conditions and the earthquake zone according to formula (5.1) and then the maximum design shear stress is calculated as per Section 5.3.1.

In a given situation if the maximum design shear stress is less than the failure stress by a suitable margin then the structure can be assumed to be safe.

This hypothesis of the failure criteria is used to calculate the predictive performance of the circular adobe models in Chapter 8.

5.4 Theory of reduced scale model testing

The theory of reduced-scale model and the application of the theory to the model testing in this research project are presented in this section.

For the behaviour of a small-scale model to accurately simulate the corresponding behaviour of a full size structure, the theory of reduced model should be applied. Moncarz and Krawinkler (1981) cited that small-scale model structures were fabricated and tested with the purpose of investigating the accuracy of prototype response predictions. In order to accurately compare the results it was necessary to apply the modeling theory. Krawinkler (1988) also referred that scale effects in both static and dynamic models for earthquake testing should be considered.

The theory established the rules according to which the geometry, material properties, initial conditions and boundary conditions of the prototype and model can be related. Therefore, the behaviour of the reduced-scale model can predict the behaviour of the prototype. The laws of similitude can be derived through dimensional analysis involving an entire set of scaling laws defining the prototype and model correlation (Tolles & Krawinkler 1990b). In order to achieve modelling requirements especially for dynamic test, there were three basic model types as true replica model, models with artificial mass simulation and model with gravity forces neglected (Moncarz & Krawinkler 1981). Table 5.2 shows a listing of similitude requirements.

Table 5.2: Similitude requirements (Moncarz & Krawinkler 1981)

Model scaling parameters	True replica model	Artificial mass model	Ignoring gravity model
Length (l)	l_r	l_r	l_r
Time (t)	$l_r^{1/2}$	$l_r^{1/2}$	l_r
Frequency (f)	$l_r^{-1/2}$	$l_r^{-1/2}$	l_r^{-1}
Velocity (v)	$l_r^{1/2}$	$l_r^{1/2}$	1
Gravitational acceleration (g)	1	1	Ignoring*
Acceleration (a)	1	1	l_r^{-1}
Mass density (ρ)	E_r / l_r	augmented**	ρ_r
Stress (σ)	E_r	1	1
Stain (ε)	1	1	1
Modulus of elasticity (E)	E_r	E_r	E_r
Displacement (δ)	l_r	l_r	l_r
Specific stiffness (E / ρ)	l_r	augmented**	1
Force (F)	$E_r l_r^2$	l_r^2	l_r^2

Subscript notation: r refers to the ratio between model and prototype (E. Leroy Tolles 2000).

**Effects of gravity are neglected because this theory assumed that the effects of gravity forces are minor* (E. Leroy Tolles 2000).

***Mass of the building augmented by adding additional structurally ineffective mass to the building* (E. Leroy Tolles 2000).

Accordingly, the prototype material was used in the model for this research project, Tolles and Krawinkler (1990b) cited that *the input accelerations be increased by the factor* $1/l_r$ *and the time be compressed by the factor* l_r.

Krawinkler (1988) also reported *effects of scaling on the response of models of masonry and adobe structures and elements* that small-scale adobe models in seismic tests had some considerable issues as follows:

- *The number of cracks decreases with a decrease in model size.*
- *Increasing mortar strength and bond strength between mortar and brick compared to prototype behaviour. The main reasons appear to be size effects due to the increased surface-to-volume ratio in models.*
- *A larger increase in strength quantities governed by tension (e.g., bending and "shear") than by compression.*

- *In static testing, the only scale effects result is scaling time compared to the dynamic response that slow testing results in a decrease in strength and deterioration.*
- *In dynamic model tests the scaling laws for forces, time, and other dependent dimensional quantities can be derived through dimensional analysis.*

The issues mentioned in this section were not considered to be of principal significance since the purpose of this research was to study the global response characteristics of the adobe models. The reduced-scale models' failure performance should be nearly the same as found in the prototype. However, the response of the small-scale model structures still contained the global characteristics of a prototype which can provide useful data for understanding the behaviour of circular adobe structures.

For this research project, the study on scaling effect between prototype and scaled models will be further investigated in Section 9.5.3. The results will be applied to dynamic tests.

5.5 Calculations of static design loads of the existing circular adobe houses

This section presents the calculations of static design loads of the existing circular earthen houses from the three case studies mentioned in Chapter 4.

These three case-studies have been carried out in different regions and most of them used different static equilibrium equations and factors to calculate lateral forces. China and India also have their own earthquake codes whereas Malawi does not have any existing code. However, these existing earthquake codes may not give reliable outcomes. Wilbowo et al. (2008) cited that the earthquake intensity in Chinese Earthquake Code was lower than what it should be. For example the Chinese earthquake Code GB50011-2001 classified the peak ground acceleration (PGA) of the Fujian province as 0.10g but the global seismic hazard map by GSHAP indicated the PGA value of the Fujian province was in the range of 0.40-0.80g (Figure 5.5). Therefore, the author had designed to use the static equilibrium equation stated in

AS1170.4 to calculate static shear forces for the three cases with consistent outcomes. In addition, the global seismic hazard map was used to indicate the peak ground acceleration's values for all case studies (see Figure 5.6).

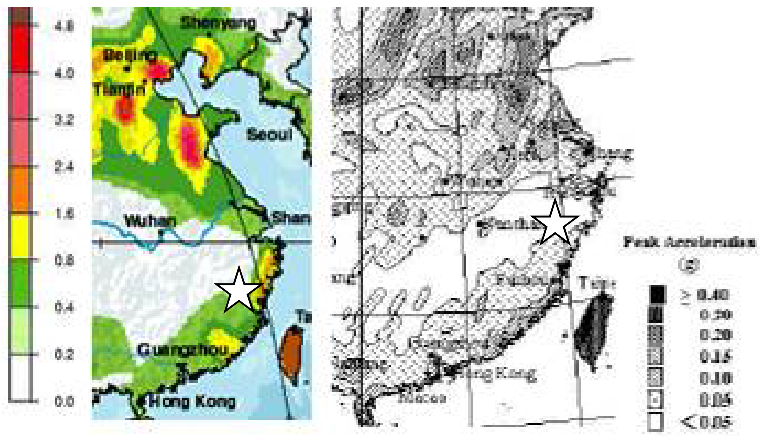

Figure 5.5: Comparison between the seismic zoning maps produced by China Earthquake Administration (CEA) (right) and that produced by the Global Seismic Hazard Assessment Program (GSHAP) (left).

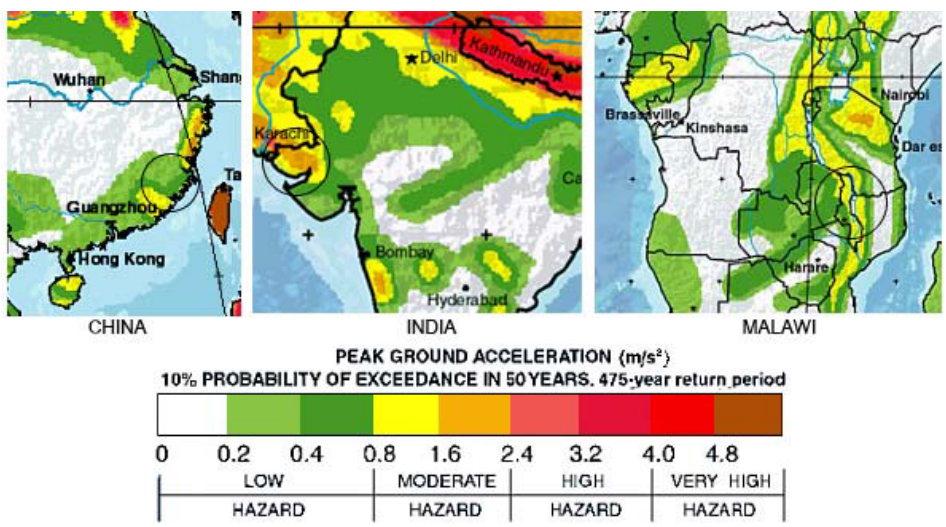

Figure 5.6: Comparison of the peak ground acceleration for each case study's region relying on the global seismic hazard map.

Prior to calculating the static lateral forces, the dimensional configurations of these three buildings were summarized using data from the previous study in Chapter 4 (see Table 4.2). In order to get consistent calculations conditions, similar wall heights and diameters of two case studies, India and Malawi, were applied. In addition, the smallest size earthen building in China was selected.

The probability factor (k_p) for the annual probability of exceedance can be obtained from Table 3.1 of AS1170.4 which gives the probability factor from the global seismic hazard map of 1.0 for 1 in 475 annual probability of exceedance (return period of 475 years).

The hazard factor (Z) for each area is determined from the zoning colour of each seismic hazard map (see Figure 5.6) and then compared with the hazard map of Australia from AS1170.4 to get the approximate value.

The site sub-soil condition was assumed to be class D_e 'soft soil' for all cases.

The ductility and performance forces (S_p / μ) was 0.616 for adobe structures.

The fundamental periods of the structures for these cases are calculated by using equation 5.3 defined in Section 5.2. The spectral shape factors are applied from Table 6.4 of AS1170.4.

The specifications and factors related to existing circular adobe buildings are presented in Table 5.3.

Table 5.3: Comparitive parameters of the existing circular adobe buildings

Parameters	Hakka house	Bhunga house	Yomata house
Height (*m*)	6.5 (2 stories)	2.2	2.2
Outside diameter (*m*)	17.0	3.0	3.0
Wall thickness (*m*)	1.0	0.33	0.20
Total weight of structure* (*kN*)	9,560**	103	66
Sub-soil type	Soft soil	Soft soil	Soft soil
Probability factor (k_p)	1.0	1.0	1.0
Hazard factor (Z)	0.07	0.16	0.09
Natural period of structure	0.25s	0.113s	0.113s
Spectral shape factor ($Ch(T)$)	3.68	3.68	3.68

*The total weight of structure is the sum of wall and roof loads.

**A sum of the outer ring wall, inner ring wall and roof load.

We used formula (5.1) to calculate the horizontal equivalent static base shear forces (V) of the buildings. The calculated results for each case are presented in Table 5.4.

Table 5.4: Comparison of the horizontal forces of three case studies' buildings

Adobe house	The horizontal equivalent static base shear forces (V) *kN*
Hakka	1,517
Bhunga	37
Yomata	13.5

The calculated results indicate the highest horizontal forces for Hakka house, followed by Bhunga and Yomata houses, respectively. It can be noted that the total weight of structures has a significant effect on their seismic resistance.

5.6 Summary

This chapter presented details of the simple static earthquake design method covering the following components:

- Description of the equivalent static load method for determining earthquake forces, explained in details in Australian Standard AS 1170.4.
- Description of the relationship between design loads from the earthquake code and tilt table performance, including the hypothesis of a failure criterion as link between prototype and model behaviour.
- Description of the theory of reduced model testing, which describes the scale effect factors for both static and dynamic tests.
- Detailed calculation of the natural frequencies of circular structures.
- Description of the calculation of static design loads of the existing circular adobe houses, which presents the comparison results of the three case studies.

Chapter 6 Brick Fabrication and Material Property Tests

6.1 Introduction

This chapter describes the procedure of brick fabrication undertaken for the static-tilt-table test, in addition to a number of material property tests of adobe prisms. The static test was undertaken in Thailand. The experimental work was, therefore, carried out using the laboratory facilities of the Faculty of Engineering, Naresuan University (NU), Phitsanulok province.

The objective of brick fabrication was to make good quality adobe bricks and mortar, and to ensure the bricks have consistent quality (as bench mark for adobe bricks made in Australia, as described in Chapter 9).

There were a number of tests undertaken on adobe prisms. The prisms were tested in compression. The objectives of material testing were to obtain some characteristic material properties of adobe bricks.

6.2 Brick fabrication

All the adobe bricks used in this project were made by hand, using traditional methods. The brick dimensions were based upon a prototype brick of 300mm x 200mm x 100mm, normally used in Thailand (Uthai Phat Ra Kun 2004). Typical bricks were 1:3 scale of the original dimensions: 100mm x 67mm x 33mm. Each typical scaled brick weighed approximately 375 g. All bricks were fabricated using combination of raw soil, rice husk and sand. The mortar was also used with same recipe as the mixture. All adobe bricks and prisms were fabricated using the same raw materials in the same location and with the same process.

The detailed fabrication process is described below:

1. First, a number of trial bricks were made using various proportion of materials. The dry components were manually mixed using raw soil plus rice husk and sand additives until a suitable mix of ingredients was achieved for the test

bricks. These dry ingredients were placed into the large mixing hole lined with a plastic layer and manually mixed. Then a small amount of water was added as required and mixed to the desired consistency. The mud was left for two nights to let the mixture settle and break down the clay particles as suggested by (Dowling 2006; IAEE 1986; Lengen 2008).

2. After drying, more water was added until it is malleable enough to place into the moulds. The proper combinations of mixture were determined by trial and error. A simple test was done by rolling out some earth into a cigar-shape and carefully flattened by fingers to form a " *ribbon*" as long as possible. The length of ribbon was measured at its break point. A suitable length for adobe bricks is between 5 – 15 centimetres long (Doat et al. 1991).

3. The appropriate mud sample was placed into moulds made of steel. The mixture was pressed down to eliminate any air and smoothed off at the top of the brick by a trowel and the mould removed vertically in one brisk movement. The moulds were cleaned in water after each brick set. The bricks were left to dry under the sun approximately 3-4 days. Then they were rotated until all surfaces were totally dry. The dry bricks were then moved into the storage area to protect them from rain and further drying.

4. A number of sample bricks were manually inspected and then a simple field test was carried out to determine overall suitability of the dry adobe bricks. Robustness assessment was undertaken by dropping a number of sample bricks onto firm ground to check their toughness under impact loading (Walker & Standards Australia 2002).

5. After testing, it was found that the suitable proportions of materials by volume can be expressed as raw soil : sand : rice husk = 2:2:1.

6. Finally, a large number of bricks, in 1:3 scale, were fabricated using the same ratio and procedures described above. They are placed into a dry storage area for drying after fabrication.

Figure 6.1: Mixing of mud for adobe bricks.

Figure 6.2: Making adobe bricks by mould.

(a) (b)

Figure 6.3: (a)Drying of adobe bricks; (b) Stacked adobe bricks.

Additionally, sedimentation test was conducted to estimate the proportion of the constituents of the soil (Walker & Standards Australia 2002). The soil was tested using a glass container filled with the selected soil and water. The mixture was shaken and allowed to settle until the water become clear. The result shows the soil composition of the brick and mortar used for the static-tilt-table test is:

Sand	= 85 %
Silt + Clay	= 15%

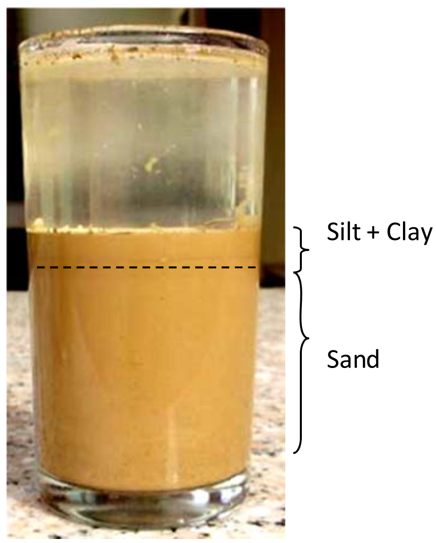

Figure 6.4: Sedimentation test.

This outcome from the sedimentation test was further used as the bench mark to determine the quality of earth used in the dynamic testing section (see Chapter 9).

6.3 Material property testing

The most important strength properties of the earth building materials can be identified by examining the modes of failure from simple field tests, such as ribbon test and robustness test (Tolles & Krawinkler 1990b). Compression tests are standard tests to determine the properties of compressive strength and unconfined compressive strength of adobe specimens. The method of manufacture and test setup were based on the Standard Test Method for Compressive Strength of Masonry Prisms: ASTM C 1314-07 (ASTM 2008). Compressive strength was obtained from maximum applied loading and cross-sectional area of specimens, whereas, unconfined strength was obtained by applying an aspect ratio correction factor to calculated values (Walker & Standards Australia 2002). The method for evaluating the results of these tests was assessed by using the Appendix H of AS 3700-2001.

6.3.1 Specifications

Five adobe prisms were fabricated and tested in a compression-testing device. The specifications of the adobe compression prisms are shown in Table 6.1 below.

Table 6.1: Specifications of compression prisms

General specimen configuration	Three layers of adobe bricks (horizontal stack)
Dimensions (L x W x H)	150mm x 200mm x 255mm
Specimen age (at testing) ~	160 days
Mortar thickness	~ 10 mm
Average specimen height (H)	246.6 mm
Average H/W ratio	1.68
Specimen drying condition	Air/sun dried on plastic surface. Temperature range : 22°C - 34°C. Humidity range : 60%-80%.
Drying load	3 half bricks (1:1 scale)
Specimen quantity	5 prisms fabricated
Specimen weight	9.5 – 10.3kg
Average specimen density	1,738 kg/m^3

The compression prisms were constructed using the same combinations of raw materials at the same time as the small-scale adobe brick fabrication undertaken in the static-tilt-table test. The 1:1 scale of adobe bricks was constructed and then sliced in half in length by saw cutting, in order to make their handling and transportation easier. The prisms were constructed using 3 layers of the bricks and stack bonded. The mortar used in the prisms was made of the same dry mix as the bricks. The mortar joint of prisms was approximately 10mm.-12mm. in thickness. All specimens were cured for 28 days and were tested 35 days after the time they were construction. The constructed sequence for compression prisms is shown in Figure 6.5.

(a) Full scale wooden mould

(b) Mud was placed into mould

(c) The bricks were dried in direct sunlight

(d) Dry bricks halved in length

(e) Place mortar

(f) Align and smoothen

(g) Check level of prisms and enclose with plastic bag for drying.

Figure 6.5: The sequence of construction for adobe compression prisms.

6.3.2 Testing method

A total of five compression tests on the adobe prisms were conducted during the second year of this research program. These tests were undertaken in compliance with ASTM C 1314-07 (ASTM 2008). The test machine was the Compressive Test Plant *ToniPACT II* located at the Faculty of Engineering, Naresuan University (NU), Thailand (see Figure 6.6). This machine was Grade A, according to AS 2195-2005: Calibration and Classification of Force-measuring Systems (Standards Australia 2005). Its upper platen also has an spherical seat tilt-able by 3 degrees. All specimens were placed in the testing machine and loaded until failure (see Figure 6.7).

Figure 6.6: Compression machine at NU.

The compressive strength was calculated by using equation (6.1) below:

$$f_c = \frac{P}{A} \tag{6.1}$$

Where:

f_c = compressive strength (kPa)

P = maximum load (kN)

A = surface area (m^2)

The unconfined compressive strength (C) of each specimen was calculated by using equation (6.2).

$$C = K_a \frac{P(kN)}{A(m^2)} (kPa) \tag{6.2}$$

Where:

P = Maximum load (kN)

A = Area of specimen (m^2)

K_a= The correction factor which depended on height-to-thickness ratio *(h/t)* of specimens

To calculate the *h/t* ratio for each specimen the height and the least lateral dimension of that specimen was used and the correction factor was then determined. However, they are not reliable for the aspect ratio correction factors of adobe masonry to account for *h/t* ratio which indicated different values between the Australia Standard AS 3700-2001 (Standards Australia 2001) and American Society for Testing and Materials standard ASTM C 1314-07 (ASTM 2008). If the correction factor stated in AS 3700-2001 were used, the average aspect ratio correction factor would be approximately 0.76. On the other hand, if the ASTM C 1314-07 was adopted then the average correction factor would be approximately 0.88. Therefore, in order to have interpretable results, the decision made was to stay with AS 3700-2001 and was also covered the later tests. The test result was shown in Table 6.2.

Figure 6.7: Compression test with specimen C1.

6.3.3 Results

The results from the compression tests are shown in Table 6.2.

Table 6.2: Results from compression tests of adobe prisms

Specimen	**H/T ratio**	**Surface Area** (m^2)	**Max Load P** (*kN*)	**Prism Strength** f_c (*kPa*)	**Unconfined Compressive Strength*** (*kPa*)*
C1	1.65	0.035	31	885.7	669.8
C2	1.68	0.033	31	939.4	713.8
C3	1.7	0.035	28	800	609.8
C4	1.67	0.034	29	852.9	647
C5	1.71	0.033	30	909	694
Average	1.68	0.034	29.8	877	666.9
SD	0.02	0.001	1.30	53.6	40.6
CoV (%)	1.0	3.0	4.0	6.0	6.0

Notes:

SD = Standard Deviation
CoV = Coefficient of Variation
* Determine the aspect ratio correction factor from AS 3700

Failure modes

Generally, there were two types of failure patterns in this compression prisms tests as face shell separation (Figure 6.8a) and Cone & Shear (Figure 6.8b).

(a) *(b)*

Figure 6.8: Types of failure pattern of compression prisms (specimen C3 & C5).

These failure patterns appear as typical vertical splitting cracks which are normally noticed in the masonry prisms. Vertical splitting cracks are due to differing deformation characteristics of brick and mortar, even though they are made from the same material as there densities are different.

From the test results in Table 6.2, it can be concluded that an average of the unconfined compressive strength of adobe bricks undertaken for the static-tilt-table test was 667 kPa. The results revealed that in this research the compressive strength was slightly lower compared with the other adobe research (presented and discussed in Chapter 9). It was assumed that the low strength may come from the size effect of adobe prisms that have a low height-to-width ratio of prisms. Tolles and Krawinkler (1990b) cited that the strength of adobe prisms was dependent on the proportion of soil, the drying condition and the size effect. They reported from their adobe research that 1:5 scale prisms were approximately 35% stronger in compressive strength than 3:4 scale prisms made of the same material, and referred this outcome to different drying conditions of the specimens as well as the size effect. Jeanette and Klaus (2004) cited that the compressive strength in clay prisms should have a minimum slenderness of 3 in order to get a reliable outcome. Another opinion about strength due to size effect was reported by Dowling (2006) who claimed that the height-to-width ratio (H/W) of the adobe prisms tested may affect the outcomes of the compressive strength. Heathcote and Jankulovski (1992) also claimed that strength of tested prisms definitely decreases with increasing aspect ratio.

In addition, the result of this section also indicated a value of the Coefficient of Variation (CoV) of 6% which showed that there was some variability in these tests. It is clear that for the adobe prism testing, more attention should be placed on quality control for both soil properties and prism characteristics. However, the CoV value in this research seems to be acceptable when compared with other strength tests (see Chapter 9).

The results from this section are discussed in greater detail in Section 9.2, where they are compared with other results from this research compression tests and with other adobe research.

6.4 Summary

In this chapter the process of brick fabrication undertaken for the static tilt-table tests has been described. Some representative material characteristics for this research has been obtained in the process. A number of standard evaluation methods were used to ensure the manufacture of good quality and consistent bricks. The chapter has also presented the processes and results of a sequence of compressive strength tests using adobe prisms.

Experimental work has been carried out in order to determine mechanical properties of adobe material. Results obtained from the compressive strength test along with the conclusions and recommendations are given as follows:

- The mean value of unconfined compressive strength of adobe prisms was found to be 667 kPa.
- Two failure modes were observed during testing the prisms as face shell separation and Cone & Shear.
- Results reveal that in this research the compressive strength is slightly lower which may come from the size effect of adobe prisms. Therefore, an investigation on the size effect of adobe prisms should be conducted in the next set of compression tests.
- Results also suggest that any further testing on adobe prisms should put more consideration on quality control for both soil properties and prism characteristics.

Chapter 7 Seismic Capacity Comparison between Square and Circular Plan Adobe Construction using Tilt-table Testing

7.1 Introduction

This chapter investigates the seismic capacity comparison between square and circular plan unreinforced adobe buildings. These two symmetrical plans have significant bearing on the performance of buildings during strong earthquakes. However, there is no evidence that indicated the best seismic performance between these two layouts of adobe structures. The test results of these comparative experiments give simple and effective solutions for construction of new adobe buildings located in seismic hazard areas. The result from this testing can assist in decreasing damage and death from earthquake activities in seismic risk areas.

This chapter provides a detailed comparative analysis and discussion of results of seismic capacity between two symmetrical shapes, i.e., a square and circular model of unreinforced adobe walls. Static tilt-table tests were carried out for seismic performance evaluation of both structures. The lateral component of model weight was used as a parameter to quantify the maximum seismic force for each model.

Two dimensional compact plans of 1:3 scale for both square and circular models, were selected. The square and circular layout for the adobe models were designed and constructed to study its response against lateral forces. This chapter provides the information on the fabrication, testing and results for the square and circular adobe walls. Comparative analysis was also carried out for the square and circular models.

At the end of the chapter the social aspects of circular buildings is presented, and the discussion on why most guidelines and manuals concentrate only on square and rectangular buildings, and not circular buildings is presented.

7.2 The relationship between the static design load and tilt table testing

Tests of adobe buildings can either be done by applying static design loads or using tilt-table. The static design method relies on the assumptions that an equivalent static load can replace the earthquake action as specified in section 6 of AS 1170.4 (see details in Chapter 5). The equivalent static force is presented by the following expression:

$$V = k_p \times Z \times C_h(T_1) \times (S_p / \mu) \times W_1 \tag{7.1}$$

In the tilt table testing, the structure is subjected to a constant acceleration (due to gravity load) when it is tilted-up by a tilt table. The horizontal force in this case (*HF*) is equal to the weight of the structure times the cosine of the tilt angle as given by the following equation:

$$HF = \sin\theta \times W_1 \tag{7.2}$$

Figure 7.1 shows the weight of the model (W) is transformed to lateral force (H_F) when tilted at θ angle.

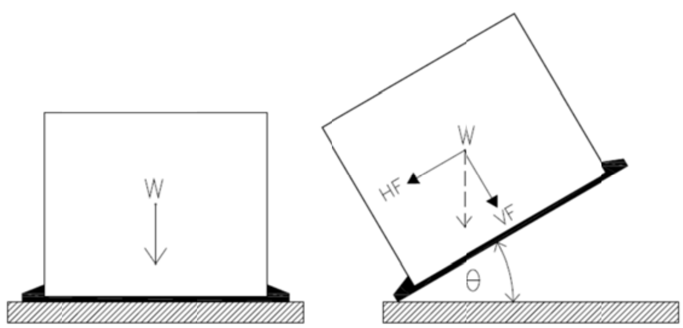

$V = H_F$

Figure 7.1: Conceptual scheme of the static testing.

Therefore, the failure angle from the tilt-table test can be used as an indication of the ultimate horizontal force the earthquake imposes on the structure.

7.3 Static tilt table

A static tilt-table was set up to evaluate the seismic performance of this type of structure. The tilt-table tests were undertaken at the Faculty of Engineering, Naresuan

University, Thailand. The static-tilt-table was constructed with 5 mm steel plate of dimensions 1.5 x 1.5 m with a checkered plate floor surface on top. A hydraulic floor jack was installed in order to lift the tilt table with the maximum model load of 2,000 kg. It can be tilted from 0 to 55 degrees indicated by a half circle roamer. Figure 7.2 shows the details of the tilt table.

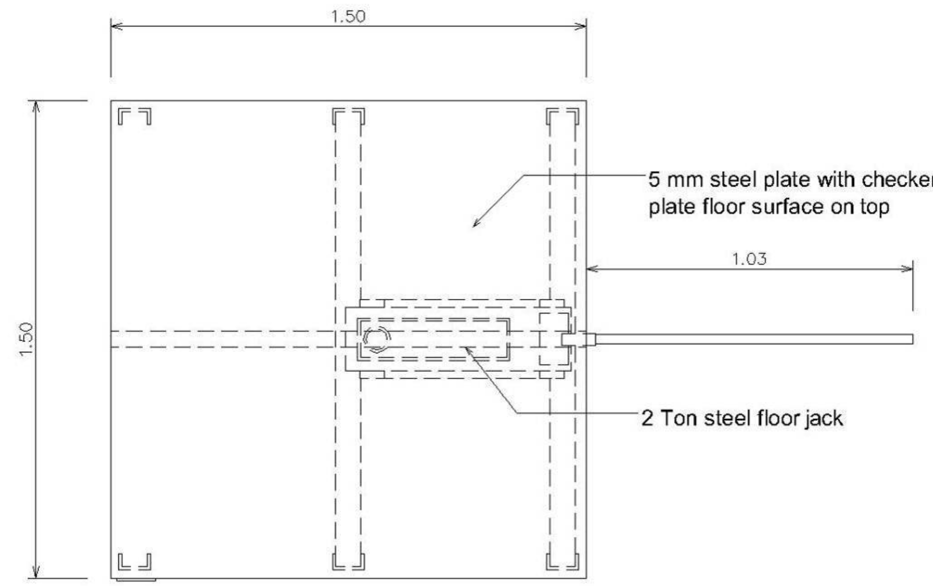

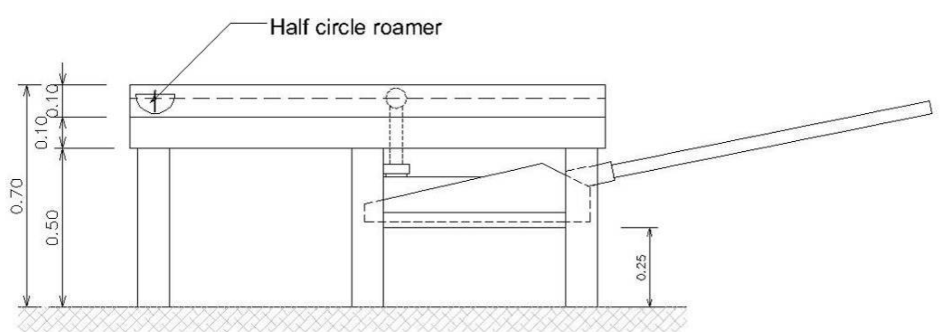

Figure 7.2: Tilt table configuration and dimensions.

Figure 7.3: Construction of the tilt table.

Figure 7.4: Tilt testing of a square adobe model.

7.4 Specimen fabrication and specifications

Two small-scale models (1:3 scale) of adobe structures were built with square and circular plans. The bricks and mortar were made from the same raw material using combinations of raw soil, rice husk and sand with the selected mix of 2:2:1 (see more detail in Chapter 6). The bricks were laid in stretcher bond with mortar joints of about 10 mm thick. The wall was attached to the steel base plate with the same mortar to bond the bricks. The square and circular models were constructed with the same height-to-thickness ratio (*h/t*) of 26.45. The formula 7.2 (given in Section 7.2) was used to calculate the ultimate horizontal force (H_F) for the first shear crack and the complete failure angles of both models. Table 7.1 shows the specifications of two models.

Table 7.1: Comparison of specifications between square and circular models

Model shape	*Wall thickness (mm)*	*Plan Dimension (m)*	*Wall height (m)*	*Roof load pressure (kN/m^2)*	*Total roof load (kN)*	*Total wall load (kN)*
Circular	31	1.2 (Diameter)	0.82	2	2.25	1.56
Square	31	1.2 x 1.2	0.82	2	2.25	1.98

Table 7.1 shows that the square wall is heavier than the circular one due to the larger wall area. In order to give a better comparison, the ultimate horizontal force for each model test was expressed in terms of the percentage of the maximum horizontal force compared to model's self-weight. These two test results were then discussed, and the seismic capacities of the square and circular models compared.

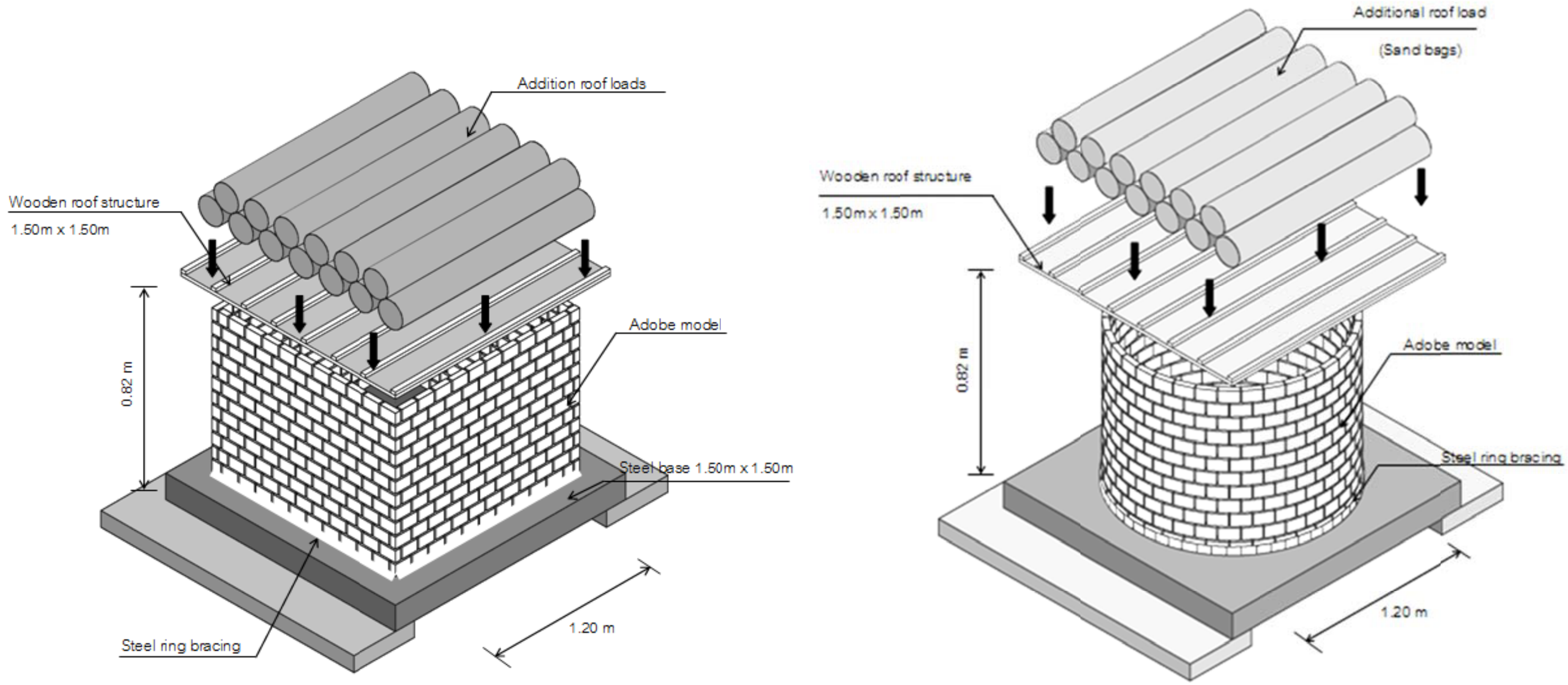

Figure 7.5: Square and circular specimens' configurations and dimensions.

7.5 Results of the specimens tested

The tests began once the constructed specimens were dry. The roof cover made from ply-wood was installed, and sand bags were placed on it to achieve the required load on the model's wall. All sand bags were laid in the same direction. The test was recorded by a number of video recorders. The table was slowly and smoothly raised by a hydraulic jack until the adobe model collapsed. The first cracking angle and the angle at which the model totally collapsed were recorded for comparison of the two models' performance. Figures 7.6 and 7.7 show the testing sequence of the square model and Figure 7.8 and 7.9 show the testing sequence of the circular model.

Figure 7.6: Tilting the square specimen and first crack appearing at 20 degrees.

Figure 7.7: The failure modes of the square specimen when tilted further.

Figure 7.8: Tilting the circular specimen and first crack appearing at 29 degrees.

Figure 7.9: The failure modes of the circular specimens when tilted further.

From the observations, the failure mechanism of the square specimen in the static test was: vertical corner cracking was induced by shear or tearing stresses and followed by the overturning of the wall panel (Figure 7.7). A lack of mechanical fixing at the corners allows greater out-of-plane displacement of the wall panels. The top of the wall had a larger response, which caused a greater pounding impact, thus inducing greater stresses that lead to the complete wall failure.

For the circular specimen, it was clear from the observations that the first shear cracking appeared on the side of the wall, starting from the top edge (Figure 7.8). The other cracks occurred when the table was tilted further. The model rapidly approached failure when the front part of the wall tended to rotate and eventually separated from the rest of the model (Figure 7.9).

The comparison of the results from the square and circular specimens were carried out. The first cracking and the complete failure angles were used to calculate the maximum lateral force for both models at each stage. Table 7.2 and Table 7.3 give the comparative results of these static tilt-table tests.

Table 7.2: Results of the square specimen subjected to static tilt testing

	First shear crack	*Complete failure*
Angle (degrees)	20	25
Horizontal force (*HF*)	1.45 kN	1.78 kN
Percentage of the max. horizontal force compared to model own weight	34.3%	42.3%

Table 7.3: Results of the circular specimen subjected to static tilt testing

	First shear crack	*Complete failure*
Angle (degrees)	29	32
Horizontal force (*HF*)	1.73 kN	2.02 kN
Percentage of the max. horizontal force compare to model own weight	45.4%	53.0%

Tables 7.2 and 7.3 provide a comparison between the first cracking angles and the failure angles of both specimens. The results show that the circular adobe structure performed better than the square one with a higher percentage of horizontal force resistance. Mauro Sassu (n.d.) also stated that a circular floor plan of vernacular buildings offers the best resistance to seismic forces, and a box-shaped building performs poorly with out-of-plane forces and separation at the wall corners. Ole Vanggaard (2003) noted that a circular building has greater static stability due to the shell action of cylindrical wall which has excellent static stability to resist compression force and transfer lateral force.

This test outcome suggests that circular plans should be considered for design and construction of adobe houses located in seismic hazard areas. A comparison with window and door openings for these two shapes would be worthy of further investigation to confirm any advantages or disadvantages of circular buildings.

In the next chapter, a comprehensive testing of the seismic capacity of circular adobe models with various configurations and roof loads were conducted. The circular adobe model in this section was then used as the typical model (specimen 1A) for comparison with the other dimensional models.

7.6 Social aspect of circular buildings

The results from the previous section indicate that a circular adobe building has better seismic resistance than a square one. At the present time, there are considerable number of guidelines and manuals which contain construction details and recommendations for the configurations of unreinforced adobe houses in earthquake prone areas. However, these guidelines and manuals concentrate only on square and rectangular plan buildings. Therefore a question arises: ***why***, even though there are a number of well documented existing publications citing that circular buildings have better seismic resistance than square or rectangular buildings (Minke 2001; Sassu n.d.), circular buildings are still ignored in building guidelines and manuals?

About one-third of the world's population live in unbaked earthen buildings with about half of the population in developing nations (Houben & Guillaud 1994; Wojciechowska 1967). However, most of these dwellers built earthen houses with their traditional simple shapes as square or rectangular plans (EERI & IAEE 2009). Even though, some of these countries are located in seismic hazard risk areas such as El Salvador, Peru, Iran, Guatemala, Kyrgyzstan, etc. Their traditional vernacular housing's plan are based on square or rectangular design and it may be difficult to encourage them to build using a circular layout. Pratt (2010) pointed out that "*The thought of making a life change can be so intimidating*". People may also have concerns on the space efficiency of circular buildings, or the construction methods they could use due to limited experience and knowledge on circular buildings. This may well be the hypothesis to answer the above question.

On the other hand, there are some groups of people living in earthquake hazard risk countries using circular adobe plans as their traditional vernacular houses, such as in China (*Hakka*), India (*Bhunga*) and Malawi (*Yomata*) (EERI & IAEE 2009). The local people in these areas have learned the principles of seismic resistant construction by a "trial and error" process. Therefore, they are confident in using a circular plan for their own houses rather than the other shapes.

It can be said that the issue may come from the social aspects of a circular building. Some people may see that circular adobe buildings have problems with their functional efficiency or/and difficulty in construction. There are some comments when asking about living in a circular house:

> *"Square plan provided more space efficient space than a circular plan. Because it is hard to be managed and it is difficult to put furniture into a round shape." (Mazlin 2008)*
>
> *"Circular plan would be more difficult to build. But could be very interesting to live in." (Demand Media Inc. 2009)*

These two assumptions are further discussed and investigated as follows:

Space efficiency in circular adobe houses

A circular plan is seen to be less space efficient than a rectangular plan due to the fact that it is difficult to fit with commercially built furniture. However, this is not an argument when talking about general buildings. While most of the areas using adobe construction for residential buildings are in developing countries their adobe houses are small due to their limitation of construction technologies. They may have only one or two separate living areas in one building space. The furniture is simple and maybe built from natural material matching with their earthen walls. Most of the furniture in adobe house are built-in and connected to the wall panels to leave the centre area open to be used as the hall way (Maneewong 2009). Beds, tables and chairs can be made by earth material. Shelves can be easily carved into the adobe walls. Roy (2006) claimed that circular is a simple shape to build in term of enclosing the maximum amount of space with the least amount of perimeter wall material. Figure 7.10 shows the space efficiency of circular adobe houses.

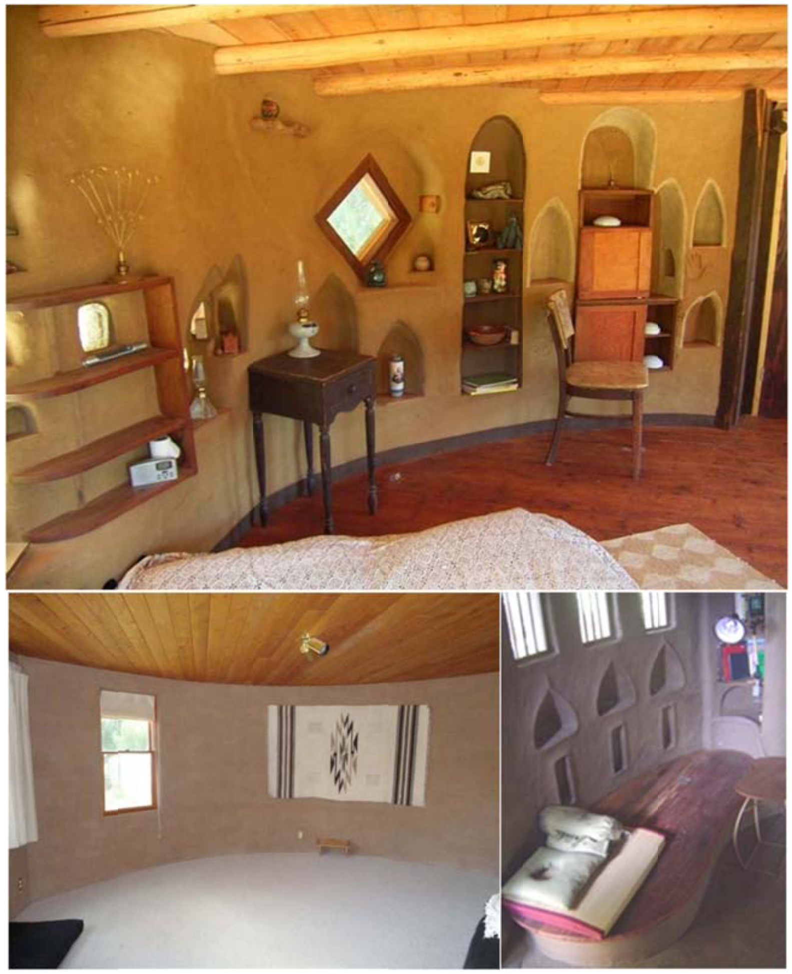

Figure 7.10: The performance of functional areas in circular adobe houses.

The limitation on functional areas may not be an issue when the focus is on small adobe buildings as there is not much difference between circular and rectangular plans. There is a limitation on space due to the buildings being smaller and due to the nature of their construction.

The difficulty in construction

Circular building in general may be more difficult to construct when compared with square or rectangular buildings but this is not true for adobe structures. Circular adobe walls are easier to lay than a straight-wall plan (Uthai Phat Ra Kun 2004) (see Figure 7.11). The rectangular and square constructions experience some difficulties with brick bonding at wall corners (Ket 1985). A long straight wall also needs wall supports every 3 metres or so whereas this is not necessary for circular walls (Uthai Phat Ra Kun 2004). The circular building has also greater static stability due to their shell action of cylindrical walls (Vanggaard 2003). Therefore, a circular shape is easier to construct when compared to other shapes.

Figure 7.11: Circular-adobe-wall construction.

Finally, it is clear from the investigation and discussion above that a circular layout for adobe construction is as space efficient and easier to construct than a square or a rectangular layout. The hypothesis that people are unaware of the fact and lack information regarding circular-adobe building needs to be addressed. Therefore, publication of this research and making the findings available to all areas using adobe construction methods may contribute to this area, and it can encourage future builders to use this type of construction. It will also challenge adobe researchers to further study circular adobe buildings.

7.7 Summary

The successful comparison tests between square and circular adobe walls revealed the following outcomes:

- Test results indicated that the static tilt-table testing gives reasonable results when the seismic response of adobe structures is investigated.
- The result of these comparative experiments indicates that circular structures perform better than the square ones.
- The outcome of these experiments gives simple and effective solutions for construction of new adobe buildings located in seismic areas.
- Further comparative studies of square and circular adobe structures with openings in various configurations should be conducted to verify the advantages of circular structures and study the failure behaviour of the structures.
- Test results challenge guidelines and manuals for adobe constructions as most of them recommend square layout for the most effective seismic resistant buildings.
- Lack of experience and knowledge on circular adobe construction restricted its use for better seismic performance.

Chapter 8 Capacity Estimation of Circular Adobe Buildings by Tilt-table Testing

8.1 Introduction

The primary aim of this thesis is to develop a simple methodology that can evaluate the existing circular adobe houses, and to provide design recommendations for circular structures located in seismic risk areas. From extensive literature reviews, it appears that static testing using a tilt-up table can be developed to achieve this objective.

This chapter presents series of static tests conducted to study the performance of unreinforced circular adobe buildings subjected to quasi-static earthquake forces. Nine small-scale circular adobe models (1:3 scale) were built with a variety of configurations and roof loads. Static tilt tests were carried out to investigate the failure modes of circular adobe structure and its failure mechanism.

The relationship between the static design load and tilt-table testing is explained in this chapter. The chapter also describes the preparation, testing and observations from the circular adobe specimens' experimentation. The detail testing sequence is described, and the observed damages for each specimen are presented.

The results in this chapter gave a better understanding of the earthquake performance of circular buildings, to predict the performance of existing circular structures in seismic regions.

The tilt-table tests were undertaken at the Naresuan University (NU), Thailand during the third year of research.

Specimen 1A is taken as a benchmark model to compare with the other models with varying roof loads, wall thicknesses and heights. Table 8.1 shows the specifications for each circular adobe model tested as part of the tilt-table testing.

Table 8.1: Small Scale Adobe Models: specifications

Model Set	***Wall Thickness*** *(mm)*	***Diameter*** *(m)*	***Wall Height*** *(m)*	***Roof Height*** *(m)*	***Roof Load Pressure*** *(kN/m^2)*	***Total Roof Load*** *(kN)*	***Total Wall Load*** *(kN)*
1A	31	1.2	0.82	0.94	2	2.25	1.56
2A	31	1.2	0.82	1.00	3	3.38	1.55
3A	31	1.2	0.82	1.06	4	4.51	1.55
2B	45	1.2	0.82	0.94	2	2.25	2.23
3B	60	1.2	0.82	0.94	2	2.25	2.93
2C	31	1.4	0.82	0.94	2	2.25	1.82
3C	31	1.0	0.82	0.94	2	2.25	1.29
2D	31	1.2	0.96	1.08	2	2.25	1.82
3D	31	1.2	0.67	0.79	2	2.25	1.27

This chapter also contains the effectiveness comparison of the test models between roof loads, wall height-to-diameter ratios and wall height-to-thickness ratios. The comparative details are described as follows:

- The test results on model 1A, 2A and 3A were selected to determine the effect of roof loads on seismic resistance capacity. Each model had a variety of additional weights on the top. The roof loads of model 1A, 2A and 3A were 2 kN/m^2, 3 kN/m^2 and 4 kN/m^2, respectively.
- The test results on model 1A, 2C, 3C, 2D and 3D were selected to determine the effect of wall height-to-diameter ratios on seismic resistance capacity. Each model had a variety of wall height-to-diameter ratios. The ratios of model 1A, 2C, 3C, 2D and 3D were 0.68, 0.58, 0.82, 0.80 and 0.56, respectively.
- The test results on model 1A, 2B, 3B, 2D and 3D were selected to determine the effects of wall height-to-thickness ratios on seismic resistance capacity. Each model had a variety of wall height-to-thickness ratios. The ratios of model 1A, 2B, 3B, 2D and 3D were 26.4, 18.2, 13.6, 30.9 and 21.6, respectively.

This chapter provided the objective outcomes which are necessary for the detailed discussion and comparative analysis in the following chapter.

8.2 The hypothesis of the typical failure mechanism

The hypothesis of the typical failure mechanism of circular adobe walls under seismic action is discussed. A horizontal load applied to a circular wall with a vertical axis is typically termed a transverse shear load (Teng & Rotter 2004). This transverse shear load causes a tensile failure in-plane of the cylinder masonry wall. The failure pattern is a crack through the mortar and brick interface due to differential drying conditions. This hypothesis is learned from the lessons of the previous circular-adobe-model testing in Chapter 7. Figure 8.1 shows the conceptual typical failure pattern of a circular adobe structure in static tilt-table test.

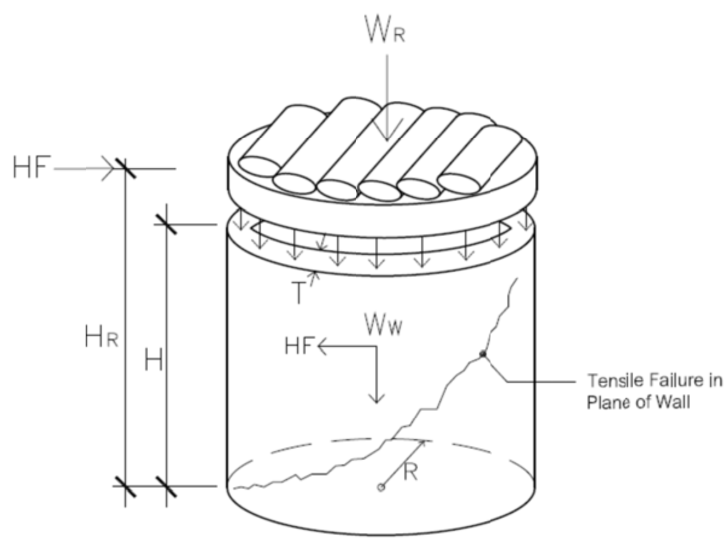

Figure 8.1: Conceptual failure pattern of a circular adobe model in static tilt testing.

This hypothesis of the failure pattern is then compared with the testing results in this chapter and will be discussed in greater detail in Section 8.7.

8.3 Specimen design and construction

All circular adobe specimens were fabricated by the author of this thesis. The walls were constructed with bricks and mortar and their fabrication was discussed in Chapter 6. Each model structure was constructed in a similar manner. The walls were constructed with the adobe bricks and mortar of the same material. Each specimen consisted of a different number of bricks due to the difference in the specifications. The specimens had a variety of roof loads, wall thicknesses, wall diameters and wall heights. The bricks were laid in stretcher bond with about 10 mm thick mortar joints. Each model wall was built directly on the checkered plate of the tilt table with additional steel bracing connected at its base. This steel ring was installed in order to prevent sliding which occurred from the failure surface friction between the checker plate and the bricks. The 1:3 scaled circular adobe models were subjected to the lateral loads produced by their own weights and loads on the roof when tilted by the tilt table. The details of model preparations and testing procedures are presented in Section 8.4. The observed damage and failure mode of each model are also described and presented by photographs. A typical specimen configuration is shown in Figure 8.2.

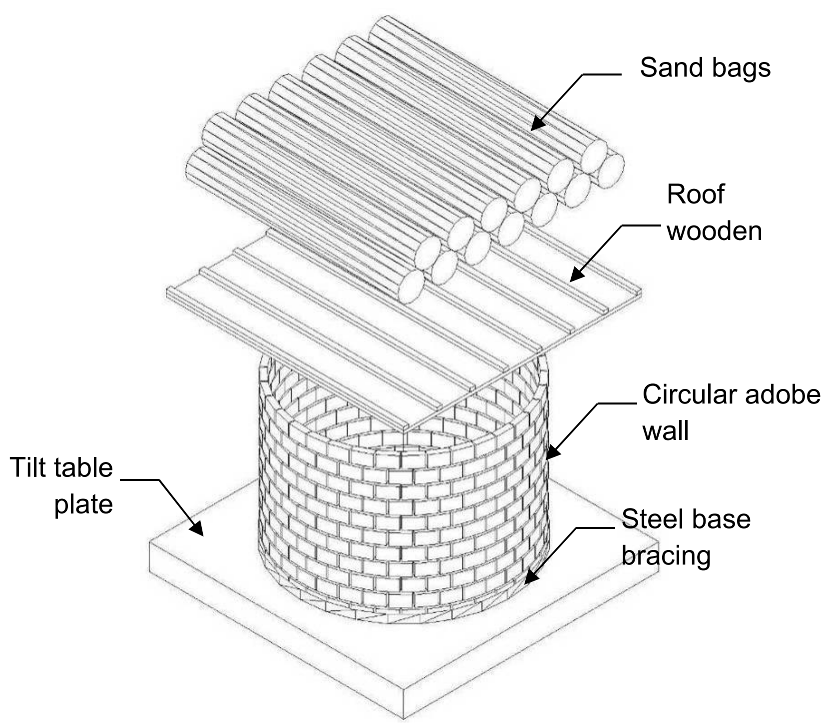

Figure 8.2: Typical specimen configuration.

Figure 8.3 shows the sequence of a circular-adobe-wall construction. The details of construction sequence are described below:

- Prior to construction of the brick wall, the steel plate of 1 inch in height was firmly connected to the top of a tilt table with outside required diameter (Figure 8.3(1)).
- The adobe bricks were placed directly on a steel checkered plate on the top of the tilt table. The wall of each model is single wythe (a single adobe brick). The first layer of wall was laid inside the ring bracing. The gap between the ring and the brick was packed with mud mortar (Figure 8.3(2)). Each model consisted of different amount and size of small-scale bricks. The bricks were laid on the long narrow side with the broad side exposed. The brickwork bonds were of stretcher pattern with about 10 mm thickness of mortar joints (Figure 8.3(3)-(4)). The bricks were laid down until they reached the required height.
- Prior to test, each completed model was cured, until all mortar joints of the circular model were dry (Figure 8.3(5)).

(1)

(2)

(3)

(4)

(5)

Figure 8.3: Construction of a circular adobe specimen.

8.4 Detail of experimental procedures of static tests

8.4.1 Procedures of static tilt-table tests

The static tilt-table testing began once the constructed specimen was dry. Based on Thailand's weather, it was be noticed that each model will dry in 3-4 days and was ready for testing. Therefore, for these experiments it was decided to allow a minimum of 7 days for models' drying time. The roof cover made from ply wood was installed on which sand bags were placed to reach the required load on the model's wall. All sand bags were laid in the same direction. The table was slowly and smoothly raised by a hydraulic jack until the adobe model collapsed. The collapse angle was recorded in order to compare the results with other model tests. Figures 8.5 to 8.7 show the test setup sequence for the tilt-table testing.

All testing was recorded by a number of video recorders.

(a) At the bottom plate. (b) At the upper plate for laying sand bags.

Figure 8.4: The wooden roof cover with bracing.

Figure 8.5: Roof and sand bags installation.

Figure 8.6: Tilting the specimen until cracking and subsequent failure.

Figure 8.7: Reading the result of failure angle.

8.4.2 Specimen 1A

Specifications of specimen 1A :

Wall thickness	:	31 mm
Outside Diameter	:	1.2 m
Height	:	0.82 m
Roof load pressure	:	2 (kN/m^2)
Total roof load	:	2.25 kN
Total wall load	:	1.56 kN

Figure 8.8: Specimen 1A prior to testing.

Specimen 1A was built with 432 adobe bricks. The wall was built as a single-layer of adobe bricks and each course was made entirely of stretchers, the joints in each row were at the centre of the bricks in the row below (running bond pattern). The height-to-thickness ratio (*h/t*) of the wall specimen was 26.45 and the height-to-diameter (*h/d*) was 0.68. The model was built directly on the steel plate of the tilt table with a retaining ring to hold the bottom course of brickwork. After the construction, the specimen was 'cured' for a minimum of 7 days prior to testing. A roof cover and sand bags were installed before testing.

The construction of this specimen served as the typical model for comparison to the others.

Testing and results of model 1A:

The 1A specimen was tested with a roof load of 2.25 kN. The model was tilted and the first shear cracking appeared at the front side starting at the top wall of the model when the tilt angle reached 29 degrees. The model was further tilted and a second shear crack occurred on the right side. Finally, the model rapidly collapsed at 32 degrees. Test results indicated that model 1A had an initial failure with a horizontal force equivalent to 48.5 % of its own weight. The testing sequence is shown in Figure 8.9.

(1)Prior to test.

(2)The first cracking appeared.

(3)Another cracking appeared.

(4)Subsequent total failure.

Figure 8.9: Testing sequence of specimen 1A.

8.4.3 Specimen 2A

Specifications of specimen 2A :

Wall thickness	:	31 mm
Outside Diameter	:	1.2 m
Height	:	0.82 m
Roof load pressure	:	3 (kN/m^2)
Total roof load	:	3.38 kN
Total wall load	:	1.56 kN

Figure 8.10: Specimen 2A prior to testing.

Specimen 2A was built with 432 adobe bricks. The wall was built using the same procedure as for the construction of specimen 1A. The height-to-thickness ratio (*h/t*) of the wall specimen was 26.45 and the height-to-diameter (*h/d*) was 0.68 and were the same as specimen 1A. For this test the roof load pressure was increased by providing additional load, the loading was 3 kN/m^2. After the drying period for a minimum of 7 days prior to testing, the roof cover and sand bags were installed. This model was constructed to determine the effect of the roof load on its seismic resistance capability.

Testing and results of 2A

The 2A specimen was tested with roof load of 3.38 kN. The specimen was tilted and first shear cracking appeared in the left side of the wall (as shown in Figure 8.11(2)) when the tilt angle reached 25 degrees, followed by another shear cracking appearing at the opposite side and finally the specimen rapidly collapsed. Test results indicated that the model 2A had an initial failure with a horizontal force equivalent to 42.26 % of its own weight. The testing sequence is shown in Figure 8.11.

(1)Prior to test.

(2)The first crack appeared.

(3)Another crack appeared.

(4)Totally collapsed.

Figure 8.11: Testing sequence of specimen 2A.

8.4.4 Specimen 3A

Specifications of specimen 3A :

Wall thickness	:	31 mm
Outside Diameter	:	1.2 m
Height	:	0.82 m
Roof load pressure :		4 (kN/m^2)
Total roof load	:	4.51 kN
Total wall load	:	1.56 kN

Figure 8.12: Specimen 3A prior to testing.

Specimen 3A was built with 432 adobe bricks using the same procedure as previously. The height-to-thickness and the height-to-diameter ratios were the same as specimen 1A with a roof load pressure of 4 kN/m^2. After the construction, the specimen was 'cured' for a minimum of 7 days prior to testing. This model was constructed to determine the effect of the roof load on its seismic resistance capability.

Testing and results of 3A

The 3A specimen was tested with 4.51 kN of roof load. The specimen had the first shear cracking at the left side when tilted at 22 degrees and rapidly collapsed. Test results presented that model 3A had an initial failure with the horizontal force equivalent to 37.46 % of its own weight. The testing sequence is shown in Figure 8-13.

(1)Prior to test.

(2)The first cracking appeared.

(3) Cracking from another side.

(4)Totally collapsed.

Figure 8.13: Testing sequence of specimen 3A.